UTS UNIVERSITY OF TECHNOLOGY SYDNEY

Microalgae cultivation and harvesting using carbon and sulphate for lipid, protein, and biofuel production

by Lisa Aditya

Thesis submitted in fulfilment of the requirements for the degree of

Doctor Philosophy

under the supervision of Professor Long D. Nghiem and Professor Md. Abul Kalam

University of Technology Sydney
Faculty of Engineering and Information Technology

March 2025

CERTIFICATE OF ORIGINAL AUTHORSHIP

I, Lisa Aditya declare that this thesis is submitted in fulfilment of the requirements for the award of Doctor of Philosophy, in the School of Civil and Environmental Engineering, Faculty of Engineering and Information Technology at the University of Technology Sydney.

This thesis is wholly my own work unless otherwise referenced or acknowledged. In addition, I certify that all information sources and literature used are indicated in the thesis.

This document has not been submitted for qualifications at any other academic institution.

This research is supported by the Australian Government Research Training Program.

Signature:

Production Note:
Signature removed prior to publication.

Date: 07-03-2025

ACKNOWLEDGEMENT

I have experienced immense personal and academic growth during my PhD journey. I am deeply thankful to all the people who have guided, supported, and inspired me throughout this journey. I owe deep gratitude to my principal supervisor, Prof. Long D. Nghiem, for his constant support, invaluable guidance, and belief in my abilities. His extensive knowledge and vast experience have been a constant source of encouragement throughout my academic journey and personal life. I am deeply thankful for the invaluable time he has dedicated to guide my research, as well as revising my journal papers and thesis. I would also like to thank my co-supervisor, Prof. Abul Kalam and special thanks also to A/Prof. Qiang Fu for their insights, which added so much depth to my research and my personal growth.

My heartfelt thanks go to my research group members and colleagues; Luong Nguyen, Chelsey Vu, Minh Vu, Allie Nguyen, Sunny, Huihui, and Dr. Md Johir. Their collaboration, shared knowledge, and encouragement made this journey productive and enjoyable.

Finally, I owe everything to my family and extended family, especially my husband, Topan Erlangga ST., MT. for his understanding, patience, and encouragement, which helped me persevere through it all. A special thanks to my sister-in-law, Intan for her unwavering love toward my daughter, which has been my greatest source of strength.

TABLE OF CONTENTS

LIST OF PUBLICATION

1. **L Aditya,** TMI Mahlia, LN Nguyen, HP Vu, LD Nghiem. Microalgae-bacteria consortium for wastewater treatment and biomass production. 2022. Science of the total environment 838, 155871. ***[Highly cited paper in Clarivate]***
2. LN Nguyen, **L Aditya**., HP Vu, MAH Johir, Bennar, L., PJ Ralph, NB Hoang, J Zdarta, LD Nghiem. 2022. Nutrient removal by algae-based wastewater treatment. Current Pollution Reports, 8(4), 369-383.
3. **L Aditya**., HP Vu, LN Nguyen, TMI Mahlia, NB Hoang, LD Nghiem. 2023. Microalgae enrichment for biomass harvesting and water reuse by ceramic microfiltration membranes. Journal of Membrane Science, 669, 121287.
4. **L Aditya**, HP Vu, MAH Johir, TMI Mahlia, AS Silitonga, X Zhang, Q Liu, LD Nghiem. 2023. Role of culture solution pH in balancing CO_2 input and light intensity for maximizing microalgae growth rate. Chemosphere 343, 140255.
5. AK Salih, **L Aditya**, F Matar, LD Nghiem, C Ton-That. Improved flux and anti-fouling performance of a photocatalytic ZnO membrane on porous stainless-steel substrate for microalgae harvesting. 2024. Journal of Membrane Science 694, 122405.
6. **L Aditya**, HP Vu, MAH Johir, S Mao, A Ansari, Q Fu, LD Nghiem. Synthesizing cationic polymers and tuning their properties for microalgae harvesting. 2024. Science of the Total Environment 917, 170423.
7. AK. Salih; CP. Irvine; F Matar; **L Aditya**; L D. Nghiem. Photocatalytic Self-Cleansing ZnO-coated Ceramic Membranes for Preconcentrating Microalgae. Journal of Membrane Science 718, 123700.

8. B Conor, T. Lacassagne, M Pernice, M, **L Aditya,** U Kuzhiumparambil, PJ Ralph. Rheological characterization and modelling of freshwater and marine microalgae and cyanobacteria co-cultures. 2025. Algal Research.
9. S Mao, S Zhang, A Feng, C Onggowarsito, H Xu, **L Aditya,** LD Nghiem, Q Fu Precision-Engineered, Low-Polymer, Digital Light Processing 3D-printed Hydrogels for Enhancing Solar Steam Generation and Sustainable Water Treatment. 2025. Nano-Micro Letters.
10. **L Aditya,** U Kuzhiumparambil, PJ Ralph, NB Hoang, MAH Johir, TMI Mahlia, LD Nghiem. Tuning carbon and nutrient concentration ratio for biomass, lipid, and protein production. 2025. Bioresource Technology (submitted).
11. **L Aditya,** MA Kalam, U Kuzhiumparambil, PJ Ralph, MAH Johir, TMI Mahlia, LD Nghiem. Sulphate Assimilation and Growth Response of *Scenedesmus sp* and *C.vulgaris* to Elevated Sodium Sulphate Concentrations. 2025. Environmental Chemical Engineering (submitted).

LIST OF ACHIEVEMENTS

1. Winner – 2022 Faculty of Engineering & IT Research Showcase Oral presentation.
2. Winner – 2022 Women in Engineering & IT HDR Award
3. UTS Vice-Chancellor's Conference Travel Award – 2023
4. UTS Vice-Chancellor's Conference Travel Award – 2024
5. School Conference Travel Award – 2024
6. Internship Scholarship – Jul to Sep 2024 a cash value of $12,000 from IWI Australia
7. Winner – 2024 Women in Engineering & IT HDR Award
8. Winner-2024 Strategic Research Accelerator grant

LIST OF ABBREVIATIONS

APS	Adenosine 5'-Phosphosulphate
ATP	Adenosine Triphosphate
bEPS	Cell-Bound Exopolysaccharides
CO2	Carbon Dioxide
FAME	Fatty Acid Methyl Esters
GC MS	Gas Chromatography-Mass Spectrometry
HCl	Hydrochloric Acid
HNMR	Proton Nuclear Magnetic Resonance
LI	Light Intensity
LMH	Liters Per Square Meter Per Hour
MeOH	Methanol
MF	Microfiltration
NADPH/NADH	Nicotinamide Adenine Dinucleotide Phosphate Hydrogen
NaHCO3	Sodium Bicarbonate
NaOH	Sodium Hydroxide
OD	Optical Density
PAPTAC	Poly(3-Acrylamidopropyl) Trimethylammonium Chloride
PO_4^{3-}	Orthophosphate
POME	Palm Oil Mill Effluent
PUFA/HUFA	Polyunsaturated Fatty Acid/Highly Unsaturated Fatty Acids

RCO2	Carbon Fixation Rate
TCA	Tricarboxylic Acid Cycle
TMP	Transmembrane Pressure
TOC	Total Organic Carbon
TOR	Target Of Rapamycin

List of Figures

List of Tables

ABSTRACT

Microalgae have emerged as a promising platform for carbon capture for simultaneously producing renewable chemical feedstocks and biofuels to address the escalating challenge of human-induced climate change. The economic feasibility of microalgae-based systems hinges on addressing the high costs of cultivation, harvesting, and water reuse. This thesis explores strategies to optimise microalgae growth and harvesting efficiency. Results indicate that balancing CO_2 input (850 mg/L) and light intensity (1089 μmol/m²/s) significantly enhances microalgae growth rates and carbon fixation, reaching up to 4.2 g/L. Additionally, the study highlights key differences in sulphate assimilation and the impact of initial pH on two freshwater microalgae species for carbon capture from industrial sulphur-rich and acidic flue gas. *Scenedesmus sp.* utilises nicotinamide adenine dinucleotide phosphate as an electron donor, whereas *C. vulgaris* relies on ferredoxin. pH fluctuations were found to impair enzymatic functions, thereby affecting microalgal growth. Optimising micro- and macronutrient availability, along with carbon supply, allows for precise control over microalgal biomass composition, enhancing its suitability for biofuel production. Harvesting efficiency was improved using ceramic microfiltration membranes to preconcentrate microalgae solutions before polymer-based harvesting. These membranes demonstrated species-specific performance, minimal fouling (mitigated through aeration), and effective permeate water reuse, facilitating sustainable cultivation cycles. A novel cationic polymer, poly(3-acrylamidopropyl) trimethylammonium chloride (PAPTAC), was synthesised and optimised for microalgae harvesting. PAPTAC achieved 90–99% flocculation efficiency across various species by leveraging charge neutralisation and bridging mechanisms, ensuring stable aggregation

without compromising biomass quality. It outperformed commercially available polymers, underscoring its potential for scalable and cost-effective applications. The thesis advances microalgae-based systems for greenhouse gas mitigation and biofuel production by optimising cultivation conditions, enhancing harvesting technologies, and promoting sustainable water reuse. Findings in this thesis work contribute to the development of cost-effective and environmentally sustainable microalgae applications.

CHAPTER 1. INTRODUCTION

1.1.Research background

Greenhouse gas emissions have increased significantly in the past decades. One of the major contributing factors is industrialisation, which creates critical environmental issues worldwide. While some industrialised nations have developed advanced emission control technologies, these solutions are often expensive. In contrast, many developing countries struggle to afford such technologies to mitigate their emissions. This problem also impacts neighbouring countries, as it can quickly spread across borders. Notably, pollutants like carbon dioxide (CO_2) and sulphur dioxide (SO_2) have severe health consequences when inhaled continuously over long periods.

Trees represent a sustainable solution for mitigating air pollution by converting toxic chemicals into beneficial products like oxygen and biomass. However, trees require arable land and take a long time to grow. Interestingly, most of the oxygen we breathe today is actually produced by microalgae.

Microalgae are autotroph organisms utilising light energy to synthesise various high-value bioactive compounds while capturing CO_2. Due to their fast growth rate and capability to survive in harsh environments, microalgae are currently applied in various industrial areas. Biomass from microalgae can be utilised for various applications, including biochemical production, animal feed, fertiliser, and biofuel. Microalgal cells are small (1–100 μm) and negatively charged, which allows them to maintain a stable colloidal suspension in water for photosynthesis. Despite their potential, the high cost of microalgae cultivation and harvesting is a major hurdle to industrial-scale microalgae cultivation and algae-based bioproducts. For example, during the cultivation process,

maintaining optimal growth conditions is critical. An imbalance in growth factors such as light intensity, nutrient levels, or CO_2 concentration can negatively affect the growth and productivity of microalgae. For example, an imbalance between nutrient supply and light intensity can reduce their capacity to capture carbon and alter their metabolic processes. This can cause stress, leading to cell damage or death. Understanding these basic principles is essential, as failure to control these factors can result in high costs to recover the system. Monitoring of cultivation conditions is necessary to ensure cost-effective production and achieve the desired byproducts.

Harvesting microalgae is another challenge, given the size of individual microalgae cells is several micrometres and negatively charged to a suspension in water. Harvesting is an important step in microalgal biomass production, serving as an essential link between the cultivation phase and downstream applications. One common method is centrifugation, which uses hydraulic pressure to separate microalgae cells from large volumes of water. However, this method is inefficient and expensive, with harvesting costs accounting for more than 50% of the total production cost of microalgae [1]. Additionally, the harvesting process can dictate the potential applications of the produced biomass. For example, nutraceuticals, cosmetic products, and food ingredients can be derived from microalgae; however, these uses may be inapplicable if the microalgae composition is damaged during harvesting. For instance, the centrifugation harvesting method uses physical force, which negatively impacts on the biomass composition and quality.

There have been several recent and dedicated works to develop efficient and cost-effective methods for harvesting microalgae. Among these methods, membrane filtration

and flocculation have shown the potential for efficient biomass recovery, low cost, and no secondary contamination. Membrane filtration for harvesting is an efficient method since it retains all intact cells while allowing nutrients to pass through to the permeate water. This permeate water is nutrient-rich water which can be used for further cultivation. However, the issue with membrane filtration is membrane fouling, where the microalgae cells clog the membrane pores and reduce the filtration efficiency. This will require frequent cleaning for maintenance or replacement and increase the total cost. On the other hand, in the flocculation process, a small amount of flocculants (usually cationic polymers) is added to the microalgae solution to neutralise the negatively charged individual cells and aggregate them for separation by gravity or air floatation [2]. It is essential to minimise the flocculant dosage, which can reduce the cost of flocculation harvesting [3].

This thesis aims to enhance the efficiency of an integrated microalgae system, focusing on capturing CO_2 and SO_2 methods, improving cultivation and harvesting methods, and promoting water reuse. This thesis explains the interplay between light intensity, CO_2 input, pH, and total carbon uptake to analyse the underlying mechanisms and maximise microalgae growth. This thesis also investigates the growth response to elevated sulphate concentrations and pH variation. Additionally, this thesis elucidates the interplay between carbon and nutrient input to achieve the desired microalgae biomass composition. Before harvesting microalgae biomass, this thesis evaluates ceramic membrane filtration to preconcentrate microalgae solution and recycle the permeate water for further microalgae cultivation. Furthermore, it explores a series of newly synthesised cationic polymers to determine the optimal dosage and UV power, comparing them to

commercially available flocculants. The findings of this study contribute to the development of efficient and inexpensive large-scale microalgae cultivation and harvesting.

1.2. Problem statement

Greenhouse gas emission, particularly CO_2, remains a serious problem. Microalgae have demonstrated the ability to absorb these pollutants, offering a potential solution. However, an efficient and cost-effective integrated microalgae system has not been systematically explored, and several technical challenges prevent its large-scale implementation.

The challenges include the techniques of introducing CO_2 into microalgae (such as using diffusers, spargers, and bicarbonate addition). The conventional technique of CO_2 sparging showed significant CO_2 loss to the atmosphere and unstable and limited mass transfer to the water phase. The growth response to elevated sodium sulphate concentration should also be analysed to optimise the system. The other challenge is the interplay between cultivation parameters, the interplay between nutrients to enhance lipids and protein, and the underlying mechanism, which has not been systematically discussed.

Additionally, cost-effective harvesting methods need further development, particularly regarding how to prevent membrane fouling during membrane filtration. There is also a need to explore methods for synthesising the flocculants and comparing their effectiveness across different microalgae species. Finally, the reusability of

permeate water after harvesting, as well as the quality of biomass, must be evaluated to understand the system's overall efficiency and impact.

1.3.Research objectives

This study aims to develop a comprehensive understanding of integrated microalgae systems. The project objectives are to:

- Elucidate carbon and sulphur metabolism by microalgae, specifically to describe the interplay between key parameters (such as light intensity, pH, feeding rate and duration), and analyses the underlying mechanisms.
- Demonstrate and evaluate ceramic membrane filtration to preconcentrate microalgae solution.
- Determine the flocculation efficiency of different types of flocculants and newly synthesised flocculants in freshwater and seawater microalgae.
- Determine the biomass quality and the reusability of water

1.4.Thesis outline

The structure of this thesis is schematically presented in Figure 1 The thesis consists of eight chapters, as outlined below. Chapter 1 introduces the research background, focusing on the role of microalgae as a sustainable solution for mitigating greenhouse gas emissions. Chapter 2 provides a comprehensive literature review, summarising the recent studies on microalgae and their biomass application. Chapter 3 explores methods to maximise microalgae growth rates by optimising CO_2 input and light intensity. Chapter 4 investigates and elucidates the growth response to elevated sulphate concentrations and pH variation on *C. vulgaris* and *Scenedesmus*. Chapter 5 focuses on

tuning carbon and nutrient ratios to optimise biomass yield and enhance lipid and protein production, contributing to microalgal resource valorisation. Chapter 6 evaluates microalgae enrichment processes for biomass harvesting and water reuse, highlighting their potential for resource recovery in environmental applications. Chapter 7 evaluates microalgae harvesting efficiency using cationic flocculants, particularly PAPTAC, as a sustainable and scalable approach. Finally, Chapter 8 concludes the key findings of the thesis and recommendations for future research and industrial applications of microalgae-based systems. This structured approach provides a clear progression from optimising microalgae growth to practical applications in biomass production and environmental management.

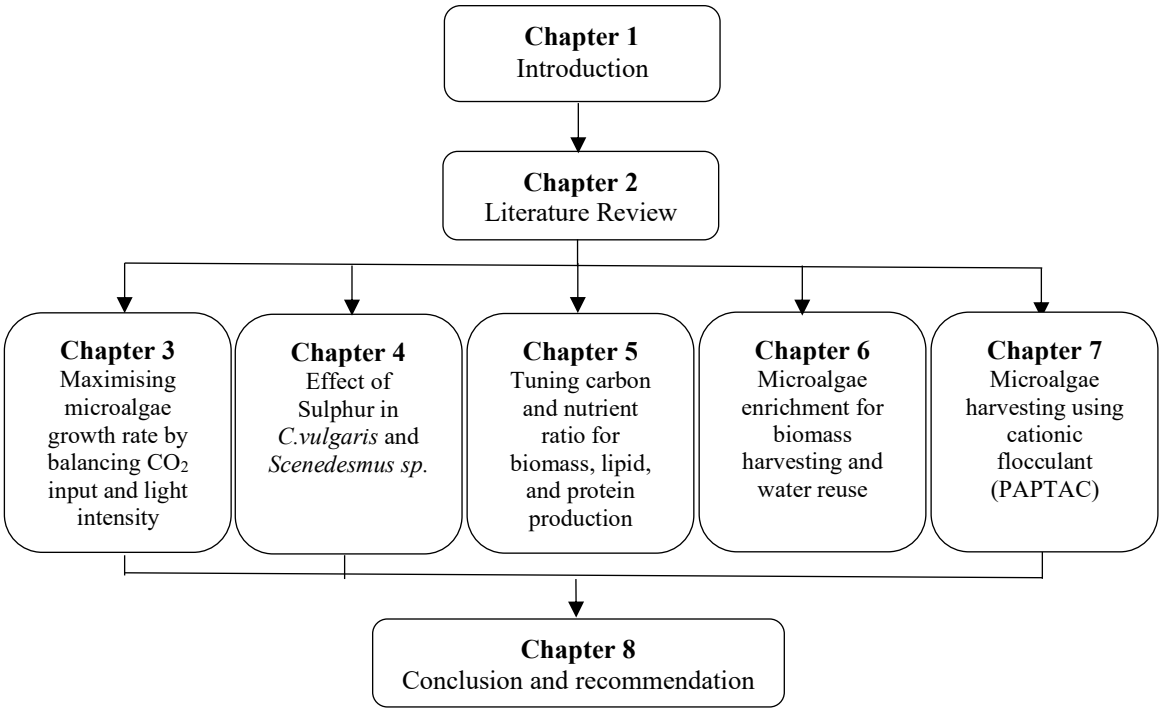

Figure 1. Schematic structure of the thesis

CHAPTER 2. Literature review

Part of this chapter has been published as the following journal article:

L Aditya, TMI Mahlia, LN Nguyen, HP Vu, LD Nghiem, Microalgae-bacteria consortium for wastewater treatment and biomass production. 2022. Science of The Total Environment 838, 155871.

2.1. Microalgae characteristics

Microalgae and photosynthesis bacteria (or *cyanobacteria*) can be found in all habitats, including water and sediment columns in freshwater and marine environments. Through photosynthesis, microalgae utilise energy from sunlight and CO_2 from the atmosphere. Then, it is used to synthesise biomass as a source of chemical energy for the overall ecosystem. Blue-green algae (or *cyanobacteria*) are strictly bacteria with photosynthesis capability. Thus, they function as microalgae in the ecosystem.

2.1.1. Pigment content and habitats

Colour is a convenient visual identification to classify microalgae. Most microalgae derive their primary colouration from *Chlorophylls* that are green. *Chlorophyll a* converts light (photons) to chemical energy. Other *Chlorophyll*s (e.g., *b, c_1, c_2,* and *d*) and *non-chlorophyll* pigments are accessory pigments to absorb a broader light spectrum. The energy is then transferred to *Chlorophyll a* for chemical energy conversion. Figure 2 shows the wavelength of light absorbance of several classes of microalgae. Carotenoids have yellow-red colours. Lutein and other primary carotenoids act as non-chlorophyll accessory pigments, while secondary carotenoids (astaxanthin and canthaxanthin) are important in cell defence processes. Primary carotenoids are tightly

tied to structural and functional components in the cellular photosynthetic machinery. By contrast, secondary carotenoids are produced in large quantities as oily droplets or a coating layer to protect microalgal cells from oxidative stress or intense illumination [4, 5]. Carotenoids are beneficial antioxidants to improve the immune system. Microalgae contain a much wider diversity of carotenoids than terrestrial plants. Microalgae are known to produce more than 40 type of carotenes and xanthophylls [6].

Phycobilin (e.g. Phycoerythrin, phycocyanin, and allophycocyanin) is another group of non-chlorophyll accessory pigment. Unlike chlorophyll and carotenoids, phycobilin is water-soluble. *Cyanobacteria* (or blue-green algae), glaucophytes, red algae, and cryptophytes can all generate phycobilin. Phycobilin absorbs light in the blueish to the red range, which is beyond the range of most chlorophyll. Phycoerythrin captures light energy and directs it to the reaction site through the phycobiliproteins and phycocyanin. Phycocyanin is used as a pharmaceutical agent because of its antioxidant, anti-inflammatory, neuroprotective, and hepatoprotective properties [7].

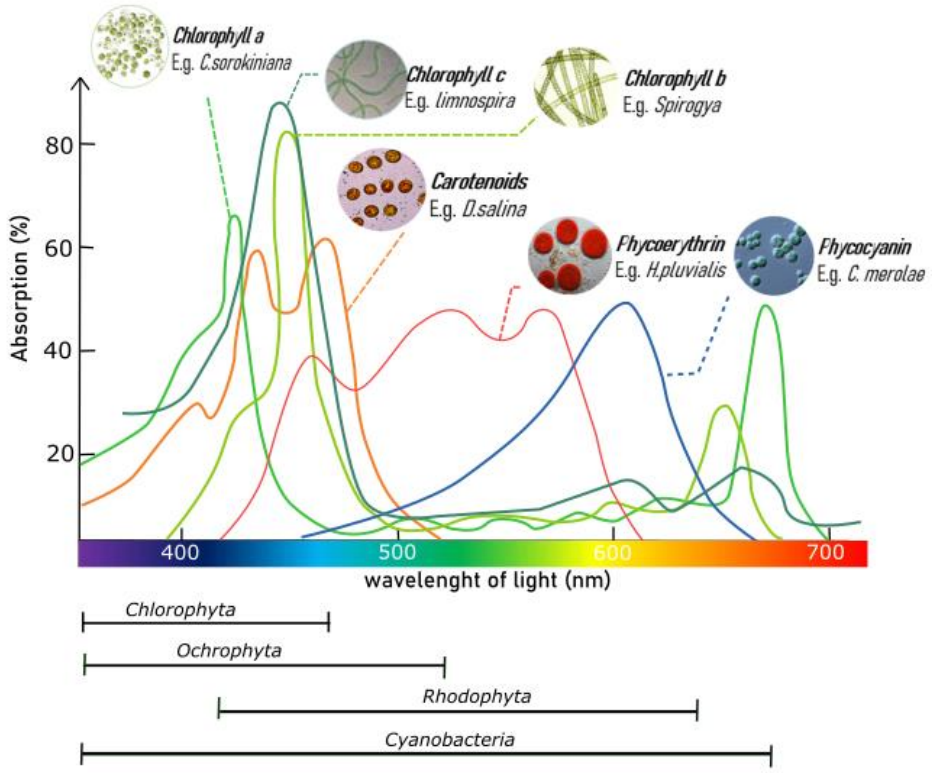

Figure 2. The microalgae pigment absorbance spectrum of light.

The production of microalgal pigments depends on environmental conditions. For example, low light intensity presents higher biomass pigment content. The light intensity of 27 mol photon/m^2/sec produced a chlorophyll content of 14.7 mg/g, while the light intensity of 54 mol photon/m^2/sec produced a chlorophyll content of 11.6 mg/g [4]. High salinity causes cell shrinkage and decreases the content of the pigment. The optimum temperature for *S. Platensis* chlorophylls and phycocyanin were 25 °C and 28 °C, respectively, while carotenoids remained reactive at up to 60 °C in *N. Gaditana* [8-10].

Bacteria do not carry out photosynthesis (with the exception of *cyanobacteria*), and thus, they can produce a broader range of pigments such as melanin, violacein, and prodigiosin. Melanin can potentially be used to visualise the in vivo interaction in the

consortia system. Melanised bacteria are also responsible for the anaerobic degradation of the organic compound trinitrotoluene in digested sewage [11]. Violacein toxin may protect microalgae from omnivorous grazers [12]. Despite the potential advantages of violacein pigment, its application for protecting microalgae cultivation still needs further investigation [13]. By contrast, prodigiosin is a natural algicide [14, 15]. Thus, bacteria producing prodigiosin pigment are not compatible with the microalgae-bacteria system.

Microalgae can thrive in both fresh and saltwater habitats. On the other hand, bacteria can only thrive mostly in a low saline environment. This is because some microalgae can regulate and exchange ions with the environment. Saline water microalgae contain more ion transporters for photosynthetic machinery, nuclear, organellar, and cellular membrane activities than freshwater species [16]. Saline water microalgae tend to have a high content of lysine, which is an amino acid for regulating ions in algal cells. In most cases, lysine content in saline water microalgae is double than in freshwater species [16].

2.1.2. Taxonomy

Microalgae can be either prokaryotic or eukaryotic microorganisms. Prokaryotic microalgae are essentially *cyanobacteria*, which can be strictly classified as bacteria. Eukaryotic microalgae include green algae (*Chlorophyta/Charophyta*), *Euglenophyta, Haptophyta, Dinoflagellates (Dinophyceae),* diatoms *(Bacillariophyceae), Eustigmatophyceae,* and red algae *(Rhodophyta).*

Cyanobacteria have *chlorophyll a* and complexes with light-activated enzymes. They are the only prokaryotic organisms that can undergo oxygenic photosynthesis.

Cyanobacteria can be found in some of the most hostile and strangest habitats. For instance, after Mount Krakatau's (Indonesia) volcanic activity, *cyanobacteria* (*Anabaena* and *Tolypothrix*) were observed at the surface of volcanic ash [17].

A notable example of the *Chlorophyta* phylum is *Chlorella*, which is spherical or ellipsoidal, with diameters ranging from 2 to 15 μm. It contains *chlorophyll a* and *b*, as well as starch for reserve material. Among *Chlorophyta*, *C. Vulgaris* is a highly utilised strain with high biomass production [18].

Euglenophyta is unicellular, motile, free-living microalgae typically found in freshwater. Due to the absence of *chloroplasts*, about two-thirds of *Euglenophyta* are *heterotrophic*. The energy storage product is arranged outside the *chloroplasts*. An example of this genus is *Euglena*. It has been recognised as a promising source of valuable biotechnological metabolites processes, like *paramylon*. [19].

The *Haptophyta* are primarily found in marine environments, with lower numbers found in freshwater and terrestrial environments. *Isochrysis aff. Galbana* is a well-known example of *Haptophyta*. Many are characterised by *calcite (calcium carbonate)* scales covering the cell (coccoliths).

Dinoflagellates (*Dinophyceae*) are unicellular *biflagellate* organisms that live in various habitats and are often found in ocean or brackish water. Only half of this taxa can carry out photosynthesis. The rest lives in symbiosis with reef-building corals and is critical in forming coral reef systems. An example of this genus is *Gonyaulax*. *Gonyaulax* belongs to red *dinoflagellates* and commonly causes red tides [20].

The diatoms or *Bacillariophyceae* organisms can be either unicellular or colonial. The wall of this genus is made up of two valves that overlap and are constructed with *silicon oxide*. The vast majority of diatoms species is benthic microorganisms. *P. Tricornutum* is the most well-known diatom [21].

The *Eustigmatophyceae* cells are *spherical* or irregularly shaped coccoid unicells. They grow individually, but they can also grow in a colony in some cases. *Nannochloropsis* is an example of a species that has drawn economic and academic interest due to its potential [22].

The red algae are a morphologically varied group that lives primarily in marine environments. These microalgae are spherical. They do not have flagella and can form loose colonies in a mucilaginous matrix. This genus species have arachidonic acid and pigments (phycobiliprotein and phycoerythrin) [23].

2.1.3. Growth forms

Microalgae tend to grow as individual cells a suspension, while bacteria tend to grow in colonies of aggregated cells as biofilm or aggregated flocs. Although less common, some microalgae can also grow in colonies, and some bacteria can grow as individual cells. Some microalgae can grow in a suspension to a certain size and then form a colony. Examples include *Collodaria, Chlorococcum sp.,* and *C. Meneghini*. *Collodaria* is unicellular microalgae that develop in single cells (up to 1 mm in size) or in colonies of a few centimetres in length [24]. *Chlorococcum sp.* Is a single green microalga that does not establish a colony [25]. *C. Meneghini* lives as solitary cells or in temporary groups of indefinite form without a mucilaginous envelope [26]. Colonial

forms are constructed from *mucilage* cells bound physically and connecting the cells. The method of colony development and the kind of colony creation is used to split joined cells by *mucilage* (Figure 3).

Cell division and cell adhesion are the two processes that allow colonies to develop. Cells in cell division stay connected after binary fission, while single cells in culture cling to each other in cell adhesion. The ratio of total biomass to cell number, growth rate, bound extracellular polymeric substances (bEPS), zooplankton effects, and species were all found to be significant variations between these two methods [27]. In the cell division process, the cell has an additional bound-extracellular polymeric substance surrounding the cells [28]. Meanwhile, no correlation was found between colony formation by cell adhesion. It can be interpreted that the adhesive polymers in the bEPS coating of a single cell can possibly be activated. Activation of this adhesion implies intercellular communication by a mechanism that has not yet been identified [27]. Cell adhesion and cell division mechanisms toward zooplankton resulted in different effects. The direct threat posed by zooplankton grazing leads to colony formation by cell adhesion. This response appears as a self-defence mechanism by microalgae cells because zooplankton has difficulties consuming the colonies [29, 30]. On the other hand, zooplankton filtrate causes colony formation through cell division [31, 32]. The distinction between cell division and cell adhesion is illustrated in Figure 3.

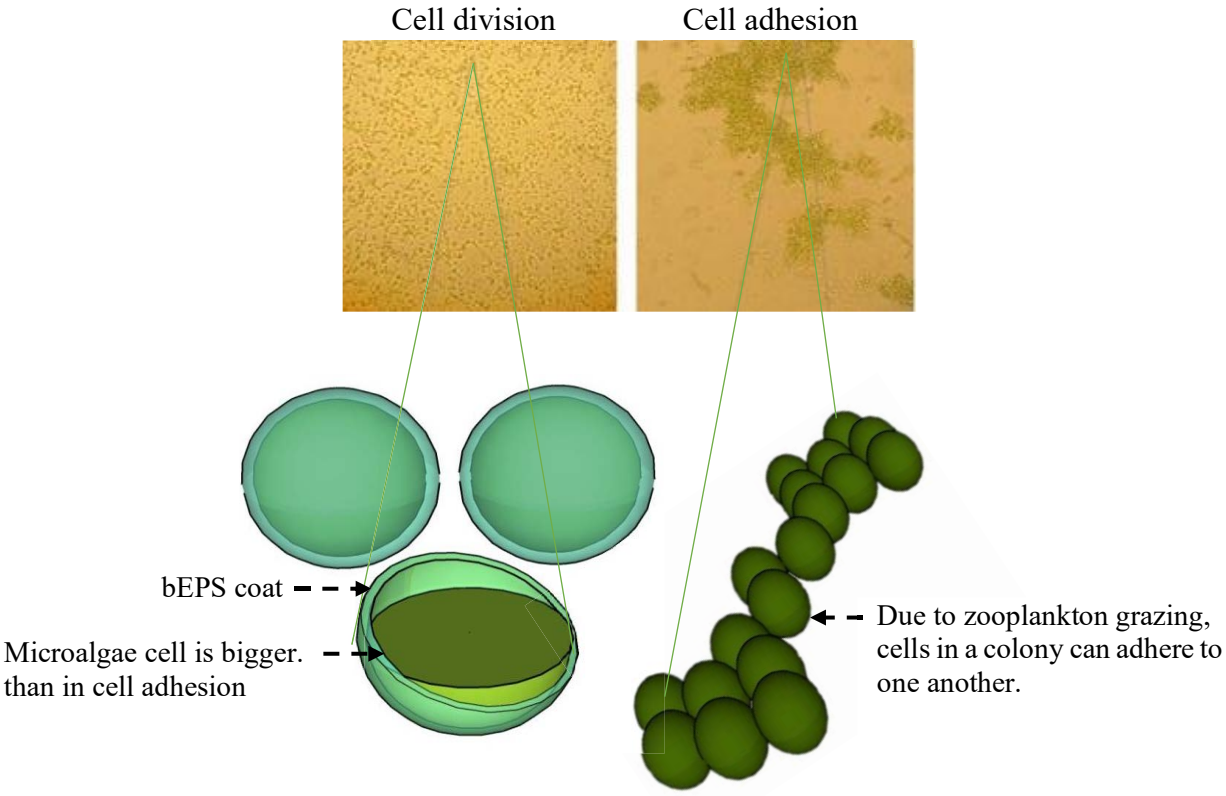

Figure 3. Cell division and cell adhesion mechanisms of microalgae colony formation.

The kind of microalgae species has an impact on the colony development process. For example, *M. Ichthyoblabe* colony formation is mostly based on cell division, while *M. Wesenbergii* colony formation is primarily based on cell adhesion [33]. It is possible that cell division and cell adhesion may be stimulated by either environmental stress or a direct danger. For example, colony formation in *M. Aeruginosa* was triggered by *Ochromonas sp,* the grazing zooplankton. When microalgae form larger colonies than single cells, zooplankton's ability to graze was diminished [34].

The type of colony formation can be divided into two types: *amorphous* and *coenobium*. In the *amorphous* colony, the cell number, size, or shape can vary. All cells

are independent and fulfil all functions of an individual. *Cyanophyta, Chlorophyta,* and *Rhodophyta* are the microalgae division belonging to this colony. *Coenobium* is a stalk, most of them can be found in *Chlorophyta* division, in which the cell has a structured arrangement with a specified number of cells. An exemplar of this conformation is in *S. Quadriculata* colon-forming. The strain may have 2, 4, 8, 16, or 32 cells arranged linearly inside the umbilicus, with lengths ranging from 8.2 to 9.6 μm and widths varying from 2.4 to 8.2 μm [35]. A new bacteria phenotyping technique allows the identification with an accuracy above 99.4%. This method can be used to examine the form of the colony in the microalgae-bacteria consortium system [36].

2.2. Microalgae-bacteria consortium for wastewater treatment

Wastewater discharge is a major pathway for nutrients (i.e. Phosphorus and nitrogen) depletion in ocean water [37]. Each year, around 1 million tonnes of phosphorus and 7.7 million tonnes of nitrogen are released into natural water bodies via wastewater discharge. It causes eutrophication and environmental degradation [38]. Microalgae based wastewater treatment can recover nutrients toward a circular bioeconomy [39-41]. To make microalgae work optimally and efficiently, the combination of internal and external parameters of microalgae should be explored. It includes every aspect from nutrient concentration ratio, percentage of CO_2 supply, the level of pH, the temperature of the growth medium, light intensity to metabolic engineering. Biochemical triggering is another way to stimulate microalgae metabolism. For example, phytohormones and substances, which modify biosynthetic pathways or function straightforwardly as metabolic precursors. Most of these growth-promoting substances can be generated by specific bacteria. A comprehensive understanding of the interaction between microalgae

and bacteria is essential to improve the treatment performance, such as increasing the total nutrition removal. Microalgae and bacteria interact in various ways, from symbiotic to competition (mutualism to antagonism). The interactions between microalgal and bacterial communities are based on energy and nutrition exchange, signal transduction, and gene transfer. Key interactions between microalgae and bacteria in the system are summarised in Figure 4.

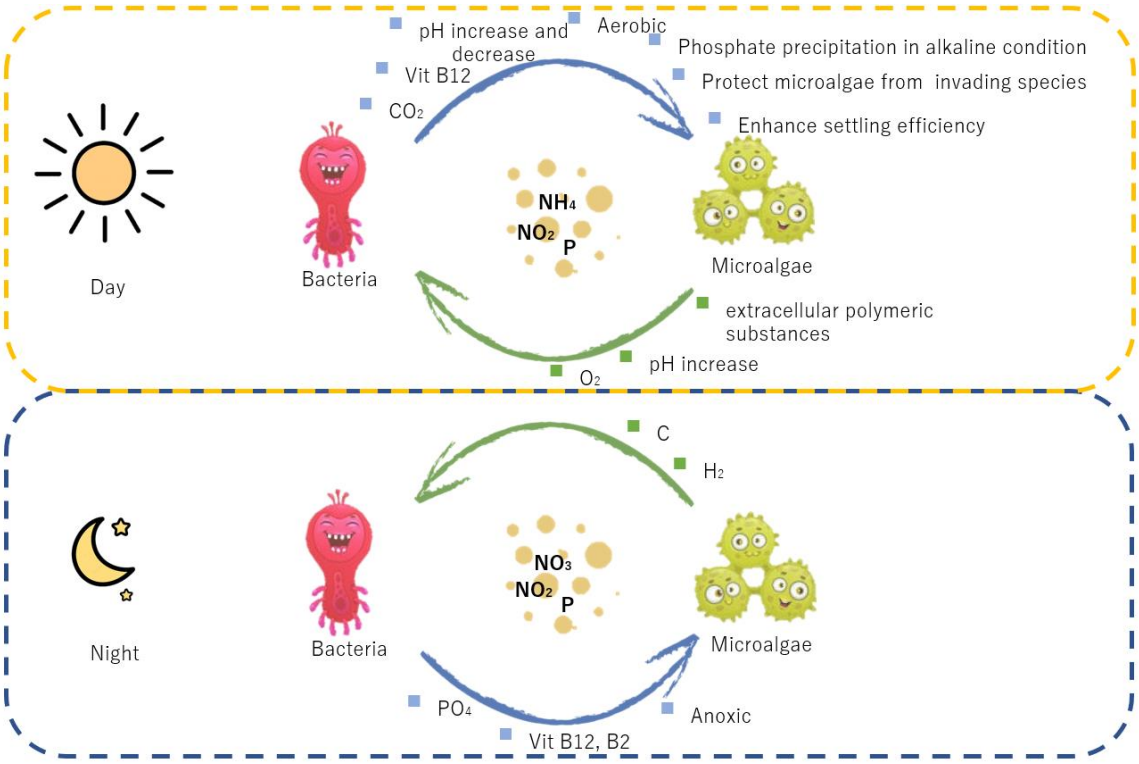

Figure 4. A generic framework for microalgae and bacteria interaction modalities

Figure 4 illustrates the exchange of carbon, energy, and key chemicals between microalgae and bacteria. For simplicity, Figure 4 is presented as a lagoon microalgae-bacteria system that is subjected to a day and night solar cycle. Several co-factors that are important for metabolic processes by microalgae and bacteria are shown in Figure 4. For example, microalgae produce O_2 for bacteria to utilise as an electron acceptor and energy

source to break down organic matter, while microalgae utilise CO_2 bacterial transpiration as the carbon source [42, 43]. The antagonism effect may also occur in a dark condition when microalgae compete for oxygen with bacteria for respiratory (conversion of biomass to energy when energy from photosynthesis is not available) and due to the decomposition of dead cells.

Vitamin B plays a vital role in the symbiotic relationship between microalgae and bacteria [44]. The bacterium *A. Brasilense* produces vitamin B_2 (riboflavin and lumichrome), plant growth stimulants during the fermentation process. These two substances impacted *C. Sorokiniana's* development and metabolism [45]. Vitamin B_{12} is produced by bacteria either in the aerobic or anaerobic pathways. Vitamin B_{12} helps control microalgae development and community composition. Photosynthesis by microalgae resulted in an increase in pH (daytime), whereas bacteria metabolism produces organic acid to lower the pH (nighttime).

Nitrogen removal by conventional wastewater is governed by a slow kinetic process involving two stages: nitrification by ammonia-oxidizing bacteria and denitrification by nitrite-oxidizing bacteria and denitrifying bacteria [46, 47]. Anammox is an alternative process that is faster and more efficient. Still, the anammox process itself cannot remove dissolved organic carbon and must also be integrated with a conventional wastewater process. On the other hand, microalgae assimilate nitrogen by using intracellular nitrate reductase enzymes, nitrate trans-membrane transporters, etc. The main advantage of the consortium system is the combined synergistic metabolism. Microalgae assimilate ammonia and produce oxygen through photosynthesis in the combined synergistic metabolism. Bacteria use oxygen to convert ammonia and nitrite

while secreting CO_2 [48]. In comparison to a single microalgae system, the consortium system removed 13.6% more ammonia, it was also 44% more than activated sludge systems [49]. This synergetic interaction also led to a rapid nitrification process [50]. To remove 60-80% of ammonia, the consortium system only required 1 to 2 days of hydraulic retention time, whereas pure-microalgae systems required 2 to 5 days [51]. Inadequate nitrogen leads to an antagonism effect (competition). It would lead to cell death and the release of intracellular ammonium [48, 49].

A microalgae-bacteria consortium system can use two distinct mechanisms for phosphorus removal: microalgae treatment after the enhanced biological phosphorus removal process and phosphate precipitation. In the microalgae treatment after the enhanced biological phosphorus removal process, the orthophosphate and CO_2 produced by bacteria can be converted to oxygen by microalgae [52]. Phosphate precipitation occurs during the daytime due to microalgae photosynthesis [53]. Microalgae photosynthesis changes the pH of the culture. Each nitrate ion creates one OH^- ion as it degrades to ammonia [54]. It allows bacteria to release algaecides. Algaecides have an antagonistic effect on microalgae, causing them to secrete extracellular polymeric substances. This situation encouraged the precipitation of phosphorus in extracellular polymeric molecules [55].

Most bacteria associated with microalgae enhanced microalgal bio-flocculation by producing polysaccharides or proteins, making the harvesting process more efficient and cost-effective [42]. Microalgae provide bacteria with organic carbon and oxygen, whereas bacteria provide fixed nitrogen, micronutrients and stimulate microalgal development [56]. On the other hand, microalgae can produce a wide range of inhibitory

compounds that can interfere with bacteria's growth. For example, microalgae can produce extracellular proteins such as dissolved amino acids and antibiotics, which inhibit bacterial growth [57]. By contrast, algicidal bacteria can produce harmful microbial substances like cellulase to disintegrate the cell wall of microalgae cells and lyse them [58, 59].

It is essential to select suitable species for the microalgae-bacteria symbiotic system. Some microalgae have a higher level of bacterial interaction than others—for example, the cell-to-cell exchange comparison of elements between the microalgae *P. Tricornutum*-bacteria and *N. Salina*-bacteria. In *P. Tricornutum*, 92-98% of cells were attached with bacteria and fixed 64% carbon, while in *N. Salina*, only 42-63% of cells had attached with bacteria and fixed just 10% carbon [60].

The nutrient removal efficiency comparison between an integrated microalgae-bacteria system and single microalgae is described in each type of wastewater origin section, namely domestic wastewater, industrial wastewater, agro-industrial wastewater, and landfill leachate. Studies on microalgae-bacteria interactions have mainly been conducted on the lab-scale since it is more restricted and less contaminated, and the results are easier to interpret. Table 1 summarises and compares nutrient removal and biomass production by a microalgae-bacteria consortium.

1 Table 1. Comparison of nutrient removal and biomass production by microalgal-bacteria consortium on various types of wastewaters (TN:
2 total nitrogen; TP: total phosphorus)

Wastewater type	Wastewater source	Microalgae	Bacteria	Initial concentration	Duration (days)	T (°C)	Nutrient removal efficiency	Biomass yield (g/L)	Biochemical composition	Ref.
Domestic wastewater	Beibei wastewater treatment plant, Chongqing	*Chlorella, chroococcus sp. And Scenedesmus sp.*	*Oscillatoria sp.*	NH_4^+-N: 40 mg/L PO_4^{3-}-P: 10 mg/L	8	22	NH_4^+-N: 99% PO_4^{3-}-P: 100%	1.5	Urocanic acid: 19.45 ± 2 μg/L	[61]
	Trento Nord treatment facility	*Chlorella and diatoms*	*Filamentous cyanobacteria* and heterotrophic bacteria	NH_4^+-N: 50 mg/L NO_3-N: 1.2 mg/L PO_4^{3-}-P: 2.8 mg/L	182	22.8	TN: 12.6 % TKN: 97% TP: 47%	~0.8	-	[62]
	Primary treated wastewater from University Rey Juan Carlos (Spain)	*C. Sorokiniana*	Activated sludge *(Rhodobacteraceae and Rhizobiaceae family)*	NH_4^+-N: 34.1 mg/L NO_3-N: 1.2 mg/L PO_4^{3-}-P: 4.9 mg/L	22	24	NH_4^+-N: 71.4% PO_4^{3-}-P: 68.3%	0.3	-	[63]
	Local WWTP in Kuala Lumpur, Malaysia	*S. Obliquus (17%)*	Activated sludge (83%)	TN: 26 mg/L TP: 6.2 mg/L	30	24	TN: 20% NO_3-N: 72%	9.3	-	[64]

							TP: 5%			
	LBZ municipal WWTP, Wuhan, China	*C. Sarokiniana,*	Activated sludge *(Nitrosomonas and Dechloromonas)*	NH_4^+-N: 25 mg/L PO_4^{3-}-P: 3 mg/L	30	25	NH_4^+-N: 98% PO_4^{3-}-P: 96%	2.5	-	[65]
Industrial wastewater	Textile Industry	*C.sorokiniana D BWC2,* *Chlorella sp*	*K. Pneumoniae ORWB 1, A. Calcoaceticus OR WB3*	NH_4^+-N: 119 mg/L NO_3-N: 110 mg/L PO_4^{3-}-P: 53.2 mg/L	7	30	TN: 71% PO_4^{3-}-P: 100%	0.67	-	[66]
	Textile Industry	Wild sample of a mixed algae	Wild sample of a mixed bacteria	TN: 74.1 mg/L TP: 86.4 mg/L	5	37	TN: 53% TP: 50%	0.1-0.5	-	[67]
	Vinegar production wastewater	*Chlorella sp*	*B. Fluminensis*	TN: 20.5 mg/L TP: 7.4 mg/L			TN: 78.7% TP: 74.8%	5.55	Notable effect on fatty acid composition rather than oil content	[68]
	Beer brewing factory	*C.vulgaris MACC360*	Native bacteria from sludge (beer brewing factory)	TN: 60 mg/L TP: 11 mg/L	3	24	TN: ~75% TP: ~75%	-	Total H_2 production: 65%	[69]
	Paper Industry	*C.sorokiniana D BWC2,* *Chlorella sp*	*K. Pneumoniae ORWB 1, A. Calcoaceticus OR WB3*	NH_4^+-N: 303 mg/L NO_3-N: 187 mg/L PO_4^{3-}-P: 77.7 mg/L	7	30	TN: 89.3% PO_4^{3-}-P: 100%	2.97	The yield of bio-crude oil: 15% (w/w)	[66]

	Leather Industry	*C.sorokiniana D BWC2,* *Chlorella sp*	*K. Pneumoniae ORWB 1, A. Calcoaceticus OR WB3*	NH_4^+-N: 89.9 mg/L NO_3-N: 162 mg/L PO_4^{3-}-P: 48.3 mg/L	7	30	TN: 55.6% PO_4^{3-}-P: 100%	0.48	-	[66]
Agro-industrial wastewater	Unsterilized palm oil mill effluent	*Scenedesmus sp.*	Anaerobic bacteria	TN: ~190 mg/L TP: ~142 mg/L	30		TN: 92% TP: 70%	-	*Actinomycetes* percentage increased	[70]
	Potato processing plant	*C. Sorokiniana*	*M. Capsulatus*	NH_4^+-N: 19 mg/L PO_4^{3-}-P: 14 mg/L	1	37	TN: 67% TP: 43%	0.21	32% carbohydrates 34.5% lipid	[71]
	Dairy wastewater from Gomati Cooperative Milk Producers' Union, India.	*Some of Chlorophyceae, C. Variabilis, P. Kessleri, P. Tricornutum, Chlamydomonas Synechocystis sp.,*	*T. Elongatus, M. Aeruginosa, Nostocales, Naviculales, Oscillatoriales, Stramenopiles, Trebouxiophyceae, Chroococcales, along with potential bacterial bioremediate*	NO_3-N: 139 mg/L NH_4^+-N: 16 mg/L PO_4^{3-}-P: 63 mg/L	14	25	NO_3-N: 93% NH_4^+-N: 100% PO_4^{3-}-P: 97%	-	18% protein 42% lipid 55% carbohydrates	[72]
	Dairy Farm wastewater	*C. Sorokiniana DBWC2* and	*K. Pneumoniae ORWB1* and *A.*	NO_3-N: 1730 mg/L PO_4^{3-}-P: 44 mg/L	7	30	NO_3-N: 84.7%	2.87	-	[73]

		Chlorella sp. DBWC7	*Calcoaceticus ORWB3.*				PO_4^{3-}-P: 100%			
	Piggery wastewater	*C. Vulgaris*	*R. Sphaeroides*	NH_4^+-N: 385 mg/L TN: 469 mg/L TP: 55 mg/L	7	28	NH_4^+-N: 100% TN: 95% TP: 96%	4.09	The combined content of carbohydrate, lipid, and protein was higher than 85%	[74]
	Piggery wastewater (20%)	*S. Almeriensis*	*Nitrospira,* and *Nitrobacter*	NO_3-N: 137 mg/L PO_4^{3-}-P: 26 mg/L	4		NO_3-N: 90% PO_4^{3-}-P: 100%		-	[75]
	Starch wastewater	*C. Vulgaris*	*R. Sphaeroides*	NH_4^+-N: 878 mg/L TN: 1492 mg/L TP: 154 mg/L	7	28	NH_4^+-N: 100% TN: 95% TP: 96%	0.96	-	[74]
Landfill leachate	20% Erin Landfill site, Chesterfield, UK	*C. Vulgaris*	*Nitrosomonas*	N-NH_3: 491 mg/L PO_4^{3-}-P: 320 mg/L	8		N-NH_3: 99.2% PO_4^{3-}-P: 100%	2-fold	Increased total organic carbon degradation	[76]
	10% lagoon in Nicosia	*Chlorophyceae species (Chlorella sp, Scenesdesmus sp,*	*Cyanobacteria (Microcystis sp, Oscillatoria sp),*	NH_4^+-N: 256 mg/L NO_3-N: 874.8 mg/L PO_4^{3-}-P: 97.5 mg/L	14	18	NH_4^+-N: 99.8% TN: 99.1 mg/L	-	The relative toxicity of the leachate was reduced in relation to the	[77]

		Stigeoclonium sp)					PO_4^{3-}-P: 98.8%		phenol removal.	
	Sandtown Landfill in Felton, DE.	Wild sample of a mixed algae	Wild sample of a mixed bacteria	NH_4^+-N: 5.1 mg/L	366		NH_4^+-N: 83%	-	-	[78]
	30% dumpsites landfill, Chennai, India	*C. Pyrenoidosa*	Bacterial nitrogen fixation	TN: 228.4 mg/L PO_4^{3-}-P: 31.6 mg/L	20	26	TN: 70% PO_4^{3-}-P: 89%	2.8	-	[79]

3

4

5

2.3.1. Domestic wastewater

Domestic wastewater is a nutrient-rich resource. The concentration of nutrients in residential wastewater varies depending on climate, socioeconomic conditions, and several other factors. Untreated domestic wastewater, on average, contains 59–653 mg/L of total nitrogen and 10-16 mg/L of phosphate [80, 81].

A key benefit of the microalgae-bacteria consortium system over a single system is higher efficiency and faster nutrient removal. The photosynthetic activity of *C. vulgaris* provided sufficient dissolved oxygen for nitrifying bacteria, which boosted the ammonia removal rate. Ammonium removal was mostly accomplished by nitrifying bacteria with support from microalgae. As a result, the ammonia removal rate was higher than algae and bacteria monocultures [82].

The other advantages of the consortium system are flocculation and aeration. An enclosed culture system of microalgae-bacteria to treat municipal wastewater had been reported by Foladori et al., [62] at a plant of 100,000 person equivalents in capacity at Trento Nord in Italy. Even though real wastewater had significant changes in influent concentrations, this microalgae-bacteria consortium maintained high and stable removal efficiency [83]. Furthermore, dense flocs might be produced by a combination of *Chlorella*, *Diatoms*, filamentous *cyanobacteria*, and heterotrophic bacteria. This system resulted in a self-sustaining therapeutic approach and may not necessitate extra aeration [83]. This behaviour differed significantly from wastewater treatment using pure *Chlorella.* Without adequate mixing, pure microalgae might settle to the bottom and gradually perish, impacting nutrient removal efficiency [84, 85].

Species selection must be considered for optimal performance. For example, *S. Obliquus* and activated sludge bacteria were utilised to treat local wastewater treatment

plants in Kuala Lumpur, Malaysia [64]. However, it could only remove 20% of total nitrogen after 30 days. Previous results suggest that *C. Sorokiniana* microalgae is more compatible with *Rhodobacteraceae and Rhizobiaceae* family than with the *Nitrosomonas or Dechloromonas* in activated sludge. The *C. Sorokiniana* and activated sludge *(Rhodobacteraceae and Rhizobiaceae* family) removed 98% of nitrogen and 96% of phosphorus within 7 hours [63]. While, *C. Sorokiniana* and activated sludge *(Nitrosomonas and Dechloromonas)* were only able to remove 71.4% of ammonia nitrogen in 14 days, since the microbial needed about 9 days to achieve steady-state condition [65]. This comparison indicated that species selection is one of the prerequisites for the effectiveness of treatment, and each species has a different survival rate. The species selection is also important for obtaining the required biomass quality for further use.

2.3.2. Industrial wastewater

Microalgae-bacteria remediation of industrial-derived wastewater is an alternative treatment method for removing nutrients with reduced chemicals and energy consumption. Industrial wastewater can have a high concentration of specific contaminants. Thus, an axenic (pure) microalgae culture system may not be sufficiently resilient to thrive in industrial wastewater [86]. Factors such as extreme pH and toxicity from specific contaminants in industrial wastewater can inhibit an axenic microalgae system. In the microalgae-bacteria consortium system, the bacteria could support the microalgae. For example, microalgae used bacteria-produced siderophores as iron replacements in iron-deficient environments. Gaseous exchange (CO_2-O_2) between microalgae and bacteria also helps the consortium to be more resilient to unfavourable environmental conditions [66]. The microalgae-bacterial consortium was also more

compact than the combination of each individual system [68]. Their interconnections can share metabolites and the ability to endure periods of nutrient limitation, combating invasion by other species and maintaining microorganism stability, providing robustness to environmental oscillations.

2.3.3. Agro-industrial wastewater

Agro-industrial wastewater tends to have higher nitrogen and phosphorus concentrations than domestic wastewater [70, 72, 73]. Botanical food processing effluent differs depending on the fruit or vegetable used—for example, palm oil mill effluent (POME) wastewater was treated with three native microalgae (*Coelastrella sp*. UKM4, *Chlamydomonas sp.* UKM6, and *Scenedesmus sp.* UKM9) [70]. The raw POME contained *Actinobacteria, Bacteroidetes, Planctomycetes, Firmicutes* and *Proteobacteria*. Over 80% of nitrogen was removed from both sterilised and raw POME. A sterilised POME could only remove 10% of the phosphorus, whereas a raw POME could remove up to 70% [70]. Bacteria were eliminated in the sterilised POME, which explained the 60% difference in phosphorus removal efficiency. Botanical food processing wastewater is the most environmentally friendly, and it may be utilised as fertiliser, animal feed, and biofuel. The biomass of *P. Purpureum* that flourished in POME was rich in essential minerals, including Fe, K, and N. These are crucial nutrients for plant development. Thus, this biomass was appropriate for conversion to biofertilizer [87]. After sage and potato processing wastewater treatment, the consortium biomass could be used as animal feed [71, 88]. The biomass from coffee processing effluent boosts methane yield by up to 87% and could be easily converted into biofuel [89].

Dairy wastewater tends to have higher nitrate content than most other wastewater [72, 73]. Pure microalgae work slowly on this type of wastewater [90, 91]. It is possibly

because the ratio between nutrients was insufficient for its metabolism. The pure microalgae culture could only remove about 65% of nitrate (from the initial concentration of 62.7 mg/L) after 6 days of treatment [92]. On the other hand, the microalgae-bacteria consortium removed more than 85% of 1730 mg/L [73]. The presence of nitrate-reducing bacteria helps higher nutrient removal. The lipid content of the microalgae-bacteria consortium biomass was more than 45%. This could be due to the nitrogen present mostly in the form of amino acids. It also had a high lactose content. Overconsumption of lactose would be stored as fats. This biomass is a viable candidate for protein supplements for animal feed, biofertilizers and defatted biomass as feedstock for bioethanol production [93, 94].

S. Almeriensis, *Nitrospira,* and *Nitrobacter* removed 90% nitrogen from animal effluent in 2 days [75]. In contrast, pure microalgae (*Scenedesmus sp.*) Required 9 days to remove 83% of nitrogen [95]. The addition of bacteria to the system improved nutrient removal and duration efficiency. However, ammonium toxicity is the main drawback of microalgal growth in piggery wastewater [74]. Pre-treatment, such as dilution, filtration, and the addition of chemical solutions, is required to minimise the high-strength ammonium. An integrated system can help build a circular economy in the future. The process begins with the nutrient-rich faeces from animals treated using anaerobic digestion and microalgae. The microalgae biomass are then harvested and fed to the animals [96].

2.3.4. Landfill leachate

The main components of landfill leachate, which may harm the environment, are ammonium toxicity and xenobiotics [77]. Microalgae could be killed immediately if ammonia concentrations exceed 80 mg/L [97]. Due to their high toxicity, lengthy

persistence, and low biodegradability, many xenobiotic chemicals negatively influence microalgae. The addition of denitrifying bacteria and phenol-degrading bacteria aided the microalgae's adaptation. The denitrifying bacteria consume nitrogen, whereas microalgae consume phosphorus. As a result, the removal efficiency was higher than pure microalgae treatment [76, 98].

In recent decades, the landfill leachate has been diluted to be treated effectively. Landfill leachate has high turbidity and thus low light penetration. A novel tubular photo-bioreactor using a rotating optical reflector has been proposed by Porto et al. (2021). This technique improved removal efficiency by over 21% compared to conventional photo-bioreactors [98]. The summary comparison of the consortium and pure microalgae system can be seen in Table 2.

Table 2. A comparison of the culture efficacy for wastewater treatment of microalgae and a microalgal-bacteria consortium.

Parameter	Pure microalgae treatment	Microalgal-bacteria consortium treatment
N removal (of 40-50 mg/L NH_4^+-N)	58% [99]	99% [61]
P removal (of 60 mg/L PO_4^{3-}-P)	10% [70]	70% [70]
Dissolved oxygen (mg/L)	< 3 [70]	< 2 [70]
Duration (to remove >83% of 137 mg/L NH_4^+-N)	9 days [95]	2 days [100]
Biomass production	2 fold [70]	4 fold [70]
Lipid productivity	17% [101]	42% [72]

Operation cost	Need additional aeration and More space because the water level must be maintained below 15 cm [84]	Costless (may not necessitate extra aeration) [83]

2.3. Microalgae-bacteria consortium biomass utilisation

Biomass from the microalgae-bacteria consortium can be utilised for various applications, including biochemical production, animal feed, biofertilizer, and biofuel [40, 102, 103]. The cultivation process ultimately dictates potential applications of the produced biomass. Nutraceuticals, cosmetic products, and food ingredients can be made from microalgae; however, these applications are unsuitable for a consortium system due to wastewater input and the bacterial component. Thus, only compatible applications are discussed below when considering the type of microalgae for each desirable end-product.

2.3.5. Biochemicals

Microalgae can be an excellent source of biochemicals, given the high content of lipids, carbohydrates, proteins, and other specific biochemicals. Some microalgae contain up to 40% of their overall mass in fatty acids, such as *C. Reinhardtii* 49.9% [104] and *I. Galbana* 47% [105]. These fatty acids might be used for nutritional and therapeutic purposes [106]. *C. Stigmatophora* (~55%) and *C. vulgaris* (>52%) are examples of microalgae with high carbohydrate contents [107]. Carbohydrates from microalgae, apart from alcohol, could be converted to bioplastic and can be produced using wastewater [108]. *Cyanobacteria* also produce *exopolysaccharides* which could be utilised as a gelling agent, thickening, stabilising agent, bio-lubricants, and anti-inflammatory agents [43, 106]. Protein in microalgae is generally found in the form of amino acids. *S. Maxima* and *S. Platensis* had all the necessary amino acids in quantities acceptable for diabetes

and obesity treatment [109, 110]. *Cholecystokinin* may be activated by proteins from microalgae or plants, which can lower cholesterol levels. They also play an important role in the human enzymatic process [104]. Figure 5 compares the biochemical composition of common microalgae strains [111-114].

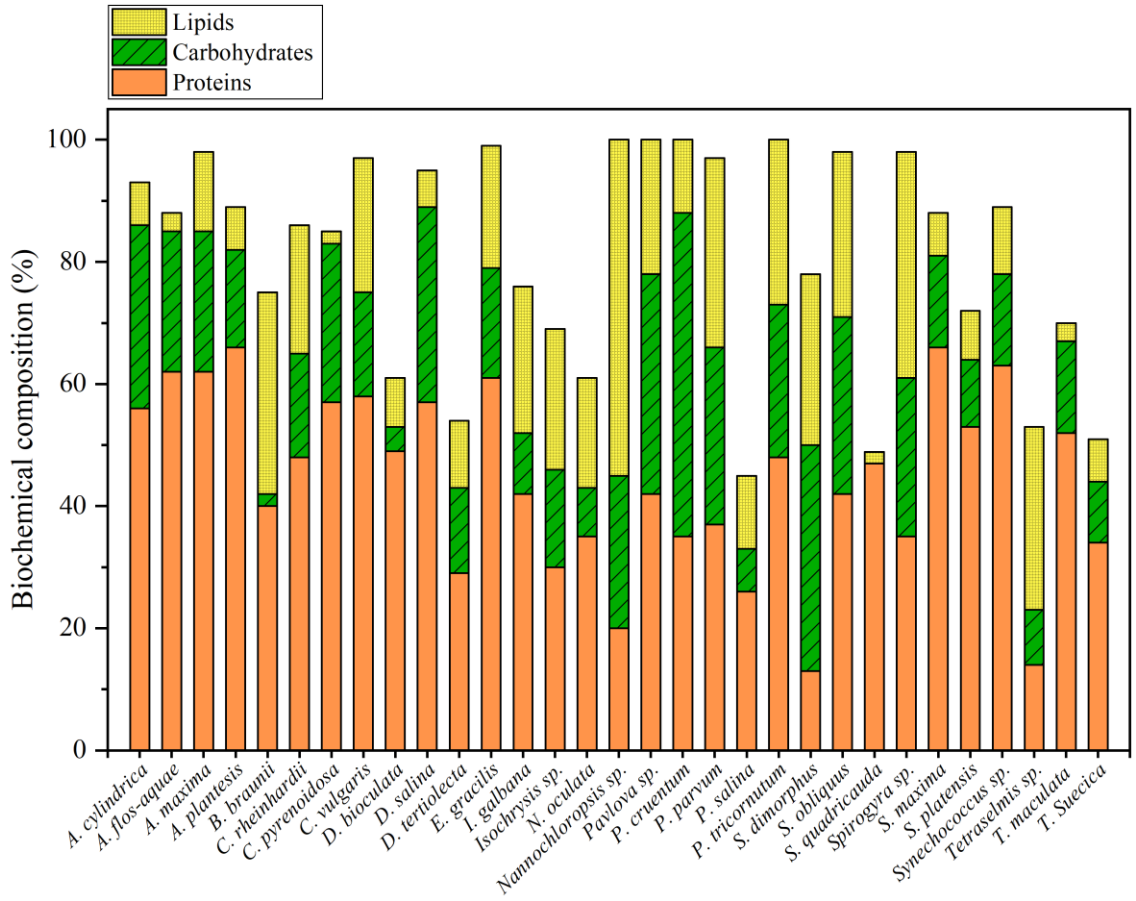

Figure 5. Macromolecule organic compounds composition in common microalgae.

Adding bacteria to microalgae culture changes the biochemical composition significantly. Microalgae-bacteria consortium of *A. Brasilense Cd* and *A. Protothecoides UTEX 2341* improved the protein up to 40-60% [115]. The consortium system of *M. Capsulatus* and *C. Sorokiniana* enhanced carbohydrates by 42% and lipid by 15% [71]. The pigment levels also increased rapidly [116]. However, due to the interaction with

bacteria, the lipid enhancement could be in the form of extracellular polymeric compounds.

2.3.6. Animal feed

Microalgae is a treasure trove for dietary supplements for aquaculture and live stocking. For instance, feeding ornamental goldfish (*Carassius auratus*) with microalgae had improved colouration [117]. *Nannochloropsis sp.* Used in finfish hatcheries had showed enhanced DPA/EPA levels. When poultry birds (chickens, ducks, turkeys, and quail) were fed microalgae, their body weight rose dramatically [118-120]. When chickens were given *H. Pluvilais, N. Gaditana*, and *Spirulina sp*., they had more muscle pigmentation, antioxidant components in the liver, and carotenoid colouration in egg yolks [121]. Astaxanthin is a red pigment that contains antioxidants and other health advantages [122]. It helps treat various cancers, prevent heart disease, and many others. Astaxanthin is found in many sea species, such as lobsters, salmons, shrimps, and crabs. In fact, sea species such as wild salmons have pink flesh as they eat plankton containing astaxanthin. Farmed salmon has a light flesh which is appealing to customers. In the past, synthetic astaxanthin was fed to farmed salmon to recreate the natural pink colouration similar to wild fish. Synthetic astaxanthin contains impurities that may pose a health problem to the consumers; thus, they are banned in several countries such as Australia and New Zealand. Here, the *H. Pluvialis* microalgae can offer a perfect solution to farmed salmon. They offer a natural source of astaxanthin to farmed salmon. They were 90 times more effective at providing the pink colour to salmon flesh than synthetic astaxanthin without any toxicity effect. Additionally, the microalgae-bacteria consortium system can produce stronger aromas than pure culture, enhancing its attractiveness as a feed for animals [123]. The consortium system, however, frequently occurs in flocs. Hence, using

such flocs as feed could harm the animals' health by obstructing shrimp gills and even cause death. Agro-industrial wastewater is the most suitable wastewater for producing animal feed using the microalgae-bacteria consortium.

2.3.7. Biofertilizers

Microalgae cultivated in wastewater can be used as a biofertilizer or soil additive [124]. Soil nitrogen and phosphorus levels and several other plant-required trace elements (Ca, K, Fe, and Mn) can be improved by microalgal biomass. When combined with soil phosphorus solubilising organisms, microalgal fertilisers exhibited a greater phosphorus release in non-sterile soil [125]. The biomass derived from landfill leachate can be directly converted into biofertilizer. The biomass should be blended with palm oil to be used as a biofuel, since this biomass contains low monounsaturated acids [77].

Microalgae (including *cyanobacteria*) application to tomato plants showed a considerable increase in the biochemical and metabolomics connected to the plant's defence systems [126-128]. Another research found that utilising filamentous microalgae strain as bio-fertilizers enhanced the dry weight of wheat plants by 30% and its biochemical composition [129, 130]. The symbiotic system between microalgae and bacteria can easily transform organic and inorganic chemicals into plant-digestible molecules, making them efficient biofertilizers [131].

2.3.8. Biofuel

It is widely accepted that the third generation of biofuel is a fuel produced from microalgal biomass. Microalgae cultivation does not compete with the production of food on arable land. Microalgae grow much faster than land-based energy crops and can double their biomass within a few hours [132]. Microalgae lipid yield is 15–300 times greater than traditional oil crops, and since it is an aquatic plant, it does not compete for land with

food crops [133]. Around 0.7–30.6% of free fatty acids and 4.1–77.5% of triglycerides were contained in microalgae lipid [134, 135]. Microalgae also contain unsaponifiable matter (0.4–20.9% of hydrocarbons, 0–83.2% of phytol, and 7.8–90.0% of sterols) and *Chlorophyllides* (5.8–16.8%) [135]. This unsaponifiable matter can be readily converted to biodiesel and aviation fuel [136, 137]. Biodiesel production from microalgae to blend with or completely replace jet fuel has been demonstrated in recent years [137]. The addition of bacteria can double lipid content and productivity by the *indole-3-acetic acid* released by plant growth-promoting bacteria [49]. The high lipid content may also relate to nutritional deficiency caused by microbial competition between microalgae and bacteria. This technique is advantageous for large-scale biofuel production [72]. Domestic wastewater is a viable option for microbial biofuel production since it can be grown continuously on a large scale.

Sustainable aviation fuel from microalgal lipids can be produced by transesterification and hydro-processing. The lipid quality depends on microalgae strains. For example, *T. Maculata* had a less than 4.5% total lipid concentration. In contrast, *Schizochytrium sp.* Had a total lipid content of more than 80% [136], The unmodified biofuel *Chlorella sp. NT8a* could meet several aircraft fuel standards [137]. The current method of converting microalgae to jet fuel costs 2 to 8 times more than regular jet fuel. Although several technological innovations have been created, they have not been able to significantly reduce the aviation industry's carbon footprint [138, 139]. In the future, proper planning optimisation and simulation are required to reduce operational expenses. Immediate reductions can be achieved via improving multi-stakeholder collaboration, including biofuel producers, aircraft manufacturers, operators, and the government.

2.4.Summary

Data corroborated from this review highlights the potential of the microalgae-bacteria consortium for wastewater treatment and nutrient recovery. The review consolidates the current understanding of microalgae characteristics and their interactions with bacteria in a consortium system. Microalgae and bacteria can thrive in a variety of conditions, and interact in various ways, from mutualism to parasitism. This review discusses the comparison of recent studies on the practical implementation of pure and consortium systems in various wastewater treatments (domestic, industrial, agro-industrial, and landfill leachate wastewater). It highlights the ability of a microalgae-bacteria consortium to utilise nutrients from wastewater and produce valuable microalgae-based products. This review also discusses the potential of wastewater-derived microalgal biomass as a promising feedstock for animal feed, biofertilizers, biofuel, and many valuable biochemicals. The applications of wastewater-derived microalgal biomass are discussed, and examples are presented in this study. This review also examines major challenges and future developmental research recommendations.

CHAPTER 3. Role of culture solution pH in balancing CO_2 input and light intensity for maximising microalgae growth rate

Part of this chapter has been published as the following journal article:

L Aditya, HP Vu, MAH Johir, TMI Mahlia, AS Silitonga, X Zhang, Q Liu, L.D. 2023. Role of culture solution pH in balancing CO_2 input and light intensity for maximising microalgae growth rate. Chemosphere 343, 140255.

3.1. Research objectives

This study aimed to maximise the CO_2 capture by microalgae and to elucidate the interplay between light intensity and CO_2 input to maximise microalgae growth rate and CO_2 uptake. The effects of light intensity and CO_2 concentration in the culture solution on microalgae growth were systematically assessed and delineated. This study also examined the relationship between four key parameters, namely growth rate, solution pH, CO_2 uptake, and organic carbon release, to reveal physiological mechanisms underlying the interplay between light intensity and CO_2 input. New insights from this study could be used to guide the design and intensification of photobioreactors for water treatment, microalgal biomass production, and CO_2 fixation.

3.2. Material and method

The freshwater algal strain *Scenedesmus* sp. (UTS-LD) isolated by the University of Technology Sydney was used in this study. Stock culture was maintained at the Algae Production Facility at the University of Technology Sydney, using MaxiGro as the growth medium. This *Scenedesmus* sp. (UTS-LD) is a fast-growing strain of green algae and has been described in detail in a previous study [140].

The *Scenedesmus* sp. (UTS-LD) was cultivated in a series of 10 L enclosed transparent plastic carboy reactors with platinum-cured silicone screw caps (Figure 6). The cap had two access ports. Two flexible tubes were inserted into these ports under airtight conditions, one was used to deliver the liquid with a peristaltic pump, and the other was used for sample collection. A Masterflex Peristaltic pump (Cole-Parmer, USA) was used to supply microalgae feeding medium and carbonated water. The reactors were placed on a magnetic rotary stirrer at 750 rpm for mixing. The reactors were continuously illuminated by Arlec LED strip (ALD1042) lights with the light on for 14 hours and dark for 10 hours. An Aarke carbonator machine equipped with a PET bottle was used to produce carbonated water of up to 850 mg/L of CO_2 in concentration.

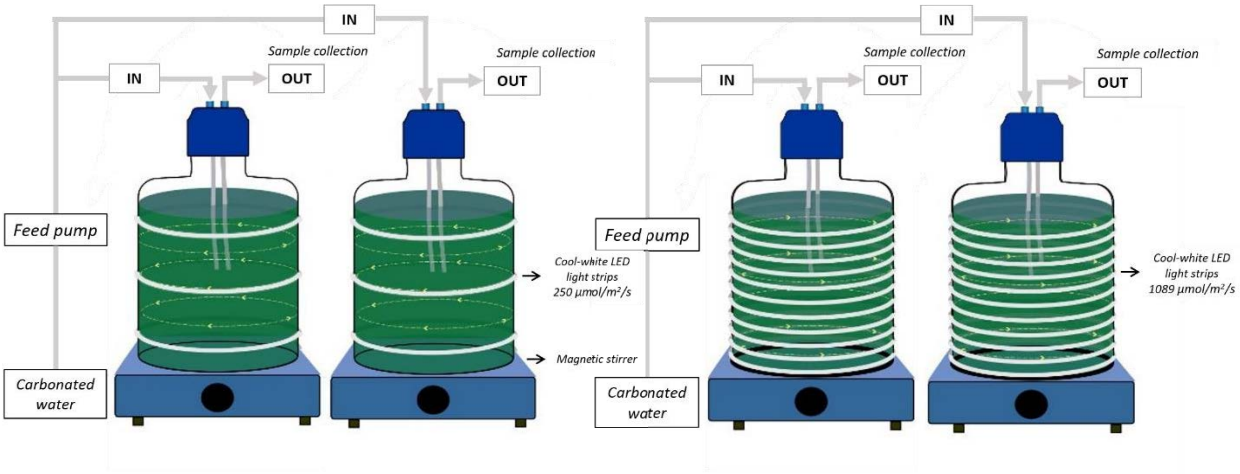

Figure 6. The schematic diagram of *Scenedesmus sp.* Cultivation in 10 L reactor.

Preliminary experiments were conducted to determine suitable techniques to introduce CO_2 to the cultivation solution and the range of key parameters such as feeding rate. The conventional technique of CO_2 sparging showed significant CO_2 loss to the atmosphere as well as unstable and limited mass transfer to the water phase. By contrast, introducing CO_2 to microalgae cultivation via carbonated water produced more reliable

results. In addition, CO_2 loss can be eliminated using enclosed photobioreactors. Thus, carbonated water was used to introduce CO_2 to the microalgae solution in this study. The range of CO_2 concentration in carbonated water and rate of carbonated water have been optimized based on preliminary experimental data.

All cultivation experiments were started at the same microalgae biomass concentration of OD_{680} of 0.1 (corresponding to 0.08 mg/ml). Light intensity was set to specific values at 250 and 1089 µmol/m^2/s. Either MaxiGro (General Hydroponics, USA) or Cell Hi F2P (Fresh by Design, Australia) was used as the cultivation media and was added to the carbonated water at 0.4 and 0.5 g/L, respectively.

The photobioreactors were kept in an air-conditioned room to maintain cultivation solution temperature at 25 °C. Every day, 50 ml of sample was withdrawn from each replicate reactors for determining the biomass concentration, pH, inorganic carbon, and total organic carbon. All experiments were performed for 14 days. Carbonated water was supplied to the photobioreactor in two different modes: (1) intermittent CO_2 transfer every 2^{nd} day and (2) continuous CO_2 transfer. In mode 1, carbonated water was transferred to the photobioreactor at 0.6 ml/min for 24 hours (first day) and no CO_2 was transferred to the photobioreactor on the second day. This cyclic pattern allows for a high CO_2 transfer rate and time for the microalgae culture to uptake the dissolved CO_2. In mode 2, carbonated water was continuously transferred to the photobioreactor at 0.6 ml/min. In both modes of operation, CO_2 concentration of the carbonated water was in the range from 30 to 850 mg/L.

The concentration of microalgal biomass was evaluated by measuring optical density (OD) after establishing a connection between dry biomass content and OD as stated in a previous study [19]. The OD of the microalgal solution was measured with a UV spectrophotometer (UV 6000 Shimadzu; Australia) at a wavelength of 680 nm in a

Quartz Glass Cuvette. The dry weight was determined by filtering 100 ml of microalgae solution through a 1.1 μm glass filter paper. The filter paper was then oven-dried for 24 hours at 60°C. The pH was measured using Hach HQ40d Multi Portable Multi-Probe Meter. Light intensity was measured using a LI-250A Light Meter equipped with a quantum sensor LI-190SA. Inorganic and organic carbon content of the cultivation solution was measured using a multi-N/C UV TOC analyser Analytic Jena. The carbon fixation rate is calculated using the following equation based on biomass production and biomass carbon content:

$$R_{CO_2} = \frac{44}{12}(C_F + C_i - C_{i+1})\,(B_{i+1} - B_i) \quad (1)$$

Where R_{CO_2} Is the carbon fixation rate (mg/L.d); C_F Is the carbon content in supplied carbonated water (g/L); C_I Is the initial carbon content in microalgae solution (g/L); C_{I+1} Is the carbon content in microalgae solution the following day (g/L); 44 is the molecular weight of CO_2; 12 is the molecular weight of carbon; B_I Is the initial biomass dry weight (mg/L/d); B_{I+1} Is the biomass dry weight in the following day (mg/L/d). The microalgae biomass dry weight was calculated considering a volume increase of 28.8% per day.

3.3. Result and discussion

3.3.1. pH regulation to optimise carbon fixation

Biomass production is governed by CO_2 concentration of the culture solution and light intensity in all experiments. Microalgae growth rate increased as CO_2 concentration and light intensity increased. Importantly, the results also show the need for balancing CO_2 input between light intensity. CO_2 is an acidic gas; thus, the dissolution of CO_2 causes a decrease in pH. On the other hand, photosynthesis consumes proton to result in

an increase in pH [141]. In the microalgae system, photosynthesis is mediated by rubisco enzyme, which has an active range between pH 6 and 10 [142, 143]. Beyond this pH range, photosynthesis by microalgae can be inhibited. Thus, the balance between CO_2 addition and light intensity is critical for regulating the culture solution pH, which in turn governs biomass growth and CO_2 uptake.

Compared to continuous transfer, intermittent CO_2 transfer resulted in half of the CO_2 input to the culture solution as described in section 2.4. However, intermittent CO_2 transfer (Figure 7A and Figure 7C) shows higher biomass production compared to continuous CO_2 transfer (Figure 8A and Figure 8C). The difference in microalgae growth rate is due to CO_2 accumulation and acidification of the culture solution, affecting the efficiency of biomass production by microalgae. Results from Figure 8 suggest that excessive CO_2 input to the culture solution is counter-productive against microalgae growth [144, 145]. On the other hand, with intermittent CO_2 transfer, the culture solution pH can be adjusted to a balanced value for optimum microalgae growth (Figure 7).

At above pH 10, rubisco enzyme denaturation can occur, causing microalgae to aggregate [142, 143, 146]. This is evidenced when high light intensity 1089 μmol/m^2/s was used (Figure 2B). The microalgae culture solution pH increased to above 10, and agglomerated cells were observed on day 14. The results from this study indicate that the alkalinisation of microalgal solutions is due to cellular H^+ assimilation [147].

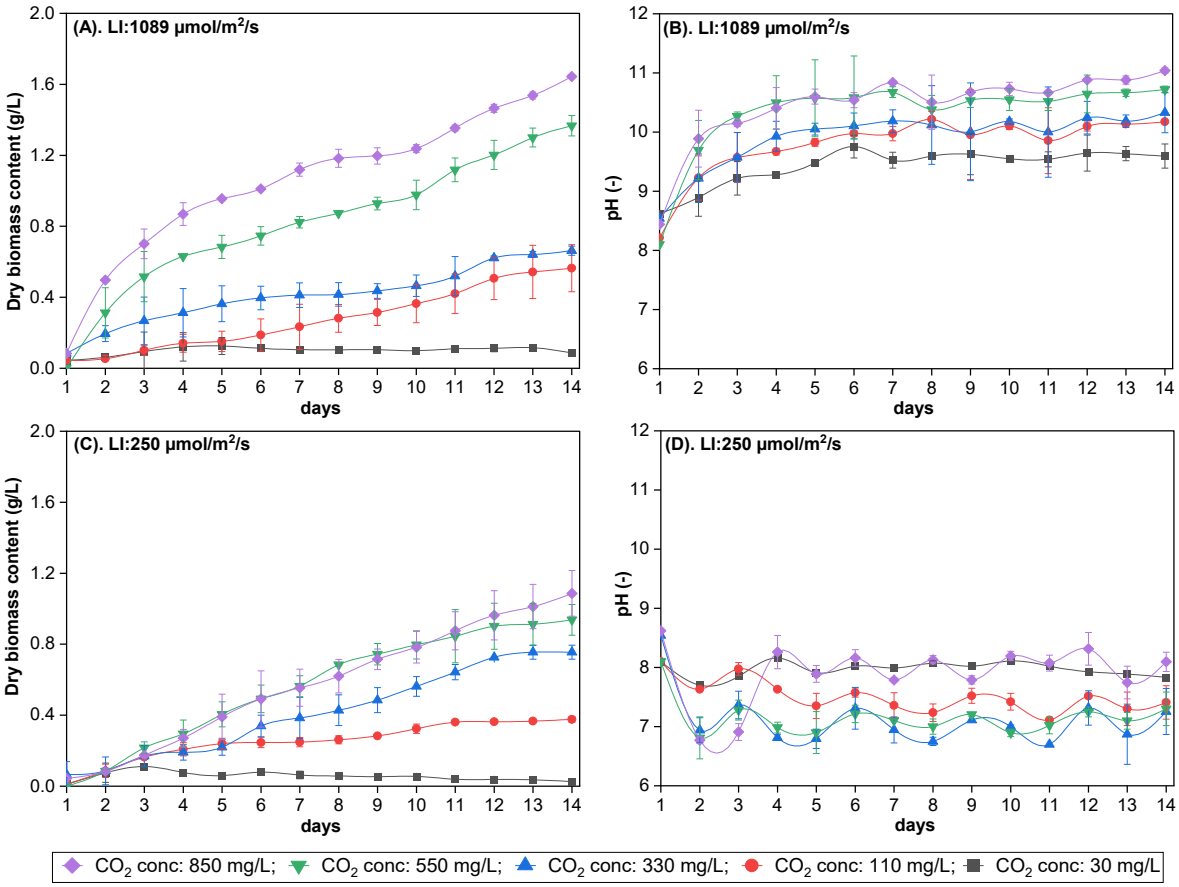

Figure 7. Biomass content in dry-weight and pH of the culture as a function of time (growing media = MaxiGro. Experimental condition: intermittent CO_2 transfer, at 0.6 ml/min feeding rate of carbonated water of CO_2 concentrations from 30 to 850 mg/L). The error bar represents the standard deviation from two replicate experiments.

In continuous CO_2 transfer mode (Figure 8), the microalgae solutions could not maintain equilibrium. For instance, when a high light intensity is applied to a CO_2 transfer with a high CO_2 concentration, the rate of photon collision with chlorophyll molecules increases, resulting in a faster rate of resonance excitation energy transfer to the reaction centres. It caused an imbalance in the photochemical reaction between the electron in photosystem II and the available H^+ (as a result of CO_2 dissolution). This reaction either slowed down or halted the electron transfer chain. This phenomenon causes severe obstruction of the opening of the photosynthetic reaction centres. This causes a pH difference between trans-thylakoids. To protect chlorophyll from deterioration,

microalgae prevented it by inactivating photosystem II reaction centres. Like its function, zeaxanthin or carotenoids will self-assemble to protect chlorophyll from light-induced damage and convert an excess excitation energy into heat. This constant reaction causes microalgae to progressively turn yellow and die. As shown in Figure 8, in light intensity 1089 μmol/m^2/s, it is indicated by a gradual decrease in pH 1-2 days prior to a decline in biomass production. A similar reaction of imbalance in photochemical reaction also occurs in CO_2 transfer with the lowest concentration. Microalgae with very low CO_2 concentrations will take longer to enter the early apoptosis phase as opposed to dying progressively. Indeed, the growth curves of microalgae with the lowest CO_2 concentration were flat (Figure 8). In other words, microalgae growth was insignificant at the lowest CO_2 input.

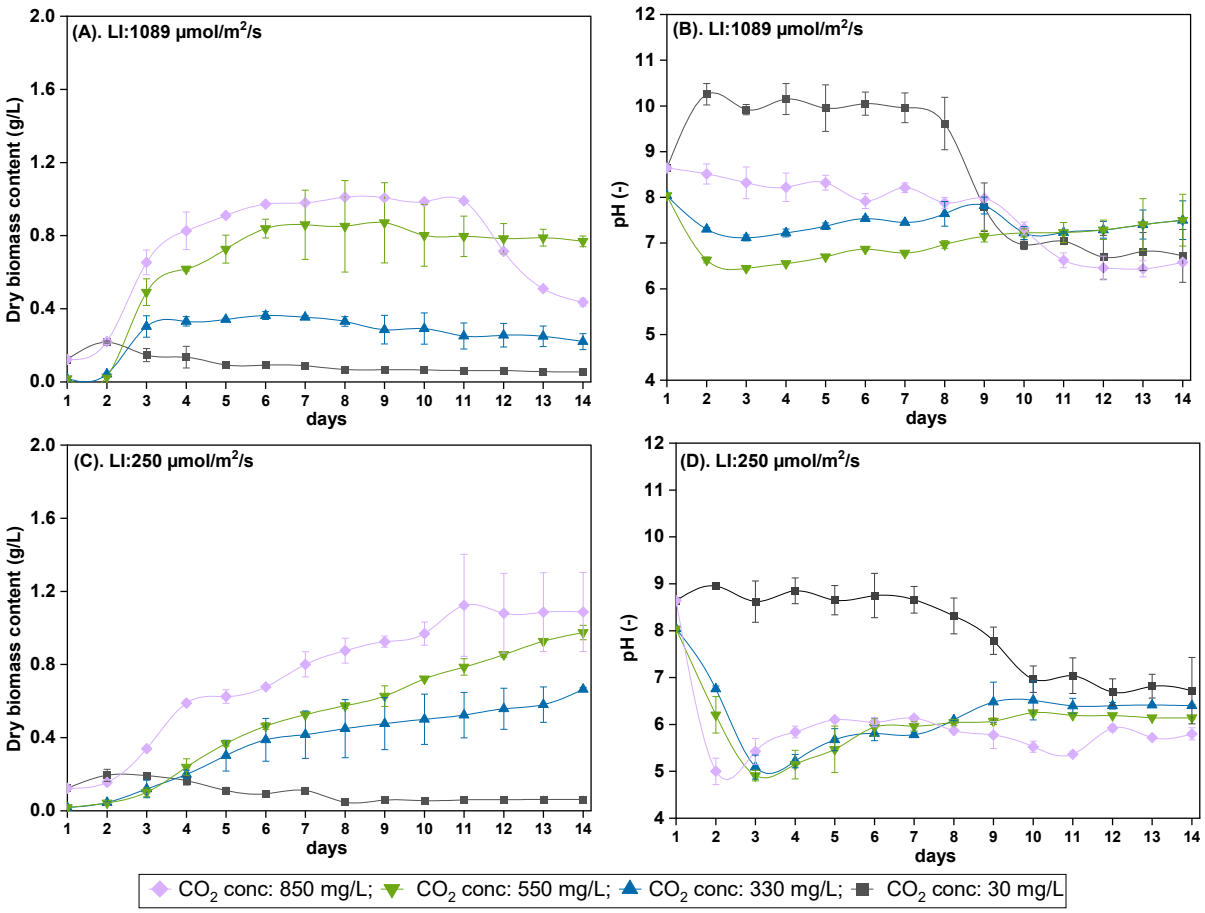

Figure 8. Biomass content in dry-weight and pH of the culture as a function of time (light intensity of 1089 and 250 µmol/m^2/s, growing media = MaxiGro, Experimental condition: continuous CO_2 transfer, at 0.6 ml/min feeding rate of carbonated water of CO_2 concentrations of 30 and 850 mg/L). The error bar represents the standard deviation from two replicate experiments.

3.3.2. Regulation of carbon assimilation

Figure 9 and Figure 10 show the residue CO_2 concentration in the cultivation solution overtime during intermittent and continuous CO_2 transfer, respectively. The cyclic pattern of CO_2 concentration in Figure 9 and 10 corresponds to intermittent CO_2 transfer of one day on and one day off. In the intermittent CO_2 transfer mode (Figure 9E), CO_2 accumulation in the culture solution was observed at the end of the cultivation experiment when light intensity was low (250 µmol/m^2/s), and CO_2 transfer was high (850 mg/L) possibly due to self-shading. By contrast, when high light intensity was

applied, CO_2 accumulation was not observed. Results from Figure 9 and 10 reaffirm that CO_2 uptake is dependent on light intensity [148].

The continuous CO_2 transfer mode resulted in significant CO_2 accumulation in the microalgae solution (Figure 10), resulting in an acidic condition that may inhibit microalgal growth. High light intensity can improve CO_2 assimilation. However, in continuous CO_2 transfer, CO_2 accumulation was observed even at the high light intensity and lower CO_2 concentration (Figure 10B).

Apart from the pH in microalgae, it is worth noting that the CO_2 molecule itself has an effect on microalgae. According to a recent study, the inhibitory effect of excessive CO_2 concentration persists even when the pH is adjusted. This is demonstrated by the lack of a strict numerical relationship between apoptosis percentage and intracellular pH [149]. This is also consistent with the findings in this study. The impact of remaining CO_2 concentrations above 100-120 mg/L results in the death of microalgae. After the CO_2 concentration reached 100 mg/L, the pH of microalgae began to decline gradually the following day, followed by their death a few days later. The remaining CO_2 concentration in microalgal solution with light intensity 1089 μmol/m^2/s, is restricted to a range, below 30 mg/L and above 160 mg/L (Figure 9).

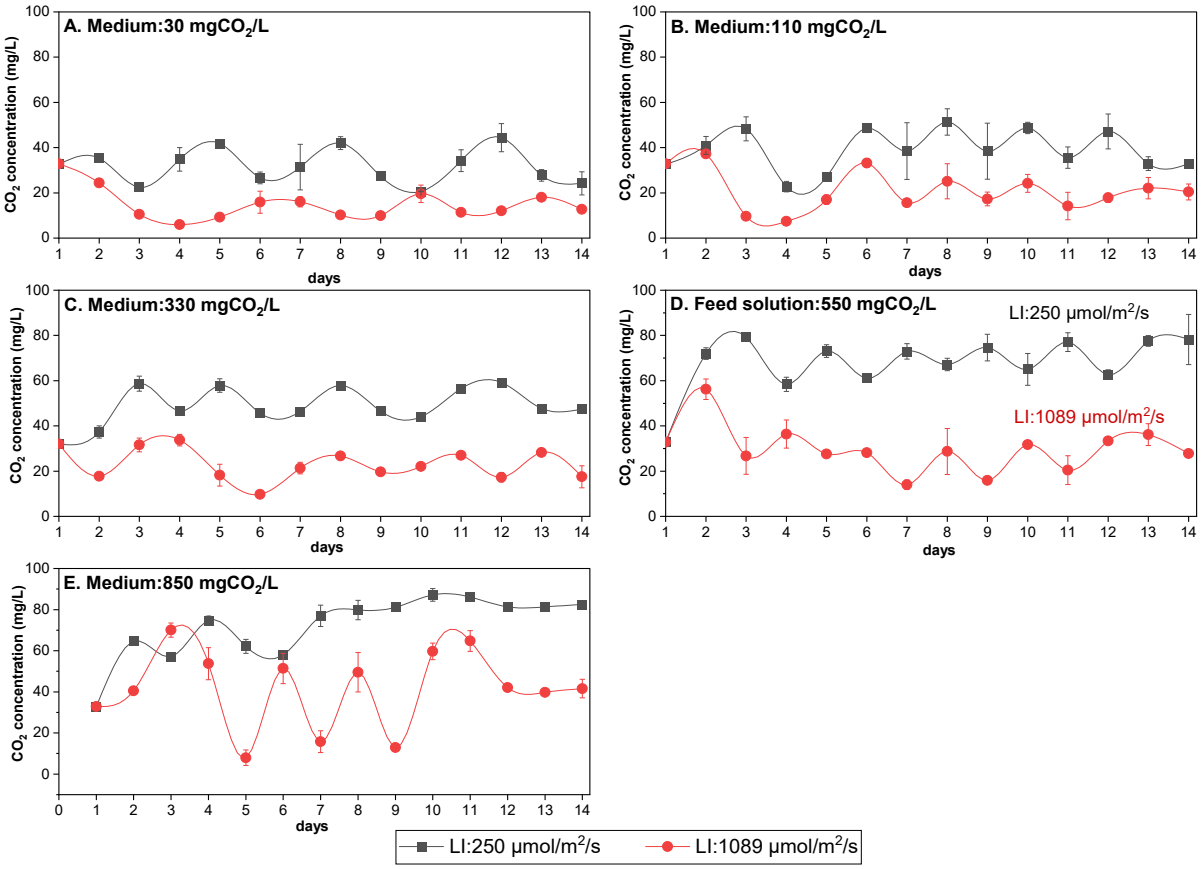

Figure 9. Residue CO_2 concentration in the cultivation solution as a function of time (light intensity of 1089 and 250 µmol/m^2/s, growing media = MaxiGro, Experimental condition: Intermittent CO_2 transfer, at 0.6 mL/min feeding rate of carbonated water of CO_2 concentrations from 30 to 850 mg/L). The error bar represents the standard deviation from two replicate experiments.

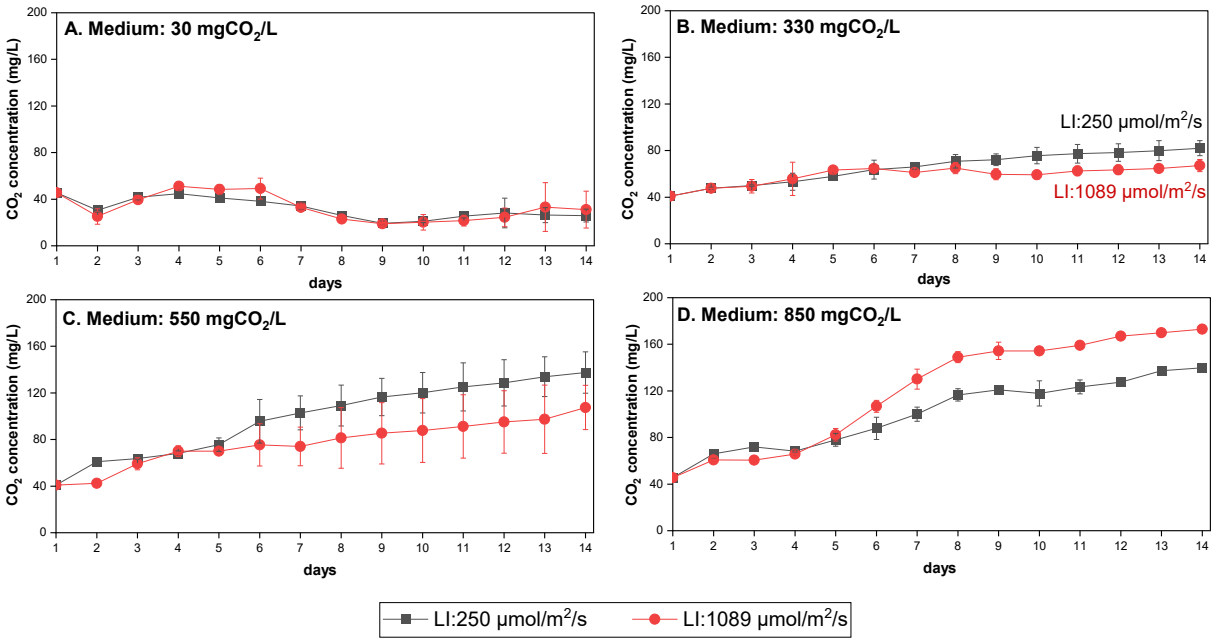

Figure 10. Residue CO_2 concentration in the cultivation solution as a function of time (light intensity of 1089 and 250 µmol/m^2/s, growing media = MaxiGro, Experimental condition: Continuous CO_2 transfer, at 0.6 mL/min feeding rate of carbonated water of CO_2 concentrations from 30 to 850 mg/L). The error bar represents the standard deviation from two replicate experiments.

Total CO_2 fixation by *Scenedesmus* sp over 14 days of cultivation is shown in Figure 11. The highest total fixation was observed with the intermittent CO_2 transfer mode at light intensity of 1089 µmol/m^2/s. The continuous CO_2 transfer mode resulted in significantly lower CO_2 fixation rate. There is no significant difference between high and low light intensity (Figure 11). This is due to the fact that continuous CO_2 transfer will continuously transmit H^+ to the microalgae solution. This disrupts the redox equilibrium in chloroplast thioredoxin systems [150]. Thereby causing the disruption of RuBisCo's activities [151-153]. The over-expression of RuBisCo consequently leads to disrupting stomatal closure and opening processes and resulted in a lower rate of CO_2 fixation. Microalgae prefer intermittent rather than continuous CO_2 transfer, as demonstrated by previous work [154]. However, other advanced study resulted that the transcriptome of microalgae indicates that the majority of genes are not regulated in sync when microalgal

growth is severely inhibited by pH or CO_2 [155].Therefore, the direct inhibitory effect on the physiological and metabolic mechanisms of microalgal cells, independent of pH alterations, is still unclear.

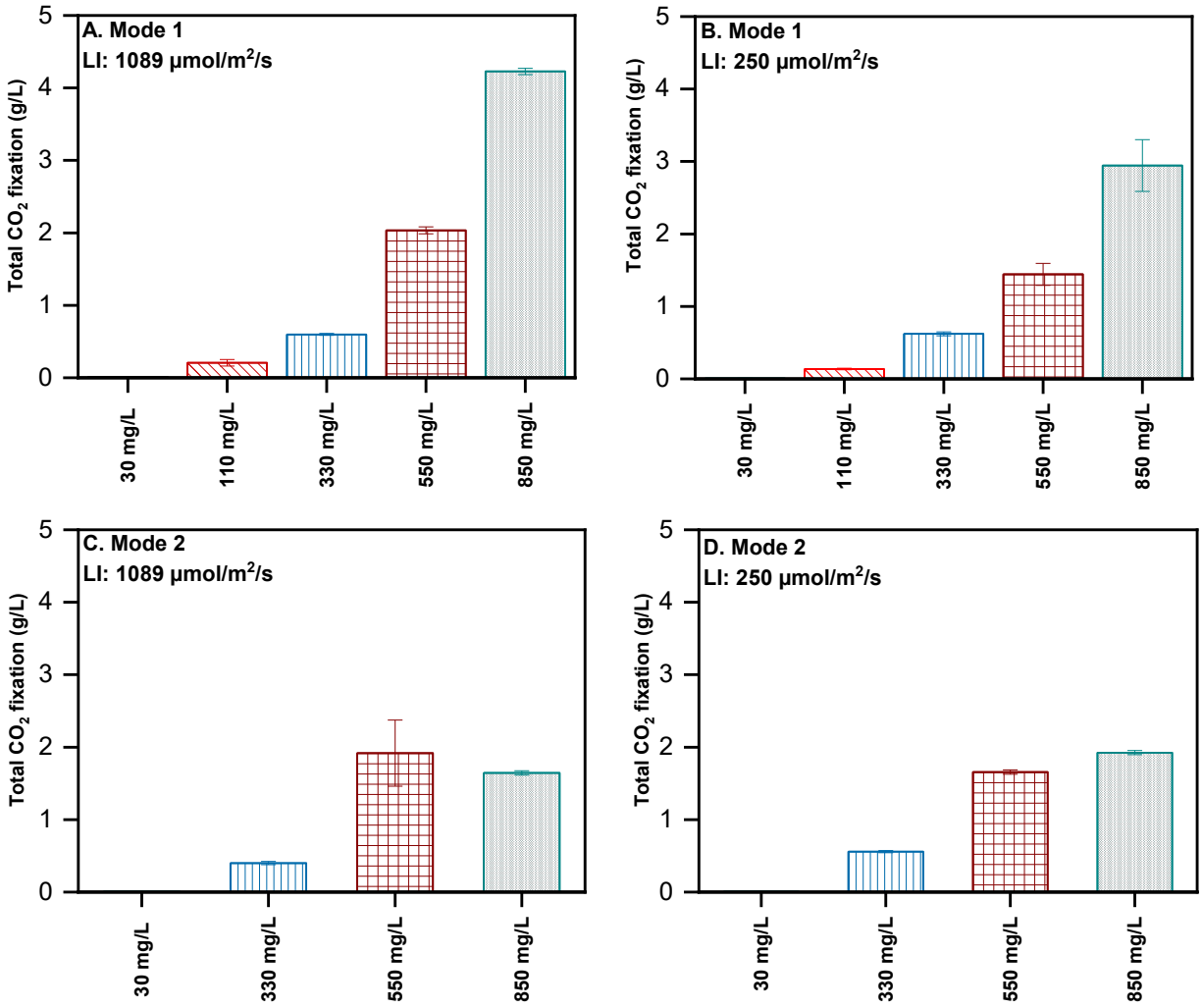

Figure 11. Total CO2 fixation by *Scenedesmus* sp over 14 days of cultivation (light intensity of 1089 and 250 µmol/m^2/s, growing media = MaxiGro, in Mode 1 and Mode 2, at 0.6 mL/min feeding rate of carbonated water of CO_2 concentrations from 30 to 850 mg/L). The error bar represents the standard deviation from two replicate experiments.

Intermittent CO_2 transfer mode produces more organic carbon than the continuous transfer mode. This is correlated to the quantity of CO_2 utilised and biomass produced

(Figure 12). Several previous studies [156, 157] have also reported enhanced organic carbon release by microalgae due to high light intensity and high CO_2 concentration. Results from this study are also consistent with microalgal CO_2-uptake mechanisms. Microalgae absorb inorganic carbon from the culture solution using carbonic anhydrase enzyme to maintain a high level of intracellular inorganic carbon for carboxylation. When converting inorganic carbon into organic carbon, the carboxylation process consumes proton (H^+) and also requires photon energy. Thus, the carboxylation process is governed by bicarbonate availability and photon absorption rate. These photons are obtained from the light source, where they are progressively absorbed by the microalgal cells' pigments [158]. In the carboxylation process, inadequate lighting would lead to photon scarcity and lengthen the lag time. As a result, in intermittent CO_2 transfer mode at light intensity of 1089 μmol/m^2/s (Figure 12) produces more organic carbon. While in the continuous transfer mode (Figure 13) were unable to achieve a balanced state of H^+ in transtylakoid membrane and adjusted pH for optimum microalgae growth.

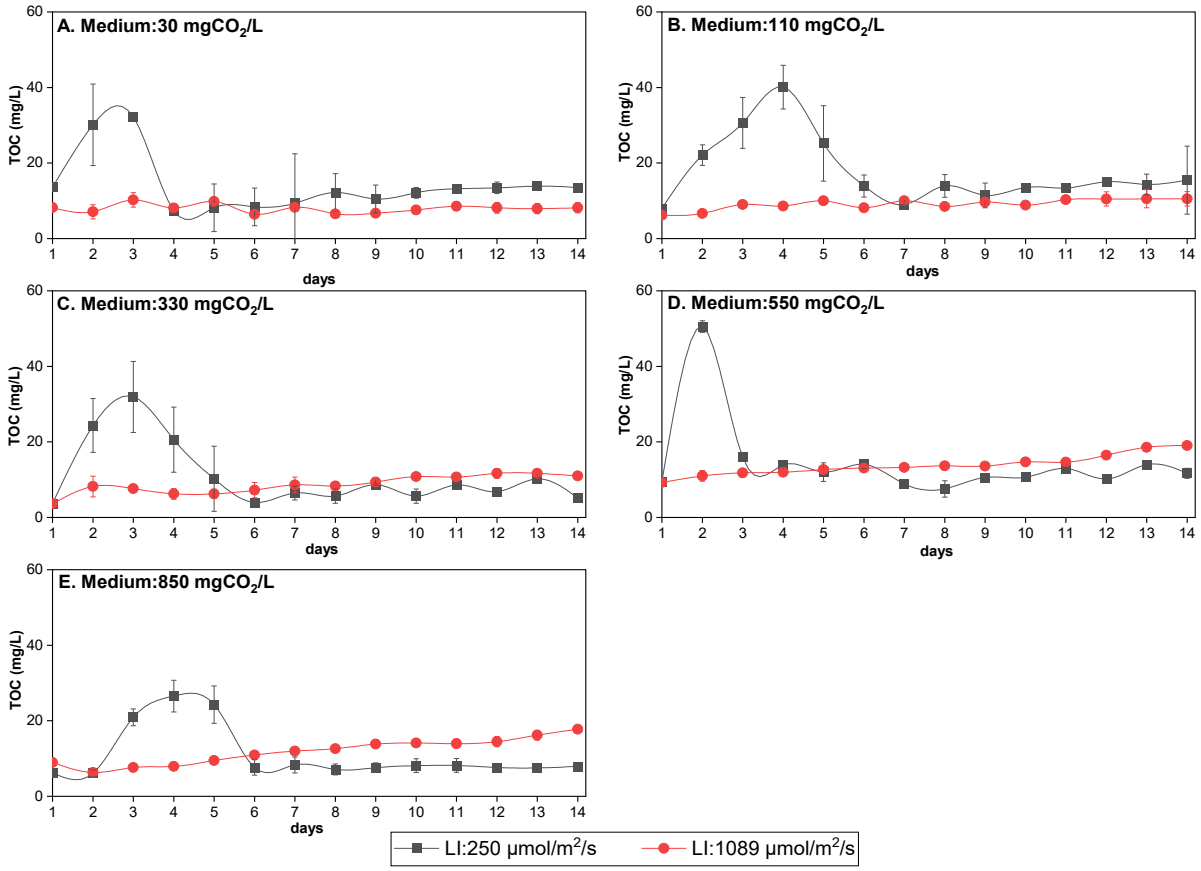

Figure 12. Total organic carbon in the culture solution (light intensity of 1089 and 250 µmol/m^2/s, growing media = MaxiGro, Experimental condition: Intermittent CO_2 transfer, at 0.6 mL/min feeding rate of carbonated water of CO_2 concentrations from 30 to 850 mg/L). The error bar represents the standard deviation from two replicate experiments.

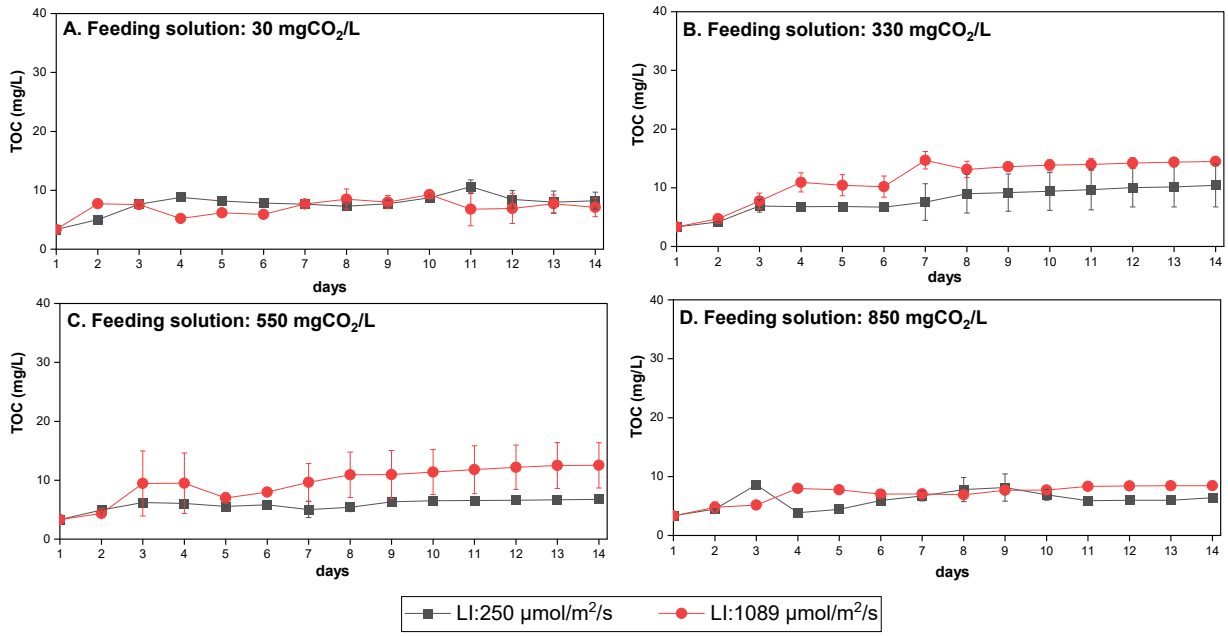

Figure 13. Total organic carbon in the culture solution (light intensity of 1089 and 250 µmol/m^2/s, growing media = MaxiGro, Experimental condition: Continuous CO_2 transfer, at 0.6 mL/min feeding rate of carbonated water of CO_2 concentrations from 30 to 850 mg/L). The error bar represents the standard deviation from two replicate experiments.

3.3.3. Impact of growth media

The effect of CO_2 concentration is medium-independent (Figure 14). The small difference in the quantity of produced biomass was possibility due to different micronutrients in these growth media. Results in Figure 14 also confirm that once nutrients are sufficient, growth media (or nutrient composition) do not significantly govern the growth rate of microalgae. In an engineering system, microalgae growth rate is governed primarily by light (photon energy) and CO_2 input.

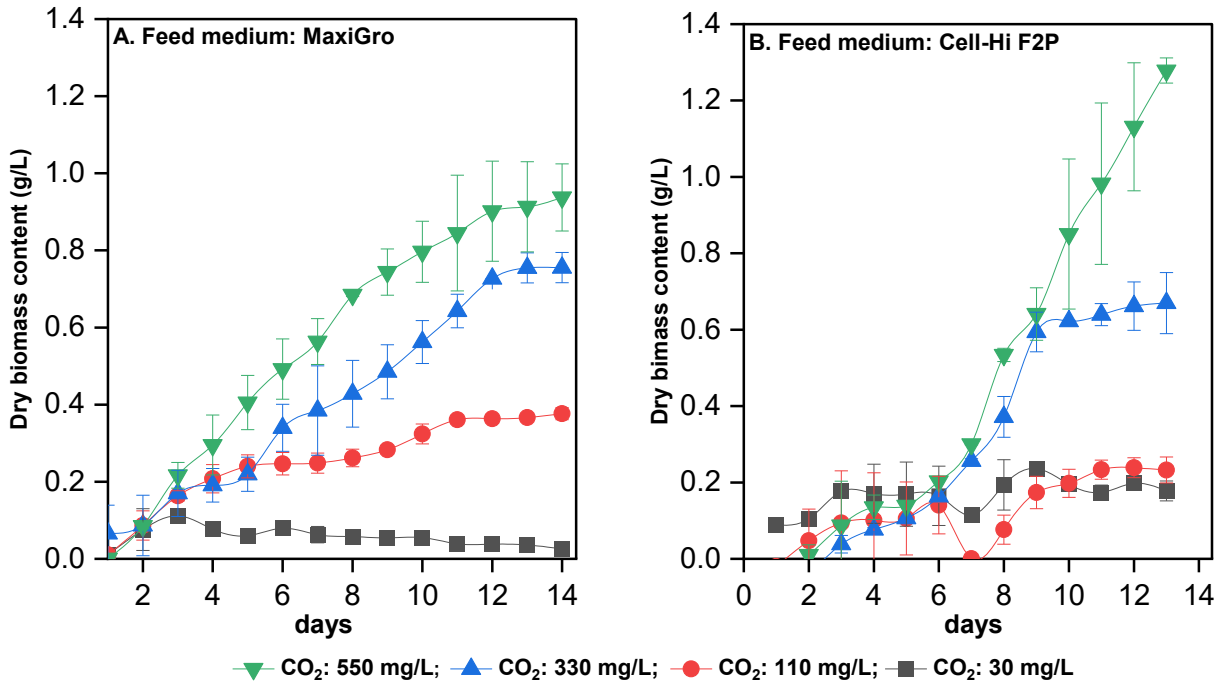

Figure 14. Comparison of *Scenedesmus* sp growth in MaxiGro and Cell-Hi F2P media (light intensity of 250 µmol/m^2/s in intermittent CO_2 transfer, at 0.6 mL/min feeding rate. CO_2 concentrations ranging from 30 to 550 mg/L. The error bar represents the standard deviation from two replicate experiments.

3.4. Summary

Results from this study affirm an increase in microalgae growth rate at high light intensity and CO_2 input. The results also show the interplay between light intensity and CO_2 input. Excessive CO_2 concentration can inhibit microalgae growth due to acidification. More importantly, light intensity and CO_2 input have opposing effects on the culture solution pH which is essential to microalgae growth. Microalgae photosynthesis is mediated by the RuBisCo enzyme that can only work in a specific pH range. CO_2 dissolution in the culture solution leads to acidification. On the other hand, the carboxylation process consumes proton and increases the solution pH. Results in this study show that by balancing light intensity and CO_2 input, high-rate microalgae growth and CO_2 fixation can be achieved. Under the intermittent CO_2 transfer mode, at the

optimal condition of 850 mg/L CO_2 and 1089 μmol/m^2/s, the highest microalgae growth rate and carbon fixation of 4.2 g/L was achieved.

CHAPTER 4. Sulphate assimilation and growth response of *Scenedesmus sp* and *Chlorella vulgaris* to elevated sodium sulphate concentrations

Part of this chapter has been submitted as the following journal article:

L Aditya, MA Kalam, U Kuzhiumparambil, PJ Ralph, MAH Johir, TMI Mahlia, LD Nghiem. Sulphate Assimilation and Growth Response of *Scenedesmus sp* and *C.vulgaris* to Elevated Sodium Sulphate Concentrations. 2025. Environmental Chemical Engineering**.**

4.1.Research objectives

This study explores how two freshwater microalgae, *Scenedesmus sp.* and *C.vulgaris*, respond to elevated sodium sulphate concentrations and pH variation, focusing on their growth parameters and biochemical composition. The investigation compares the growth patterns of the two species and the underlying mechanism. Moreover, this study also evaluates the impact of sulphate and pH separately to anticipate the impact of sulphur dioxide in flue gas on algae growth and their content. Elevated sulphate levels often induce pH fluctuations in microalgal cultures, which can further induce stress and impair growth. This study also evaluates the effects of high sulphate concentrations on the production of fatty acid methyl esters (FAME), lipids, and proteins. These biomolecules are critical for applications such as biofuel production and the development of sustainable bioproducts.

By examining the interplay between sulphate concentration, microalgal growth, and pH, this study aims to enhance the growth of microalgae to elevated sulphate

concentration and pH. The findings provide valuable insights into microalgae adaptation to sulphate stress and to identify strategies for optimising their performance in FAME production.

4.2.Material and methods

4.2.1. Microalgae and associated equipment

This study utilised two strains of freshwater green microalgae namely *Scenedesmus sp.* (UTS-LD) and *C.vulgaris* (CS-41). *Scenedesmus sp.* (UTS-LD), initially isolated in Australia by the University of Technology Sydney, and *C.vulgaris* (CS-41), obtained from the Australian National Algae Culture Collection at CSIRO Microalgae Research in Hobart, Tasmania. *Scenedesmus sp* typically appears in coenobium, appearing in this study as crescent-shaped colonies with four cells, with 12 μm in length and 3–5 μm in width. By contrast, *C.vulgaris* consists of individual spherical cells ranging from 2 to 10 μm in diameter. Both strains were cultivated in Erlenmeyer with a light intensity of 1031 μmol/m²/s. The growth media included either MaxiGro (from General Hydroponics, USA) or Cell Hi HP (from Fresh by Design, Australia), with sodium bicarbonate serving as the carbon source.

4.2.2. Experimental protocol

All cultivation experiments were initiated with 250 mL solution at the same microalgae concentration of OD_{680} of 0.1 in 500 mL Schott glass bottle reactors. The reactors were continuously mixed using a shaker, uncapped to allow gas exchange with the atmosphere, and illuminated by LED lighting (Arlec) at 1031 μmol/m^2/s. The growth medium consisted of MaxiGro and 0.6 g/L $NaHCO_3$ (Sigma-Aldrich). Na_2SO_4 in the range from 3 to 45 mM was added to individual reactors. All experiments were conducted in two replicates in a hydroponic tent at 27.0±1 ºC. The pH was adjusted to the desired

level using 1 M NaOH or 1 M HCl. 1 M NaOH was prepared by dissolving pellets in Milli-Q water, while 1 M HCl was prepared by diluting 32% HCl in Milli-Q water. The humidity probe of the digital meter was placed inside the mouth of the reactors without contacting the water surface. The measurement was recorded once the displayed values stabilised. Similarly, temperature was measured using a glass rod thermometer, which was inserted into the reactors.

4.2.3. Analytical methods

The growth of microalgal biomass was evaluated by measuring the optical density (OD) using a previously established correlation between dry biomass content and OD, as described in a prior study [140]. OD measurements of the microalgal solution were conducted using a UV spectrophotometer (UV 6000 Shimadzu; Australia) at a wavelength of 680 nm, with a 4 mL Quartz Glass Cuvette. Dry weight was determined by filtering 100 mL of the microalgae solution through 1.1 µm glass filter paper, followed by drying the filter paper in an oven at 60 °C for 24 hours.

Light intensity was measured with a Light Meter (LI-250A li-cor USA) using a quantum sensor (LI-190SA). Humidity and temperature were monitored using an Ozito 0-100%RH -20 to 60°C Digital Humidity and Temperature Meter and a glass rod thermometer.

FAME analysis was performed using a GC-MS (QP2020 Shimadzu Corporation, Kyoto, Japan) equipped with an autosampler (AOC-20is Shimadzu Corporation). The column used was an SH-Rxi-5Sil MS fused silica capillary column (30.0 m × 0.25 mm × 0.25 µm), operating in electron impact mode at 70 eV. Helium served as the carrier gas at a constant flow rate of 1.0 mL min^{-1}, with an injection volume of 2 µL, an injector temperature of 280 °C, and an ion source temperature of 230 °C. The oven temperature

followed a gradient: 50 °C (for 2 minutes) to 220 °C (4 °C/min), then to 300°C (60°C/min) for 3 minutes. FAME peaks were identified by comparing retention times with authentic standards and quantified through area normalisation and response factors.

Total lipid content was determined gravimetrically, with nonadecanoic acid (C19:0) serving as the internal standard. Dried lipids were treated with 1 mL of 1% NaOH in methanol and heated at 55 °C for 15 minutes, followed by the addition of 2 mL of 5% methanolic HCl and a subsequent 15-minute heating at 55 °C. After adding 1 mL of Milli-Q water, FAMEs were extracted using hexane (3 × 1 mL), evaporated to dryness under nitrogen, redissolved in 200 µL of hexane, and stored at −20 °C in glass vials until GC-MS analysis. This approach facilitated the simultaneous production of carotenoids and chemical building block precursors from chlorophytes microalgae.

4.3.Result and discussion

4.3.1. Growth response to elevated sodium sulphate concentrations

Results from this study show a clear relationship between microalgae growth and sulphate content of the culture solution (Figure 15). Growth response to sulphate concentration is also species-specific. *Scenedesmus sp.* and *C. vulgaris* cultures both show similar initial growth rates. Then by day 6, cultures with sulphate concentrations above 21 mM began to change to yellow. After 12 days, both species showed growth patterns distinctive from each other. *Scenedesmus sp.* transitioned through different growth phases depending on sulphate concentration (Figure 15A), while *C. vulgaris* maintained an exponential growth phase except at sulphate concentrations above 21 mM (Figure 15B). Growth rates increased across all sulphate concentrations during the initial days, consistent with metabolic activity that alkalinised the culture solution (Figure 15C and D). By day 4, pH levels in both cultures had risen above 9.5 in all reactors. However,

starting on day 6, a decline in pH were observed in both cultures. This pH reduction correlates with a transition to the declining growth phases, indicating that the microalgae no longer actively perform ion exchange during photosynthesis, marking the end of the culture's life. For instance, Figure 15C and D show that the most significant pH decreases were observed at 27 mM and 30 mM sulphate concentrations, aligning with subsequent drops in growth rate in the following days. Humidity patterns also revealed differing osmotic stress tolerance between the two species (Figure 15E and 1F). *Scenedesmus sp* showed a relatively stable pattern, whereas *C. vulgaris* fluctuated over time.

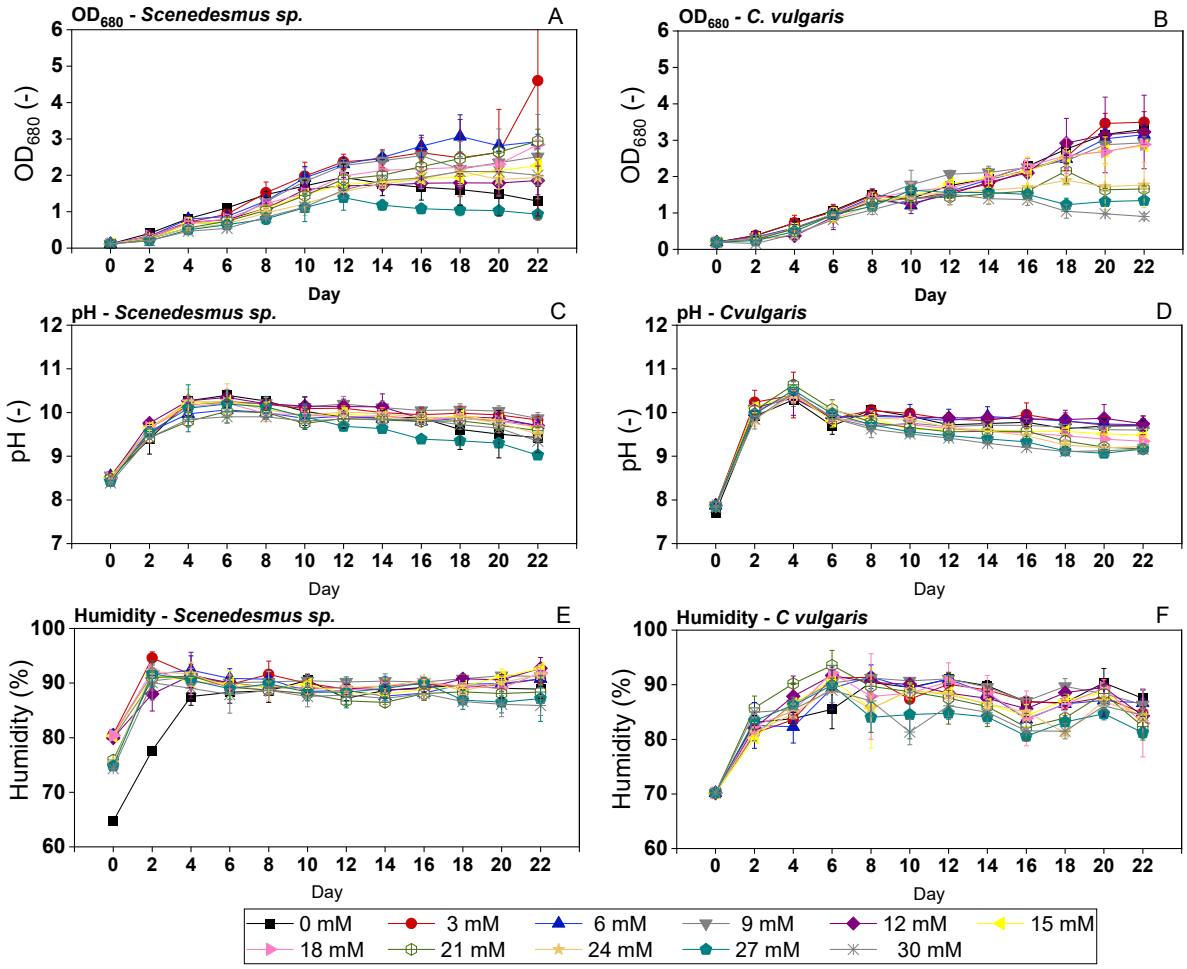

Figure 15. *Scenedesmus* and *C. vulgaris* growth rate, pH and humidity in different sodium sulphate concentrations (0-30 mM). The error bar represents the standard deviation from two replicate experiments.

The optimal sulphate concentration for Scenedesmus sp growth was within the lower-to-moderate sulphate concentration range (Figure 16). *Scenedesmus sp* showed a significant reduction in growth at 0 mM sulphate concentration compared to cultures exposed to sulphate. This indicates that some sulphate is necessary for optimal growth. Moreover, beyond a certain point, increasing sulphate concentrations led to a decline in biomass (Figure 16A). Meanwhile, *C. vulgaris* showed the optimal concentration at a relatively lower sulphate before gradually declining with further increases in sulphate (Figure 16B). This suggests that *C. vulgaris* is less tolerant to higher sulphate levels. These differences highlight the differences in sulphate metabolism pathways between the two species.

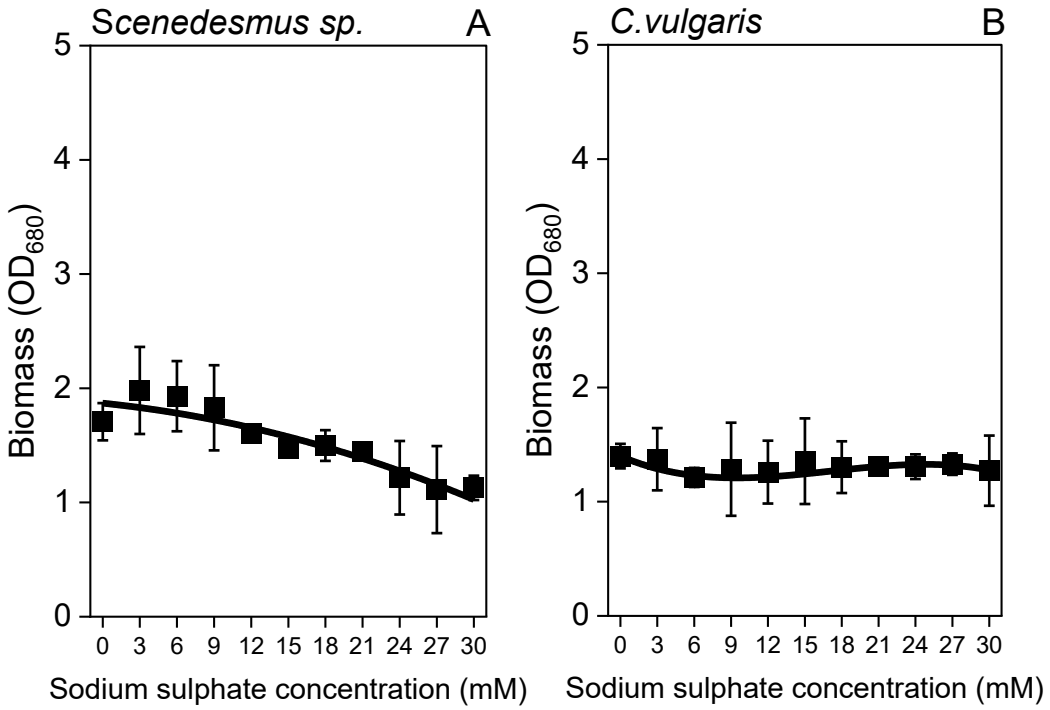

Figure 16. Average biomass production of Scenedesmus sp (A) and C. vulgaris (B) was taken after 10 days under varying sodium sulphate concentrations (0–30 mM). Error bars indicate standard deviation from two replicate experiments.

The results are consistent with previous studies, highlighting differences in sulphur assimilation mechanisms between *Scenedesmus sp* and *C. vulgaris* [159-162].

Scenedesmus sp relies on eukaryotic-specific pathways, while *C. vulgaris* employs bacterial-like sulphate transport systems, including prokaryotic-like plastid sulphate transporters on chloroplast membranes [159]. To participate in microalgal metabolic processes, sulphate must be activated via ATP sulfurylase, which converts sulphate to adenosine 5′-phosphosulfate (APS). Although both species depend on ATP sulfurylase activity, their metabolisms differ during sulphite reduction to sulphide by sulphite reductase enzymes. *Scenedesmus sp* utilises a eukaryotic-type sulphite reductase that can use nicotinamide adenine dinucleotide phosphate (NADPH) as electron donors, whereas *C. vulgaris* employs a ferredoxin-dependent sulphite reductase, relying on electrons from reduced ferredoxin generated during photosynthesis (Figure 17) [159-162].

This variation also explains the optimal sulphate concentration for each species. *Scenedesmus sp.* require sulphate when nitrogen is available and utilise NADPH for amino acid synthesis [163, 164]. Nitrogen is essential for protein synthesis, and it depends on sulphur-containing amino acids. For example, cysteine-dependent enzymes crucial for nitrogen metabolism become less active under sulphur deprivation [165, 166]. Consequently, proper nitrogen concentrations are necessary for efficient protein synthesis in *Scenedesmus* sp [161, 167]. Additionally, sulphur limitation reduces sulphur-containing compounds involved in RNA synthesis and obstructs DNA replication, ultimately inhibiting cell division [168, 169].

The reduced growth rate at higher sulphate concentrations may result from an imbalance between nitrogen and sulphate availability. Sulphur transport is an energy-dependent process in eukaryotic-type sulphite reductase. Sulphur deficiency decreases the energy allocated for sulphate transport while increasing energy use in alternative biological pathways when other nutrients are abundant [170, 171]. This shift can slow

amino acid synthesis, particularly of cysteine and methionine, leading to an accumulation of unassimilated sulphide, which may become toxic *to Scenedesmus* sp [161].

Unlike *Scenedesmus* sp, *C. vulgaris* relies on ferredoxin, a chloroplast's key electron carrier for sulphate assimilation. This process depends on light availability and photosynthetic activity, as ferredoxin receives its electrons from Photosystem I [168]. When other nutrients are abundant, ferredoxin may be redirected towards other metabolic processes, such as nitrite reduction, thereby reducing sulphate assimilation efficiency [168, 172]. Since both nitrogen and sulphate metabolism require ferredoxin as an electron donor, they are interdependent [164]. As a result, higher sulphate assimilation in *C. vulgaris* was achieved under nitrogen-limited conditions [173, 174] which explained this study result that *C. vulgaris* exhibited higher growth at the lowest sulphate concentration, while increasing sulphate concentrations led to reduced growth rates. It also has been reported that without sulphur, Rubisco and PSI and PSII proteins in a photoautotrophic culture level decreased, which aligned with this study result of decreasing growth rate in 0 mM *C.vulgaris* culture [175, 176].

The yellowing of the culture at sulphate concentrations above 21 mM in both cultures has also been reported in previous studies [177, 178]. Chlorophyll levels reduced with increasing sulphate concentrations due to the formation of reactive species, such as superoxide anions and hydrogen peroxide, during the conversion of bisulphite to sulphate. This oxidative stress led to membrane lipid peroxidation and chlorophyll degradation, inhibiting algal growth [177]. Additionally, plasmolysis and organelle decomposition, including chloroplast and nucleus breakdown, were observed in cultures with elevated sulphate levels [178].

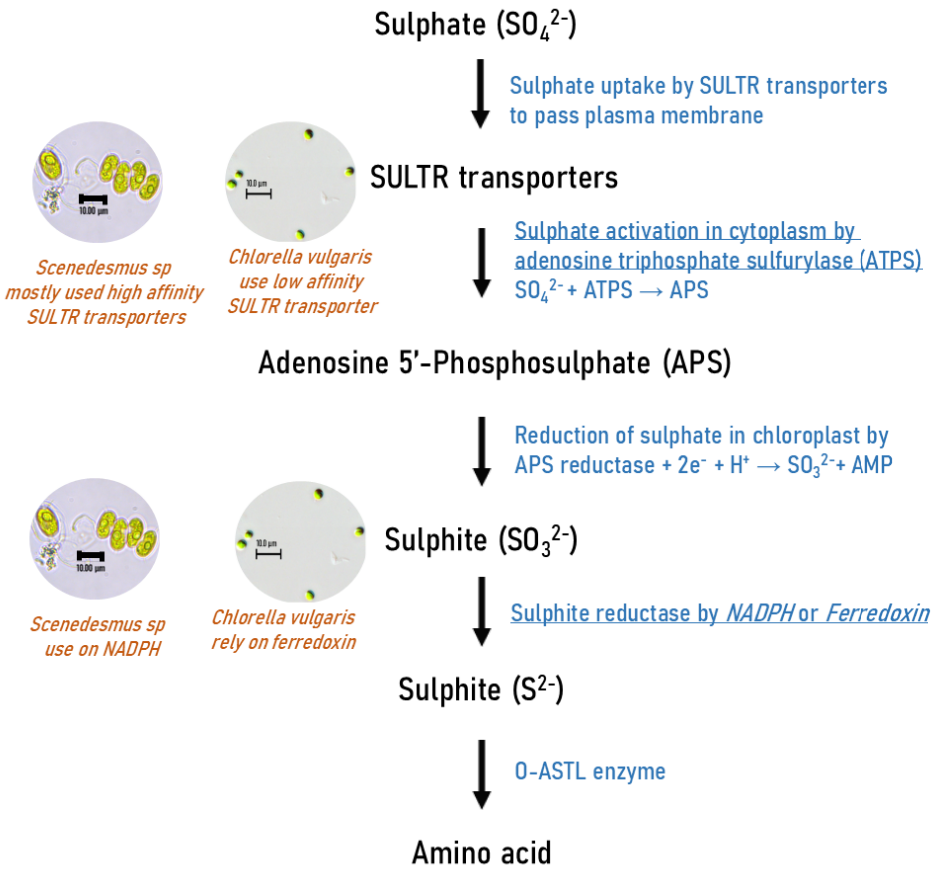

Figure 17.Sulphate metabolism difference in *Scenedesmus sp* and *C.vulgaris* [159-162].

The morphological differences between the species also influence their responses to nutrient absorption, particularly sodium ions, which can disrupt photosynthesis at high concentrations [179]. *Scenedesmus sp* has a thicker, more robust cell wall that may provide enhanced protection against ionic stress [180, 181]. Additionally, *Scenedesmus sp* is known to form colonies, potentially buffering environmental stress. These adaptations may enable *Scenedesmus sp* to maintain photosystem stability and regulate intracellular Na^+ levels under moderate sodium sulphate stress. Conversely, *C. vulgaris* has a thinner cell wall, rendering it more susceptible to environmental stressors such as salinity [182]. As a unicellular alga, *C. vulgaris* lacks the advantage of colony formation, resulting in direct exposure to stress under high salinity conditions. While *Scenedesmus sp* exhibits stable growth and photosynthetic efficiency at intermediate sulphate concentrations, high concentrations can induce stress, reducing growth or activity. In

contrast, *C. vulgaris* is more sensitive to disruptions in photosynthesis, with growth and pigment content declining at lower stress thresholds [168]. This lower tolerance to osmotic stress in *C. vulgaris* at elevated sulphate levels results in an earlier reduction in growth.

4.3.2. Impact of initial pH

Results in Figure 18 show a clear relationship between pH of the culture solution and microalgal growth. An extreme pH conditions significantly affect microalgal growth. For example, at a pH level below 4 (Figure 18A), microalgal failed to grow and the solution bleached within two days, highlighting the detrimental effects of extreme acidity. While a pH above 10 inhibits prolonged exponential growth period. This result aligns with the pH-dependent behaviour of *Scenedesmus sp* [183], and the inhibitory effect on high alkalinity and acidity [184-187]. For example, microalgal growth decreased by 55% under highly acidic conditions (pH <5) and decreased by 46% under highly alkaline conditions (pH>8), with optimal growth observed at pH 7.5–8 [184]. This is attributable to the direct impact of pH on enzymatic activity and cellular membrane stability [178].

Microalgal enzymes are highly sensitive to pH fluctuations. Extremely acidic or alkaline conditions can lead to protein denaturation and impaired enzyme performance. This, in turn, disrupts the optimal uptake of nutrients [188, 189]. For instance, the activity of ATP sulfurylase, which is crucial for ATP synthesis, is strongly influenced by the pH of the thylakoid lumen and surrounding stroma. Non-optimal pH conditions hinder ATP production. Similarly, APS reductase, another pH-sensitive enzyme, relies on the proper ionisation of its functional groups to facilitate the reaction. Acidic environments inhibit APS sulphite production, affecting the downstream synthesis of sulphur-containing compounds [171]. Acidic conditions may also lead to an imbalance in ion exchange,

reducing its bioavailability for cellular uptake and enzymatic reactions [184]. This significantly disrupts sulphate assimilation and the synthesis of sulphur-containing amino acids [188, 189]. Additionally, RuBisCo, a critical enzyme in the Calvin cycle, is responsible for CO_2 fixation during photosynthesis, and this enzyme is highly pH sensitive. Acidic pH conditions can impair RuBisCo's ability to fix CO_2, negatively affecting photosynthesis and biomass production [190, 191]. In contrast, Figure 18B shows that higher sulphate concentrations might mitigate this effect, allowing growth to continue in the exponential phase. This is because sulphate helps maintain ionic balance in high-pH environments, particularly for *Scenedesmus sp*, that utilise NADPH for sulphate assimilation [192-194].

Total biomass produced with initial pH adjustment (Figure 18) was slightly higher compared to the result in Figure 18A, consistent with findings from other studies [185, 195, 196]. The cell density in the under-controlled conditions was 1.32 times higher than when relying solely on the microalgae's natural alkalinisation ability. Therefore, pH adjustment was concluded to enhance microalgal growth [185]. Adjusting pH to optimal could also enhance lipid accumulation [195, 197].

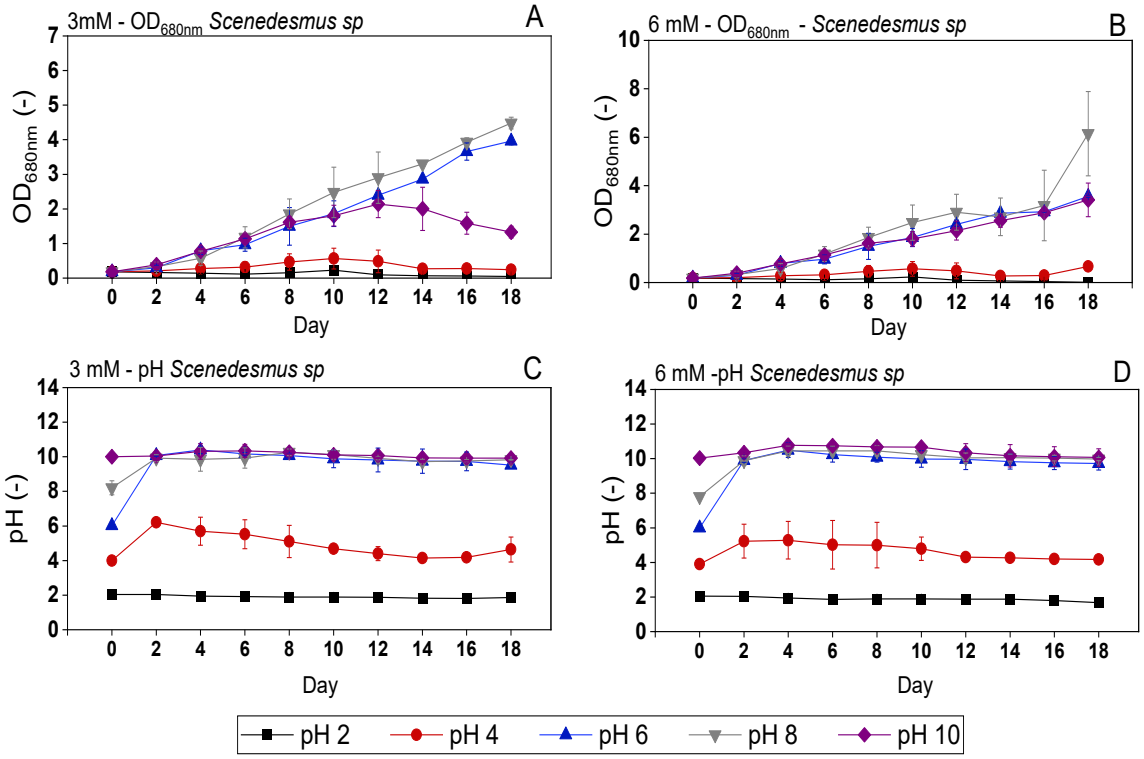

Figure 18. Impact of initial pH on the growth rate of *Scenedesmus sp* (A, B) and pH variation (C, D) under sodium sulphate concentrations of 3 mM and 6 mM, respectively. Error bars indicate the standard deviation from two replicate experiments.

Figure 19 shows that an initial pH of 8 was optimal for achieving the highest biomass production in 3 mM and 6 mM sulphate conditions. This was followed by pH 6 and pH 10. In both sulphate concentrations, biomass production at pH 6 remained relatively high, supporting the idea that *Scenedesmus sp.* can tolerate a moderate acidic to neutral pH range [197]. Cultures at pH 10 exhibited lower biomass production than those at pH 8 and 6, suggesting that although alkalinity is less detrimental than acidity, excessively high pH imposes physiological stress on the cells. Cultures at pH 4 and pH 2 were completely bleached and showed no growth, indicating severe stress and cell death under highly acidic conditions [198, 199]. This is consistent with previous studies reporting that extreme acidity disrupts enzyme activities, leading to impaired

photosynthesis process [190, 191]. A similar result was also reported that a pH below 4 caused detrimental effects on microalgae culture under various sulphate and sulphite concentrations, and low pH was the main reason for sulphate toxicity [188, 189]. Additionally, biomass production was consistently higher at 6 mM (Figure 19 A) compared to 3 mM (Figure 19B) across all cultures, further supporting our previous discussion that *Scenedesmus sp.* requires sulphate to enhance its growth [199, 200]. Apart from pH, a lower growth rate was observed in 6 mM compared to 3 mM, this is due to sulphate itself being toxic to microalgal at elevated concentrations. High sulphate concentrations can lead to excessive conversion of sulphate into sulphide, which is more toxic to microalgae. Sulphide accumulation at bisulphite concentrations above 3 mM can cause significant stress and cellular bleaching. Under these conditions, key metabolic pathways, including those related to amino acids, peptides, carbohydrates, secondary metabolites, organic acids, alcohols, nucleotides, lipids, hormones, and other bioactive compounds, are downregulated [188].

This also aligns with the previous study that shows sulphate toxicity affects microalgae by disrupting osmotic balance across the cell membrane [200]. Sulphate is transported into cells via ATP-dependent permeases and subsequently into chloroplasts, where it begins assimilation along with other essential nutrients like nitrates and phosphates. Elevated sulphate levels can interfere with cellular processes by disrupting osmotic balance and competing with nitrates and phosphates for transport and assimilation. This competition inhibits critical enzymes involved in cellular respiration, impairing energy production and overall cellular functionality [188, 190]. It is important to note that each microalgal species has its own maximum pH tolerance. Generally,

Scenedesmus sp exhibits a higher tolerance to alkaline conditions under sulphate limitation compared to *C. vulgaris* [161, 187].

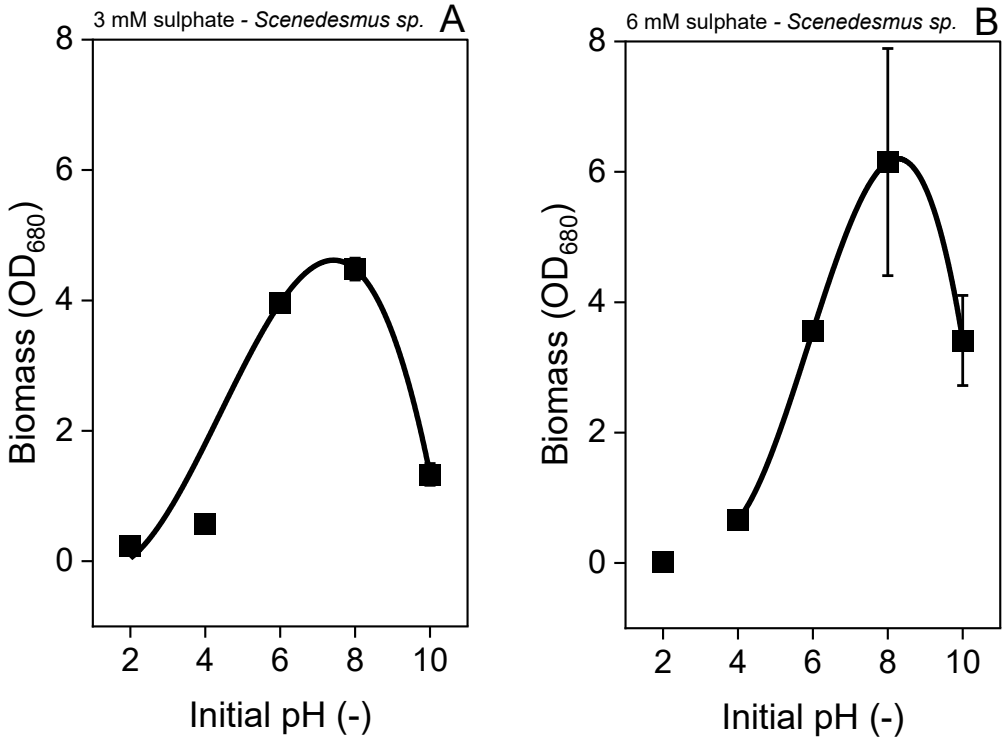

Figure 19. Biomass production of *Scenedesmus sp.* at 3 mM (A) and 6 mM (B) after 18 days of cultivation across a pH range of 2–10. Error bars indicate the standard deviation from two replicate experiments.

4.3.3. Lipid, protein and FAME content on elevated sulphate concentrations

Sulphate in culture solution negatively impacts lipid production by *Scenedesmus sp* (Figure 20). *Scenedesmus sp* was selected for its higher sulphate tolerance and lipid productivity, compared to *C.vulgaris* [161, 181, 201], to assess their lipid and protein content under elevated sulphate concentration. The increase in sulphate concentration activated redox stress adaptation, triggering the production of glutathione, which subsequently increased protein demand and reduced lipid production [160].

Protein synthesis had the highest at 3 mM sodium sulphate and decreased as the sulphate concentration increased (Figure 20). As the sulphate concentration rose, protein

production progressively decreased. For example, at 12 mM, protein synthesised was 8% lower than at 3 mM, while at 21 mM, it decreased by a further 25%. These results indicate that *Scenedesmus sp* requires an optimal sulphate concentration to enhance protein synthesis, as sulphate serves as a crucial precursor for protein formation [202]. Higher sulphate uptake facilitated the availability of sulphur-containing amino acids polyunsaturated fatty acid (cysteine and methionine), promoting protein synthesis [160]. However, concentrations beyond the optimal range led to osmotic stress, adversely affecting protein synthesis [161].

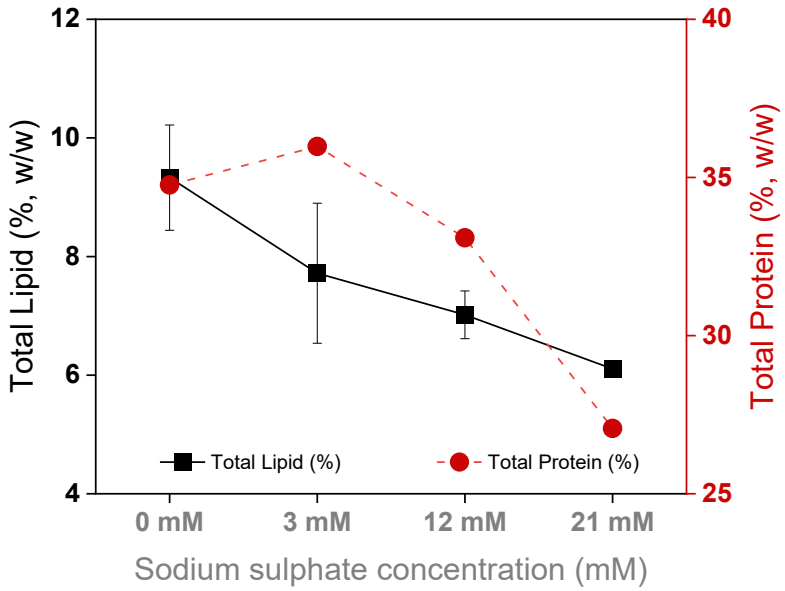

Figure 20. Total protein and lipid content of *Scenedesmus sp.* under sodium sulphate concentrations of 0, 3, 12, and 21 mM. Error bars represent the standard deviation from three replicate measurements.

An appropriate sulphate concentration enhances protein synthesis while reducing lipid accumulation [160, 161]. This aligns with our observations, which show that protein levels increased in cultures with 3 mM sulphate, while lipid levels decreased. During sulphate assimilation, ATP is consumed, generating tricarboxylic acid cycle and nitrogen metabolism, indirectly supporting protein biosynthesis [169]. The presence of sulphate

activated the target of rapamycin signalling pathway, which promoted target of rapamycin inhibition and inhibited microalgal lipid production [203]. Microalgae prioritised protein synthesis over lipid storage due to the necessity of proteins for metabolic stability and cellular resilience in a sulphate-rich environment [203].

Similar to total lipid production, FAMEs production varied based on sulphate concentration. Without any sulphate addition, the production of some methyl ester was the highest, these include Methyl palmitate, Methyl heptadecanoate, Methyl gamma-linolenate, Linolelaidic acid methyl ester, cis-9-Oleic acid methyl ester, Methyl nonadecanoate, and cis-5,8,11,14-Eicosatetraenoic acid methyl ester. Furthermore, Cis-5,8,11,14,17-Eicosapentaenoic acid methyl ester and Methyl docosanoate, had the highest production at 3 mM. Conversely, Methyl tetradecanoate, trans-9-Elaidic acid methyl ester, Methyl palmitoleate, and Methyl octadecanoate production increased by 63% at 21 mM compared to 0 mM sulphate concentrations (Figure 21).

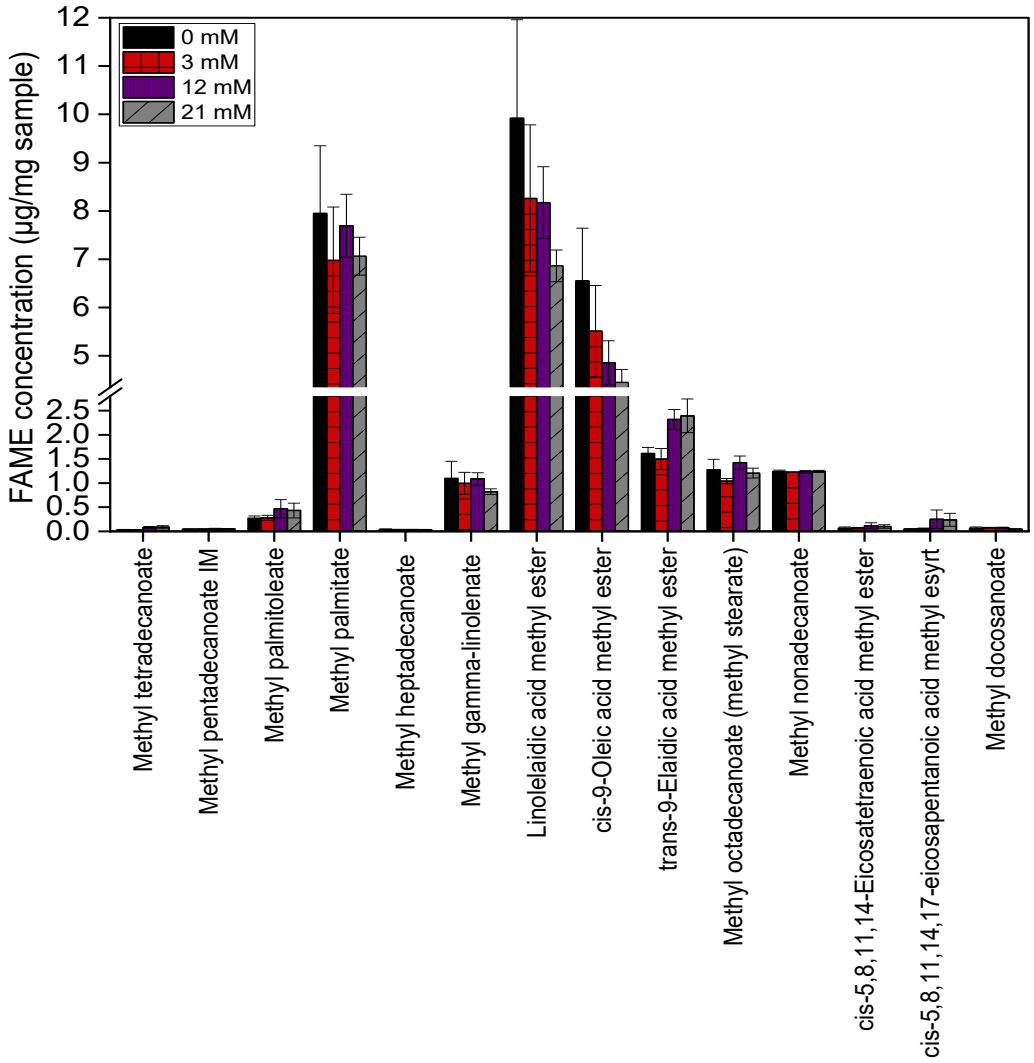

Figure 21. FAMEs production of *Scenedesmus sp* under sodium sulphate concentrations of 0, 3, 12, and 21 mM. Error bars represent the standard deviation from three replicate measurements.

A prior study showed that low sulphate concentrations enhanced lipid biosynthesis [160, 204, 205]. Similarly, at high sulphate concentrations, microalgae shift metabolic activity towards protein biosynthesis, leading to a reduction in polyunsaturated fatty acid and highly unsaturated fatty acids - derived methyl esters synthesis [160, 206]. The interplay between sulphate availability and fatty acid composition is crucial for biodiesel quality. Understanding this metabolic shift is essential for optimising cultivation strategies to enhance specific biochemical outputs based on industrial needs.

4.4.Summary

This study investigated the growth responses of two freshwater microalgae, *Scenedesmus sp* and *C. vulgaris,* at elevated sulphate concentrations. Growth response to sulphate concentration is species-specific. *Scenedesmus sp* and *C.vulgar*is cultures show similar initial growth rates. Then, after 12 days, both species showed growth patterns distinctive from each other. *Scenedesmus sp* transitioned through different growth phases depending on sulphate concentration, while *C. vulgaris* maintained an exponential growth phase except at concentrations above 21 mM. *Scenedesmus sp*. can tolerate higher sulphate concentrations than *C. vulgaris*, highlighting differences in sulphate assimilation between these freshwater species. The pH and humidity patterns were also varied between the two species. These differences were attributed to their sulphate assimilation pathways. *Scenedesmus sp* relies on eukaryotic-type reductase enzymes, while *C. vulgaris* utilises prokaryotic-like plastid sulphate transporters on chloroplast membranes. Elevated sulphate levels induced toxicity and disrupted osmotic balance. Acidic conditions disrupt sulphur metabolism and adenosine triphosphate production, impairing critical enzyme metabolism in microalgae. These results also highlight the crucial role of sulphate in regulating lipid and protein production. Microalgae prioritised protein synthesis over lipid storage for metabolic stability and cellular resilience in a sulphate-rich environment. This demonstrates that an optimal concentration is necessary to balance metabolic processes while avoiding osmotic stress and toxicity.

CHAPTER 5. Tuning carbon and nutrient concentration ratio for biomass, lipid, and protein production

Part of this chapter has been submitted as the following journal article:

L Aditya, U Kuzhiumparambil, PJ Ralph, NB Hoang, MAH Johir, TMI Mahlia, LD Nghiem. Tuning carbon and nutrient concentration ratio for biomass, lipid, and protein production. 2025. Bioresource Technology

5.1. Research objectives

This study aimed to elucidate the interplay between carbon and nutrient input to enhance lipid yield and biomass production. Two model microalgae species, namely *Scenedesmus sp*. and *Chlorella vulgaris*, were cultivated using two different growth mediums (i.e. MaxiGro and Cell Hi HP) and a range of inorganic carbon content to obtain protein and fatty acid methyl ester (FAME) for further characterisation. Microalgae biomass production, cell morphology, cell zeta potential, and biochemical composition were systematically characterised.

5.2.Material and method

5.2.1. Microalgae and associated equipment

Two freshwater green microalgae species, namely *Scenedesmus* sp. (UTS-LD) and Chlorella *vulgaris* (CS-41) were used in this study. *Scenedesmus* sp. (UTS-LD), was isolated by the University of Technology Sydney from Australian water. Chlorella *vulgaris* (CS-41), was from the Australian National Algae Culture Collection at CSIRO Microalgae Research (Hobart, Australia). The microalgae stock cultures of both species were maintained at the Centre for Technology in Water and Wastewater at the University

of Technology Sydney. These two species differ markedly in their morphology. *Scenedesmus* commonly exists as a group of cells within a larger mother wall (coenobium). In this study, *Scenedesmus* exists in coenobium of four cells in a crescent-shaped and about 12 μm in length and 3–5 μm in width. On the other hand, C. *vulgaris* occurs as individual cells in the spherical shape of 2–10 μm in diameter.

Both microalgae strains were cultivated in a series of 1-litre Schott bottles. Arlec LED cool white (ALD1042) lights were used as a light source. The cultivation media utilised in this study were MaxiGro (General Hydroponics, USA) or Cell Hi HP (Fresh by Design, Australia). This study used $NaHCO_3$ (from McKenzie's Bi-Carb) as a carbon source.

5.2.2. Experimental protocol

All cultivation experiments were started at 1-L microalgae solution at the same microalgae biomass concentration of OD_{680} of 0.2 (corresponding to 0.04 mg/mL). The bottles were continuously aerated with compressed air at 1 L/min. During the cultivation process, the bottles were left open to the atmosphere. An amount of growth medium and $NaHCO_3$ ranging from 0 to 1.2 g/L was introduced into the microalgae solution. LED lights delivered 1031 μmol/m^2/s as continuous illumination (24:0h light:dark cycle). The room temperature was 27ºC. All cultivation were measured after 10 days, and each sample had two replicates.

5.2.3. Analytical methods

The microalgal biomass concentration was assessed by quantifying the optical density (OD) using a previously established correlation between dry biomass content and OD, as mentioned in a prior study (Aditya et al., 2023). The microalgal solution's OD was

determined using a UV spectrophotometer (UV 6000 Shimadzu; Australia) at a specific wavelength of 680 nm, utilising a 4 mL Quartz Glass Cuvette. The dry weight was obtained by filtering 100 mL of microalgae solution through 1.1 μm glass filter paper. Subsequently, the filter paper was placed to a 24-hour drying process in an oven set at 60 °C.

Light intensity was measured using a Light Meter (LI-250A li-cor USA) with a quantum sensor (LI-190SA). The room temperature was measured with thermometer (Digitech QM1602) and the water temperature was measured with a glass rod thermometer. A multi-N/C UV TOC analyser (Analytik Jena) was used to characterise inorganic and organic carbon content of the microalgae cultivation solution. Total nitrogen and phosphorus were measured using TNTplus vial kits with the DR3900 spectrometer (Hach Australia). An ion chromatography (Thermofisher, Australia) was used to measure phosphate (PO_4^{3-}). The system includes a Dionex AS-AP autosampler and Dionex AS19 IC column for delivering samples in isocratic mode with the hydroxide gradient. The Zeta potential is measured by using a zeta instrument (Zetasizer Nano ZS Zen 3600, Malvern, UK).

FAME analysis was carried out using a GC-MS (QP2020 Shimadzu Corporation, Kyoto Japan) equipped with an autosampler (AOC-20is Shimadzu Corporation). The column used was an SH-Rxi-5Sil MS fused silica capillary column (30.0 m x 0.25 mm x 0.25 μm) operating in electron impact mode at 70 eV. Helium was used as the carrier gas at a constant flow of 1.0 mL min-1 and an injection volume of 1 μL, with an injector temperature of 280 °C and an ion source temperature of 230°C. The injection volume was 2 μL. The oven temperature was programmed for a gradient of 50 ℃ (held for 2 min) to 220 ℃ (4 ℃/min), 220 ℃ to 300 ℃ (60 ℃/min) and held for 3 min. FAME peaks were

identified by comparison of their retention times with authentic standards and quantified by area normalisation and response factor.

Total lipid content was determined gravimetrically. Nonadecanoic acid (C19:0) was used as the internal standard. Dried lipids were treated with 1 mL of 1% NaOH in MeOH, heated for 15 min at 55 °C, followed by the addition of 5% methanolic HCl (2 mL) and heated for 15 min at 55 °C. 1 mL Milli-Q water was added, and FAMEs were extracted by hexane (3 × 1 mL) and evaporated to dryness under nitrogen. They were redissolved in 200 μL of hexane and stored in −20 °C in glass vials until GC–MS analysis. Simultaneous production of carotenoids and chemical building blocks precursors from chlorophyte microalgae.

5.3.Result and discussion

5.3.1. Growth medium nutrient variability and microalgae responses

Detailed growth medium analysis shows marked differences in the concentration of specific macro and micronutrients between MaxiGro and Cell Hi HP (Table 3). Previous research has suggested that nutrient concentrations and growth medium may influence the growth rate and biochemical composition of mature microalgae cells.

Table 3. MaxiGro and Cell Hi HP growth medium at 1 g/L concentration. The standard deviation from two replicate measurement.

Medium compositions	MaxiGro (mg/L)	Cell Hi HP (mg/L)
TN	277±0.0	243±0.0
TP	65.7±0.0	52.4±0.0
PO_4^{3-}	-	51.64±0.2
K	145.4±1.3	272.0±0.9
Mg	21.6±1.9	7.7±0.7

Ca	7.8±2.7	1.2±5.9
Fe	1.7±1.0	5.4±1.4
Mn	1.0±0.7	0.7±0.5
Zn	0.7±0.5	0.9±0.5
Na	2.2±0.6	30.3±1.4

MaxiGro showed a higher concentration of total nitrogen and total phosphorus, which has been shown to boost microalgae biomass production [207]. Orthophosphate (PO_4^{3-}) was not detectable in MaxiGro, despite a high total phosphorus content. Previous research has shown that orthophosphate is essential for microbial activities and the lack of phosphorus in this form may induce changes in physical properties and nucleic acid synthesis [208, 209]. The absence of PO_4^{3-} in the MaxiGro medium may also impact the phosphorylation processes within cells [210]. Phosphorylation, a primary energy carrier, depends on phosphate groups derived from ATP (adenosine triphosphate). Phosphate deficiency may lead to reduced ATP synthesis and, consequently, lower protein production [211]. In agreement with the literature, results from this study also show lower protein production in *Scenedesmus* sp. grown in MaxiGro compared to Cell Hi HP. Additionally, phosphate limitation may cause changes in cell size, shape, and pigment production. It was also observed that *Scenedesmus* sp. grown in MaxiGro developed an elongated rod morphology, while those in Cell Hi developed towards a coccus shape, even though both cultures were cultivated simultaneously using the same inoculum.

Magnesium and calcium concentrations in MaxiGro were three and six-fold greater than those in Cell Hi HP, respectively. When culturing in Cell Hi HP growth media, *Scenedesmus* sp. was yellowish compared to MaxiGro despite being cultivated simultaneously. This result aligns with a prior study stating that higher calcium and

magnesium may lead to the production of secondary metabolites. These secondary metabolites have higher antioxidants and pigments [212, 213].

Magnesium plays a crucial role in the structure of chlorophyll, the molecule responsible for photosynthesis in microalgae [214]. Magnesium complexes with chlorophyll and is located at the centre of the molecule to allow for capturing light energy and conversion to chemical energy [215]. Magnesium also acts as a cofactor in many enzymatic reactions, including those involved in Calvin cycle for carbon fixation. It acts as a cofactor for ATP-utilizing enzymes. Lower magnesium concentrations could explain the observed yellowish colour in Cell Hi HP cultures, indicating chlorophyll deficiency and, thus, less efficient photosynthesis [216].

Cell Hi HP has significantly higher potassium, iron, and sodium content than MaxiGro. Potassium and iron support protein synthesis and improve osmotic balance in microalgae [217, 218]. Potassium plays a critical role in maintaining the cell's osmotic balance, since potassium manages the influx and efflux of water and other solutes, which affects nutrient uptake and metabolite transport [219, 220].

Iron plays an important role in nitrogen assimilation processes. Many enzymes involved in nitrogen metabolism require iron, such as nitrate reductase and nitrogenase. Since nitrogen is a key part of amino acids, which are the building blocks of proteins, having enough iron is crucial for producing proteins effectively [221, 222]. Higher potassium and iron in Cell Hi HP may support a more stable growth environment, since potassium and iron help in maintaining osmoregulation and electron transport chain [223]. On the other hand, sodium in microalgae is important for maintaining osmotic and ionic balance, like potassium. However, its role is often less critical in freshwater species, which tend to be more sensitive to sodium concentrations [224, 225]. High sodium

concentrations can significantly induce changes in microalgae, impacting their metabolism, growth, and survival [225-227]. For example, sodium can interfere with the electron transport chain in chloroplasts, reducing the efficiency of photosynthesis and thus decreasing the overall energy production within the cell. The severity of these effects largely depends on the specific species of microalgae [228, 229].

5.3.2. *Scenedesmus* growth in MaxiGro and Cell Hi HP media

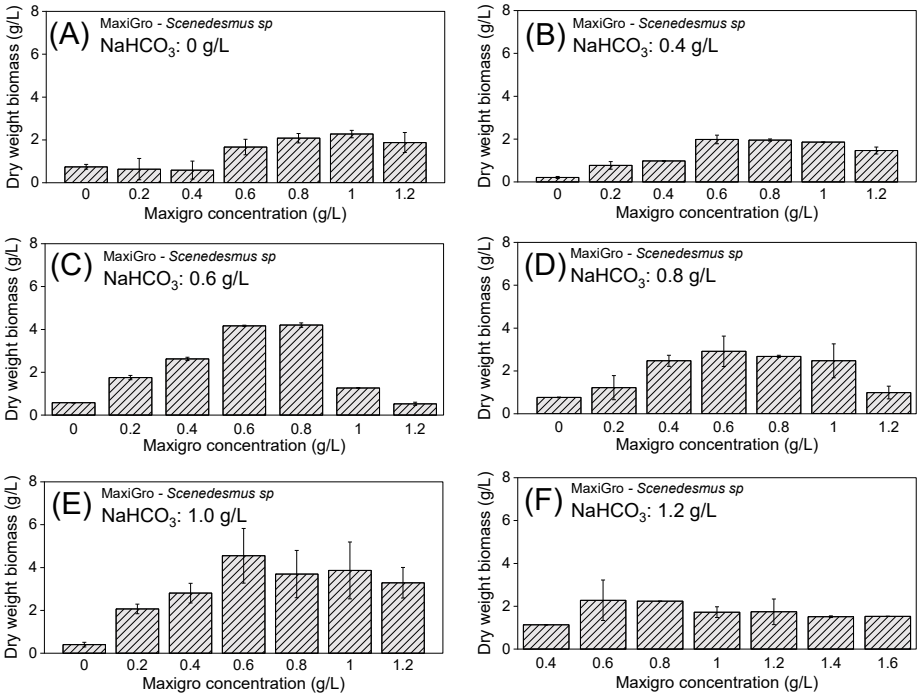

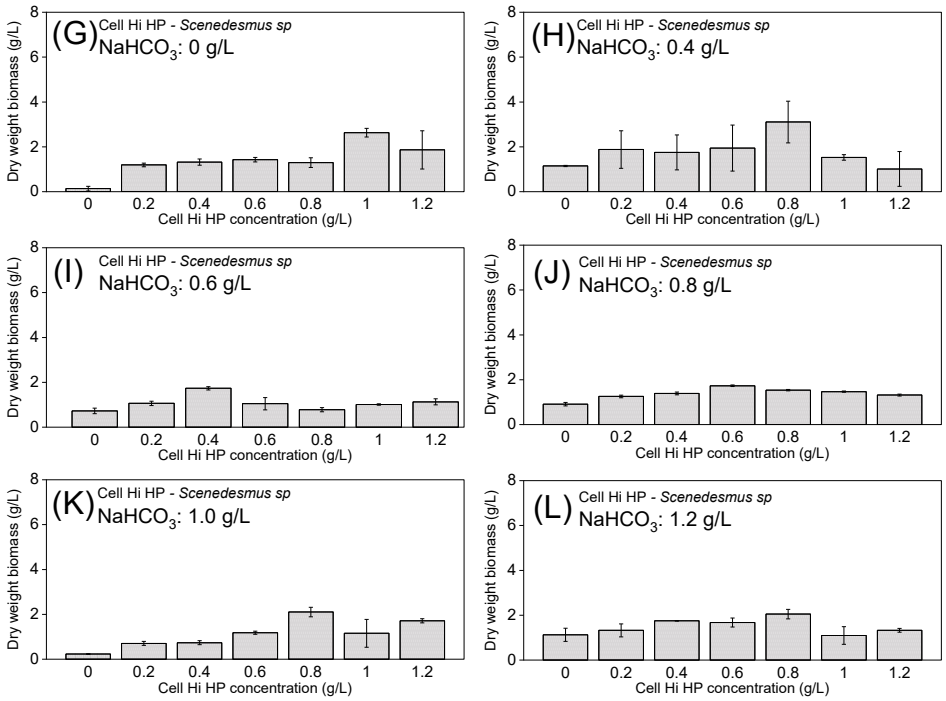

Figure 22. Dry-weight *Scenedesmus* biomass content after 10 days of cultivation as a function of $NaHCO_3$ concentration and Maxigro (A-F) or Cell Hi HP (G-L) concentration. Error bars represent the standard deviation from two replicate experiments.

Tuning the nutrient composition to match the specific needs of the microalgae species significantly improved the production of biomass and metabolite. Without any carbon addition, both growth media show a similar growth profile, achieving *Scenedesmus* optimal growth at MaxiGro or Cell Hi HP content of 1 g/L in the culture solution (Figure 22A and Figure 22G). Without no additional carbon addition, the highest microalgae concentration in mature solution cultivated by MaxiGro or Cell Hi HP was 2.4 and 2.6 g/L (in dry weight), respectively. Optimal growth increases when inorganic carbon is added to the culture solution. A notable increase in microalgae growth rate from 2.4 and 2.6 (without carbon addition) to 5.5 and 4.8 (with 1 g/L $NaHCO_3$) is shown at MaxiGro and Cell Hi HP growth media, respectively. Importantly, there is also a shift to lower growth media concentration to achieve the optimum microalgae growth (Figure

22B and Figure 22H). The highest microalgae biomass production in the stationary phase solution is shown at 1 g/L $NaHCO_3$ concentration and 0.6 g/L MaxiGo content, resulting in 5.5 g/L dry weight of biomass production (Figure 22E and Figure 22K).

Overall, Figure 22 demonstrates that when the concentration of $NaHCO_3$ is increased, the demand for growth medium decreases. This finding is consistent with previous studies, which showed that $NaHCO_3$ significantly enhances biomass and chlorophyll in microalgae, reducing the requirement for additional growth media components [230, 231]. This observation is also consistent with established science in microalgae physiology [232, 233]. Microalgae rely on multiple metabolic pathways to support their growth. When the carbon source is restricted, microalgae prioritise the production of light-harvesting substances such as chlorophyll and carotenoids [234]. These light-harvesting substances allow for more efficient photosynthesis and, thus, more carbon utilisation. These pigments are mostly proteins; thus, their production also increases the nutrient demand. Results in Figure 22 are also consistent with recent research findings. The maximum growth of microalgae has been reported at 12 mM for *Scenedesmus sp* [235] of $NaHCO_3$. Both studies highlight the role of $NaHCO_3$ as an effective inorganic carbon source that enhances biomass productivity. Both studies also affirm that exceeding the optimal level can inhibit growth due to increased pH and excessive sodium ion concentrations, which create unfavourable conditions for microalgae. Excessive amounts of sodium can disrupt the electron transport chain in chloroplasts, reducing the efficiency of photosynthesis and lowering cell energy production

5.3.3. *C. vulgaris* growth in MaxiGro and Cell Hi HP media

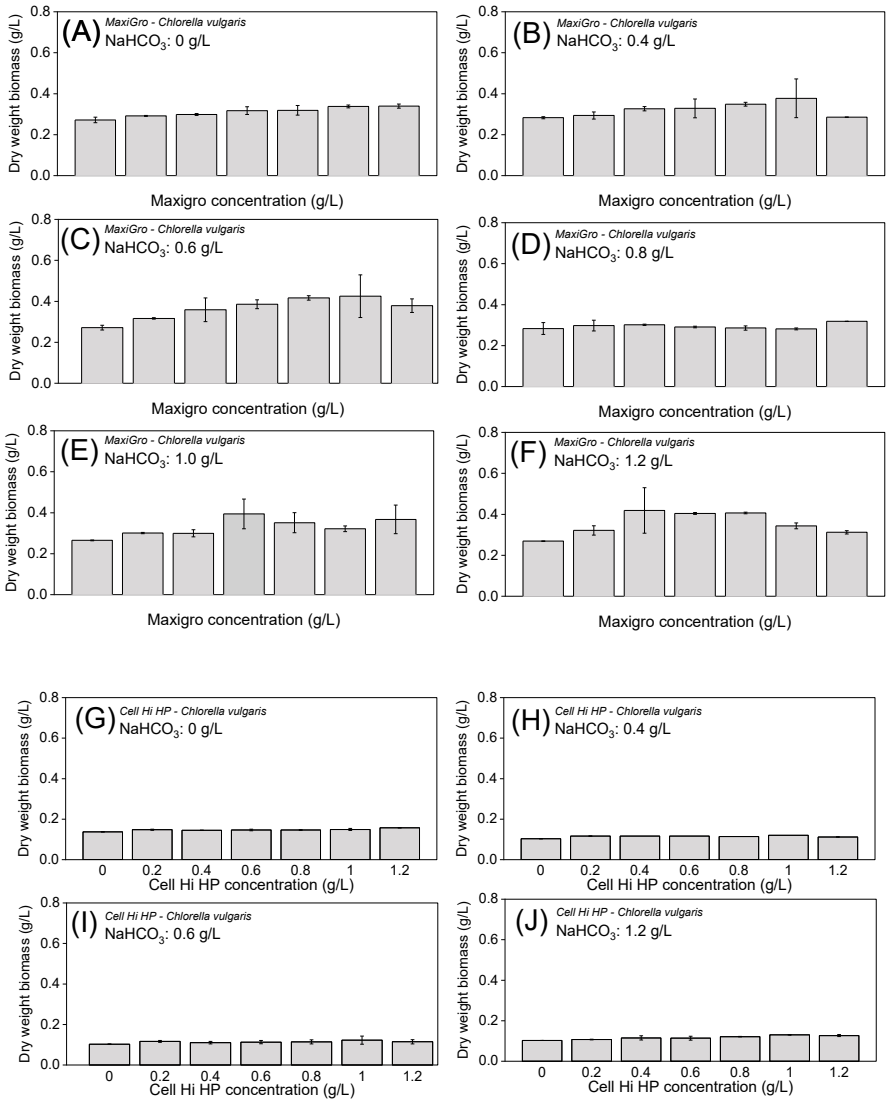

Figure 23. Dry-weight *C.vulgaris* biomass content after 10 days of cultivation as a function of $NaHCO_3$ concentration and Maxigro (A-F) or Cell Hi HP (G-J) concentration. Error bars represent the standard deviation from two replicate experiments.

C. vulgaris shows increasing growth rates as $NaHCO_3$ concentration increases (Figure 23). The optimal growth rate also shifts to lower growth medium concentrations as the $NaHCO_3$ concentration increases; a similar pattern is shown in *Scenedesmus* sp. biomass production (Figure 23). For example, when $NaHCO_3$ concentration is at 0.4 g/L,

optimal growth is achieved at 1 g/L MaxiGro. Increasing the bicarbonate to 1.0 g/L shifts the optimal growth to 0.6 g/L MaxiGro. This finding indicates that, as the concentration of $NaHCO_3$ rises, less growth medium is needed. This supports previous findings showing that the maximum C. *vulgaris* growth was 10 mM [224]. This also indicates that the right balance of $NaHCO_3$ increases *C. vulgaris* growth rate [224, 230, 236, 237].

The results also suggest that *C. vulgaris* tends to increase in cell size under high sodium concentrations, with a noticeable reduction in surface charge density. This aligns with prior findings that high sodium concentration can lead to morphological changes in microalgae, including the formation of cell surface charge due to the dissociation of sodium ions coating the microalgae cell walls [238].

C. vulgaris growth rates in Cell Hi HP medium show a significant reduction, indicating that Cell Hi HP is not a suitable growth medium for *C. vulgaris*. This might be due to the high sodium concentration, which inhibits freshwater species growth (Figure 23G-J). These results show a significant impact of medium composition on microalgae growth and physiological responses. Understanding this impact of growth media composition and $NaHCO_3$ relationships further helps to optimise and tailor biomass production of targeted algal species.

5.3.4. Effect of growth medium on cell surface charge and aggregation

Growth medium concentration and carbon concentration have a notable impact on the surface charge of the microalgae cells. The surface charge of microalgae, indicated by zeta potential, is significantly influenced by several factors, including the growth condition and pH. Growth media components strongly affect these growth conditions, particularly the aqueous medium's ionic strength [239]. The thickness of the microalgae

surface charge is significantly related to the ionic strength of their environment. The main factor affecting the ionic strength of the growth medium is multivalent metal salt. Cell Hi HP has higher multivalent metal salts from sodium, potassium, and iron; consequently, Cell Hi HP has high ionic strength. The forces attracting opposite charges become stronger in high ionic strength, accumulating the opposite ions on the microalgae's surface. This makes the electrostatic behaviour of the microalgae more pronounced, thus increasing the zeta potential value of microalgae cells [239, 240]. These results agree with the previous finding; the increased ionic strength of the culture medium increased the zeta potential of *C. vulgaris* [240]. The surface charge of *Scenedesmus dimorphus* shifted from negative to positive as the ionic strength increased [241].

The surface charge is also significantly affected by pH, which can be adjusted by altering the carbon concentration [242, 243]. Variations in $NaHCO_3$ concentration can alter the ionic strength and pH of the medium, thereby affecting the zeta potential of the cells. Studies have shown that microalgae exposed to higher $NaHCO_3$ concentrations can exhibit changes in surface charge due to the increased uptake of bicarbonate ions or hydrogen ions, which modify the ionic balance at the cell surface [244]. Moreover, zeta potential of microalgae decreases as pH values increase [240] and tends to be constant when the pH value further increases [243]. In this study, both growth media have an initial pH below 5 at the start of the experiment. However, this does not affect the surface charge values because the zeta potential was measured after 10 days of cultivation, when the microalgae had transformed the acidic environment to an alkaline.

Both species show similar patterns of zeta potential value for 0.6 g/L and 1.2 g/L of the growth medium, suggesting that the growth medium more influences specific metabolic pathways for surface charge than by $NaHCO_3$ concentration (Figure 24). Zeta

potential has critical implications for microalgae aggregation or separation. Elevated zeta potential indicates a higher surface charge, which can cause particles to repel each other or aggregate more easily [243, 245]. This leads to microalgae clumping or separating, contrary to their natural behaviour in environments. Aggregated microalgae are beneficial for harvesting since they can be collected more efficiently, reducing the cost and complexity of harvesting [246]. Changes in the growth medium can alter how microalgae aggregate. This dual impact of growth medium and $NaHCO_3$ concentration highlights the complex interplay between nutrient availability and carbon source in determining the electrochemical properties of microalgae. Thus, tailoring growth conditions to create specific characteristics is crucial for harvesting microalgae.

Scenedesmus sp. grown in MaxiGro developed towards an elongated rod morphology. On the other hand, those in Cell Hi developed towards a coccus shape, even though both were cultivated simultaneously using the same inoculum. These results align with a prior study that shows the zeta potential of microalgae changes with different conditions, affecting their aggregation behaviour [243] and morphology [247]. Additionally, both microalgae species grown in Cell Hi HP medium show higher zeta potential than those grown in MaxiGro, which can be attributed to their lower growth rates. The rapid growth rate can minimise the intercellular interaction between the cells, resulting in a strong electronegative surface charge and significant repulsion [248]. This finding is consistent with previous studies suggesting that lower growth rates can reduce zeta potential in microalgae [3, 249].

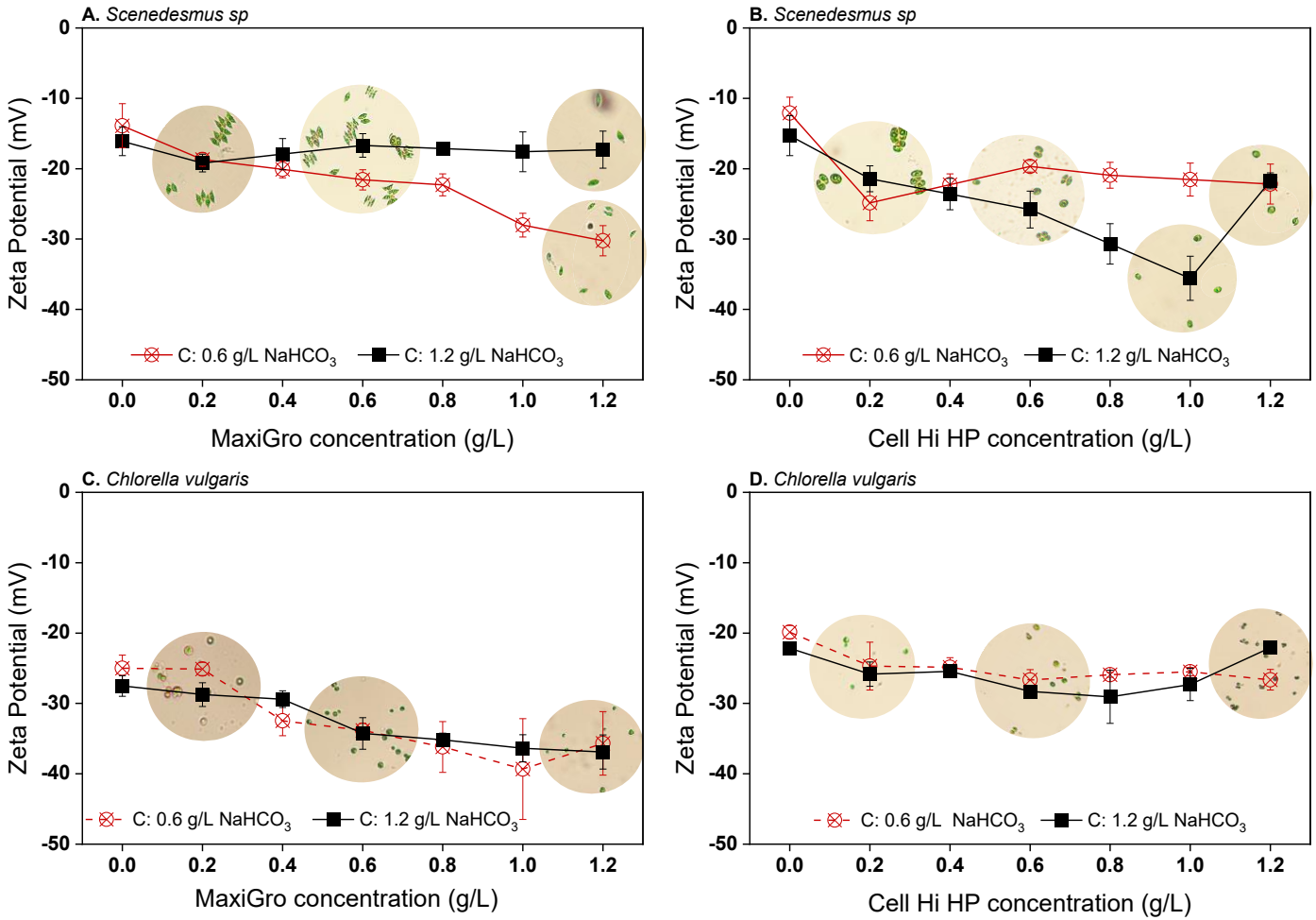

Figure 24. *Scenedesmus* and *C. vulgaris* growth after 10 days of cultivation in MaxiGro and Cell Hi HP at 0.6 and 1.2 g/L, with identical $NaHCO_3$ concentrations. The zeta potential result was more significant under 0 g/L $NaHCO_3$ concentrations. Error bars represent the standard deviation from three replicate measurements.

5.3.5. Effects of growth medium and bicarbonate input on *Scenedesmus* cell content

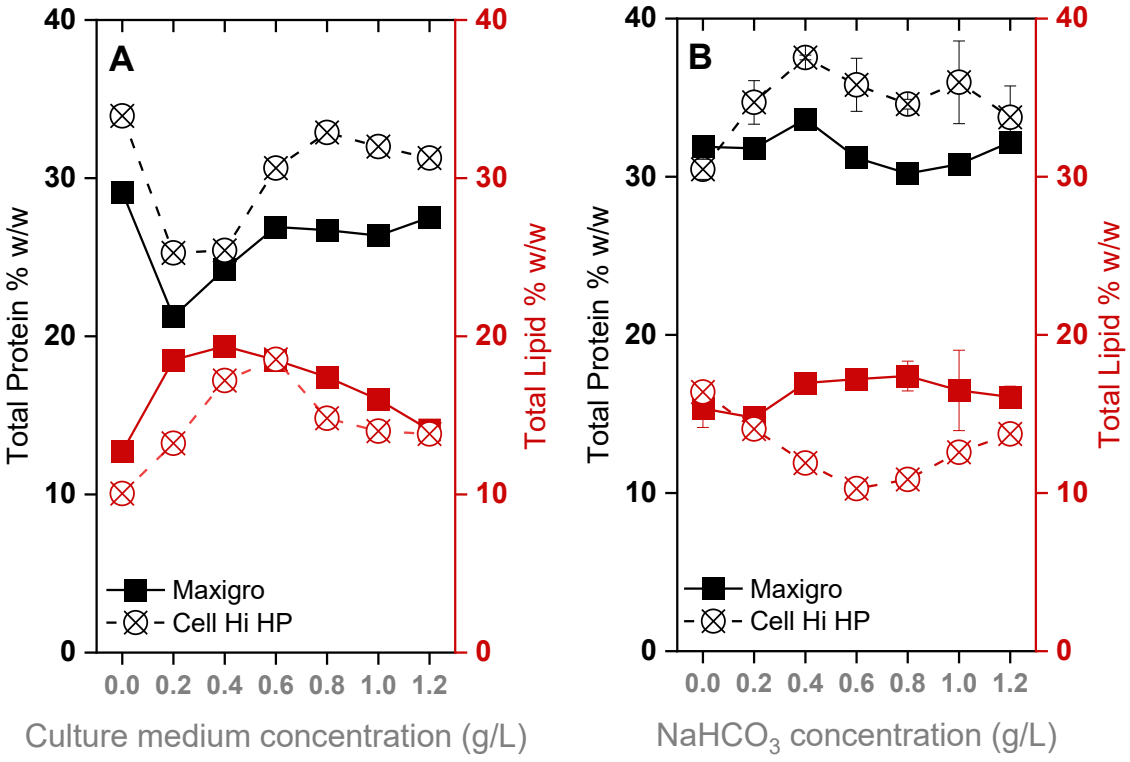

Figure 25. Total protein and lipid content of *Scenedesmus* in varied culture medium (A) concentration and varied $NaHCO_3$ (B). Error bars represent the standard deviation from three replicate measurements.

Growth medium and $NaHCO_3$ concentration can also significantly impact protein and lipid production. Protein production increases with the increased concentration of both growth mediums (Figure 25A). Protein production is also affected by $NaHCO_3$ concentration, showing the optimum condition at 0.4 g/L $NaHCO_3$ (Figure 25B). The highest protein production is achieved at 0.4 g/L $NaHCO_3$ and 0.6-0.8 g/L Cell Hi HP, reaching 37.5% w/w in Figure 25A-B.

Lipid production decreases as the concentration of both growth mediums increases (Figure 25). The highest lipid production occurs at 0.4 g/L MaxiGro and 0.6 g/L Cell Hi HP, achieving 19.4% and 18.5% w/w total lipid, respectively. Lipid production remains relatively stable with varying $NaHCO_3$ concentrations in the MaxiGro medium (Figure 25B). However, lipid production in the Cell Hi HP medium shows the lowest at 0.6 g/L $NaHCO_3$ (Figure 25B), while at a similar Cell Hi HP concentration (0.6 g/L $NaHCO_3$), it produces the highest protein. The highest lipid production is achieved at 0.6 g/L $NaHCO_3$ and 0.4 g/L MaxiGro.

These results agree with previous studies, which highlighted lipid productivity by *Scenedesmus* sp. can be enhanced by balancing $NaHCO_3$ and growth medium [250, 251]. *Scenedesmus* sp. grown in Cell Hi HP has slightly higher protein content due to higher iron levels [252], while *Scenedesmus* grown in MaxiGro has slightly higher lipid content, which is attributed to orthophosphate limitation [253]. Lipid content in *Scenedesmus obliquus* nearly doubled when phosphorus concentration was halved [254, 255]. Results in Figure 25B suggest that both microalgae species in this study are sensitive to high sodium levels since they can only occur in freshwater. The impact of sodium varies widely depending on the specific type of microalgae. Therefore, changes in sodium levels have little impact on protein production in these freshwater species. This is also consistent with a prior study, which demonstrated that under optimal $NaHCO_3$ concentration, microalgae show increased protein content, especially in amino acids such as glutamic acid, cystine, and arginine [256].

5.3.6. FAME content in varied growth medium concentrations

The production of fatty acid methyl esters (FAMEs) in microalgae is significantly influenced by the growth medium and the concentration of various nutrients. In both growth mediums, the maximum FAME production was 0.4 g/L and 0.6 g/L of MaxiGro and Cell Hi HP, respectively. This result is similar to the highest lipid concentration produced by both growth mediums. This is because lipids in microalgae mainly consist of triglycerides, phospholipids, and free fatty acids. Triglycerides are the primary precursors for FAMEs, and triglycerides react with methanol to form FAMEs and glycerol during transesterification (converting lipids to biodiesel).

Among all the FAME results, Maxigro shows higher FAME production compared to Cell Hi HP, except for Trans-9-Elaidic-methyl ester. Like its effect on lipid production, the high FAME production under MaxiGro growth medium is attributed to the higher nutrient availability in this growth medium. However, the low output of Trans-9-Elaidic-methyl in MaxiGro can be attributed to a lack of detectable orthophosphate. Trans fatty acids like Trans-9-Elaidic-methyl acid are typically formed through specific enzymatic processes, including the isomerisation of cis fatty acids. Enzymes involved in these processes require adequate energy, which is influenced by ATP's availability of phosphate groups [247].

Among the various $NaHCO_3$ concentrations tested, 0.8 g/L resulted in the highest FAME production, which probably provides the balance needed to produce maximum FAME production. Some specific FAMEs, such as methyl pentadecanoate and methyl palmitoleate, have less effect under different $NaHCO_3$ concentrations. However, this particular FAME has significant effects under different growth mediums. It is probably

because the $NaHCO_3$ concentration falls within a range that does not significantly impact their biosynthesis. Conversely, the synthesis of most methyl esters such as methyl decanoate, increased linearly with higher $NaHCO_3$ concentrations, reaching its peak at 0.8 g/L in the MaxiGro medium. Beyond this point, at 1 g/L $NaHCO_3$, its production started to decline. The same pattern was also shown in Methyl Palmitate, Methyl Heptadecanoate, Methyl Linoleate, Methyl Octadecanoic, Methyl Cis-111-Eicosenoate, Methyl Arachidonate, Methyl Erucate, and Methyl Lignocarate. This pattern suggests that synthesis for these methyl esters is closely related to $NaHCO_3$ availability within the MaxiGro medium.

The interplay between growth media and $NaHCO_3$ concentration significantly impacts the production of certain FAMEs, such as Methyl Gamma Linoleate (ALA) and Methyl Heptadecanoate. This implies that both factors significantly influence the biosynthesis of these compounds, highlighting the importance of optimising both growth medium and carbon for specific FAME production [257].

For application purposes, such as lubricant, 0.4 g/L MaxiGro is recommended. This concentration has the optimal production of FAMEs such as methyl laurate and cis-9-Oleic acid methyl ester, known for their excellent lubrication properties [258]. Methyl Tetradecanoate is also produced in significant quantities. Methyl Tetradecanoate supports cool flow properties, making the oil more efficient under varying temperature conditions [259, 260]. The presence of Methyl palmitate and Methyl Cis-11-Eicosenoate, which also has the highest production at 0.4 g/L MaxiGro, supports the optimal concentration at 0.4 g/L MaxiGro. Methyl Palmitate and Methyl Cis-11-Eicosenoate enhance the lubricity of the lubricant, reducing friction between mechanical parts [261].

Understanding the effects of different growth media and $NaHCO_3$ concentrations on FAME production is crucial for optimising microalgae cultivation for industrial applications and biochemical production [262].

5.4. Summary

This study demonstrates the importance of optimising carbon and nutrient inputs for enhancing lipid and protein production in microalgae. The result shows that increasing carbon input can reduce nutrient demand for the same growth rate. Inputting excessive nutrients or carbon can negatively impacts microalgae morphology and surface charge. Moreover, the nutrient composition of the growth media significantly influences lipid and protein production. MaxiGro has higher lipid production due to higher magnesium content, and Cell Hi HP has higher protein because of higher potassium and iron levels.

CHAPTER 6. Microalgae enrichment for biomass harvesting and water reuse by ceramic microfiltration membranes

Part of this chapter has been published as the following journal article:

Aditya, L., Vu, H.P., Nguyen, L.N., Mahlia, T.I., Hoang, N.B., Nghiem, L.D. 2023. Microalgae enrichment for biomass harvesting and water reuse by ceramic microfiltration membranes. Journal of Membrane Science, 669, 121287.

6.1. Research objectives

This study aims to evaluate the efficacy of aerated membrane filtration for microalgae enrichment and permeate reusability. This study major mechanisms governing the membrane filtration and regrowth with the permeate water for *C. Vulgaris* and *Scenedesmus sp.* Are discussed. Using the membrane to simultaneously concentrate the microalgae solution and recover the clean water for reuse, significant cost savings can be expected. This study's results contribute to optimising large-scale microalgae cultivation harvesting and permeate reusability.

6.2. Material and method

6.2.1. Microalgae

Two microalgae strains were used, namely *Chlorella vulgaris* (CS-41) from the Australian National Algae Culture Collection CSIRO Microalgae Research (Hobart, TAS, Australia) and *Scenedesmus sp.* (UTS-LD) isolated from Australia by the University of Technology Sydney. *Chlorella sp.* And *Scenedesmus sp.* Are two of the

most studied green microalgae due to their potential for a range of industrial applications including biofuel, bioplastics, and the production of other bioproducts. The *C. Vulgaris* (CS-41) is a spherically shaped green microalga of 2-10 μm in diameter. On the other hand, *Scenedesmus sp.* Is usually found in coenobium (or multicell forms). In other words, *Scenedesmus sp.* Often occurs as multiple of two cells inside a parental mother wall. *Scenedesmus sp.* Also has other self-defence mechanisms, including a thick cell wall with mucilage and long bristles at each end of the individual cell. The *Scenedesmus sp.* (UTS-LD) in this study occurs in a group of four cells, each cell has comb shape of about 12 μm in length and 3-5 μm in width. Stock cultures were maintained at Algae Production Facility at the University of Technology Sydney, using MLA and f/2 media (algaboost, Australia) for *Chlorella vulgaris* and *Scenedesmus sp.,* respectively.

6.2.2. Membrane filtration system

Submerged microfiltration (MF) system was used in this study (Figure 26). The system consisted of a flat sheet ceramic membrane module (Suzhou Dasen Electronic Material Co., Ltd., Jiangxi, China) with a nominal pore size of 0.1 μm and 750 cm^2 in total surface area. The membrane module was fully submerged in a rectangular glass vessel of 20 cm in length, 4 cm in width, and 45 cm in height. A Masterflex Peristaltic pump (Cole-Parmer, USA) was connected to the membrane module for clean water extraction. The system was equipped with a digital pressure gauge data logger to monitor the transmembrane pressure (TMP). A rectangular stone diffuser connected to an air pump was placed at the bottom of the membrane vessel for aeration. Another Masterflex

Peristaltic pump (Cole-Parmer, USA) was used to regularly supply new microalgae solutions to the system when required.

6.3. Result and discussion

6.3.1. Microalgae enrichment by MF membrane filtration

TMP increase was moderate during the enrichment process in all experiments. The observed TMP increase was due mostly to the formation of a cake layer of microalgae cells on the membrane surface [263]. Membrane fouling was specific to each individual microalgae species. Figure 26 shows notable fouling by *C. vulgaris* while *Scenedesmus sp.* Only resulted in mild fouling. Membrane fouling was lower when the module was aerated compared to non-aerated condition. Without aeration, TMP raised by over 56% and 38% for *C. vulgaris* and *Scenedesmus sp*, respectively. Due to the microalgae cell cake layer on the membrane surface, the permeate flux gradually decreased from the initial set point especially when filtering the *C. vulgaris* solution, thus, the actual permeate flux as a function of time is reported in Figure 26.

The difference in fouling rate between *C. Vulgaris* and *Scenedesmus sp.* Can be attributed to their cell dimension and morphology. Characteristics of the cake layer including porosity and compactness, are affected by cell shape and physical properties [264]. *C. vulgaris* is spherical in shape and occurs as individual cells. By contrast, *Scenedesmus sp.* Has a cylindrical-fusiform shape and occurs as a coenobium of four cells. In this study, the coenobium of *Scenedesmus sp.* Was four times larger than *C. vulgaris* in lengthy, resulting in a more porous cell cake layer and lower TMP increase as

observed in Figure 26. Because of its morphology, it only allows *Scenedesmus sp.* To adhere to membrane walls without covering the pores entirely.

Aeration could effectively reduce membrane fouling, especially when caused by a denser cell cake layer (*C. vulgaris*). The decreased membrane fouling under aerated conditions could be ascribed to the synergistic effects of buoyancy and drag force from flowing bubbles. The impact of aeration was also species dependent. At a water recovery of 40% without aeration, the TMP of *C. Vulgaris* and *Scenedesmus sp.* Reached 48 kPa and 23 kPa, while in aerated condition, it was only 20 kPa and 8 kPa, respectively. In addition to cell dimension (and thus cake layer porosity), the morphology of the cell surface can also play a significant role, as discussed in the next section.

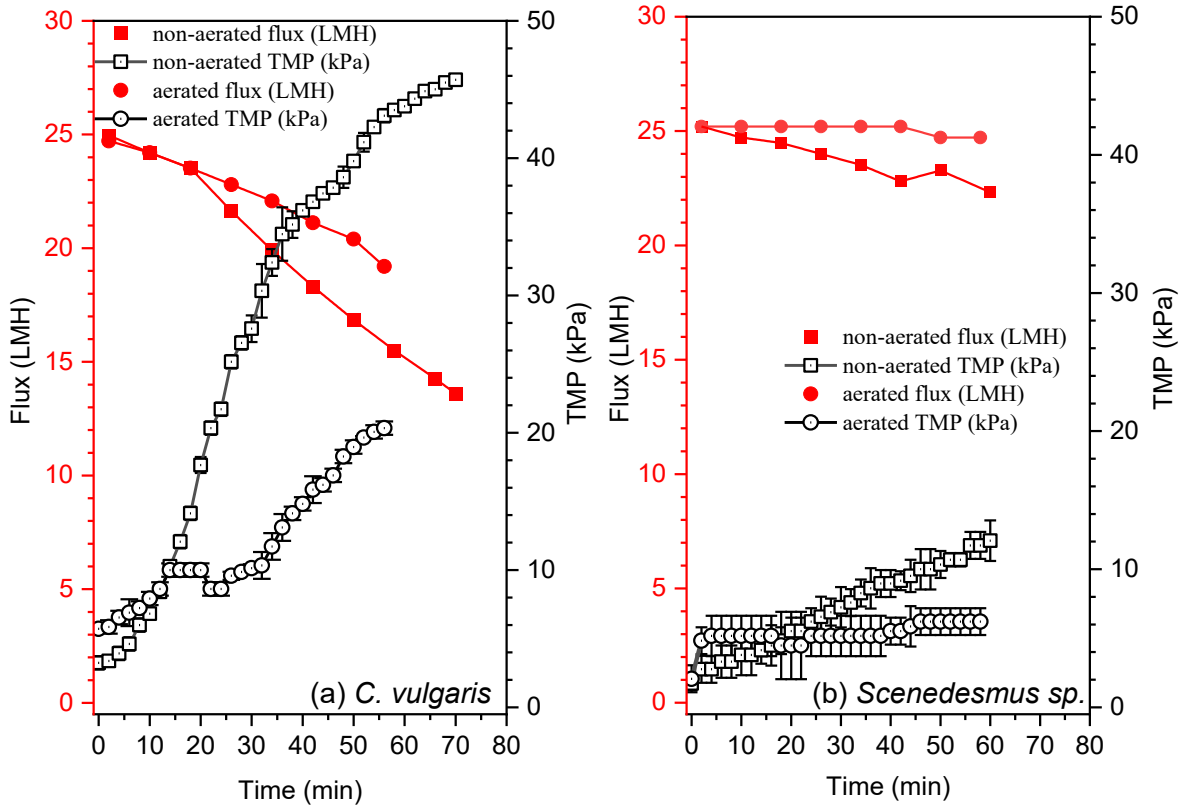

Figure 26. Comparison of TMP and permeate flux during the dewatering microalgae solution (a) C. *Vulgaris* and (b) *Scenedesmus* sp. In aerated and non-aerated conditions.

Experiments were conducted at 40% water recovery. The error bar represents the standard deviation from two measurements.

6.3.2. Backwashing efficiency

Backwashing using permeate water was efficient to restore the membrane permeability (Figure 27). TMP was restored to the original value after backwashing in all experiments. The backwashing efficiency was microalgae species-specific. When enriching *Scenedesmus sp.,* the required time and permeate volume for backwashing assisted by aeration were 1 min and 25 ml, corresponding to about 0.25% of the produced permeate volume (at 80% recovery). These values are about 5 times lower compared to those used for *C. vulgaris*. The difference in backwashing efficiency can be ascribed to the dimension, shape, and morphology of microalgal cells. The *C. Vulgaris* resulted in a more compact cake layer compared to *Scenedesmus sp* due to its size and shape.

Of a particular note, while *Scenedesmus sp.* can be effectively backwashed, visual inspection showed a tinge of green on the membrane surface, evidence of incomplete removal of all microalgae cells by backwashing. By contrast, backwashing after *C. Vulgaris* filtration resulted in a completely clean membrane surface without any residue of microalgae cells (Figure 27). *C. vulgaris* is spherical, with rigid cell walls preventing them from adhering to the membrane surface. *Scenedesmus sp.* Has a slimy outer layer with bristles on each cell. The coenobium structure of *Scenedesmus sp.* May also result in imperfectly formed cell groups. Deformed or ruptured cells can tightly adhere to the membrane surface. A broken cell can release oil droplets that easily adhere to the cell wall and the membrane surface. Although residue of *Scenedesmus sp.* was insignificant

after one filtration cycle and the membrane permeability was still fully restored, the results in Figure 28 highlight the need to evaluate backwashing efficiency after repetitive filtration cycles.

Aeration could only slightly reduce membrane fouling during *Scenedesmus sp.* Filtration but was important to enhance backwashing efficiency. After *C. Vulgaris* and *Scenedesmus sp.* Filtration, 1 min of backwashing time was required with aeration. By contrast, without aeration the backwashing time increases to 4 min to achieve the same outcome. It is evidenced that aeration can create a turbulence condition at the membrane surface to dislodge the microalgae cell cake layer.

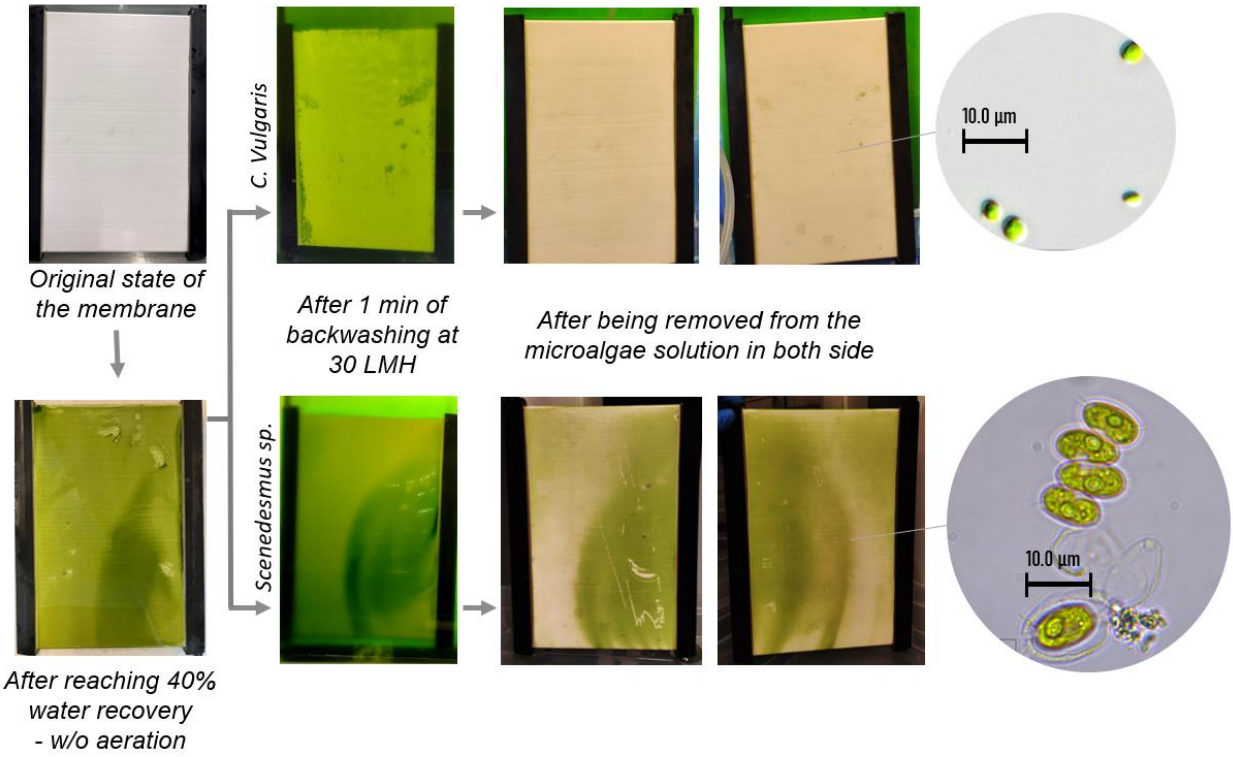

Figure 27. The ceramic membrane profile before and after backwashing of *C. Vulgaris* and *Scenedesmus sp.*

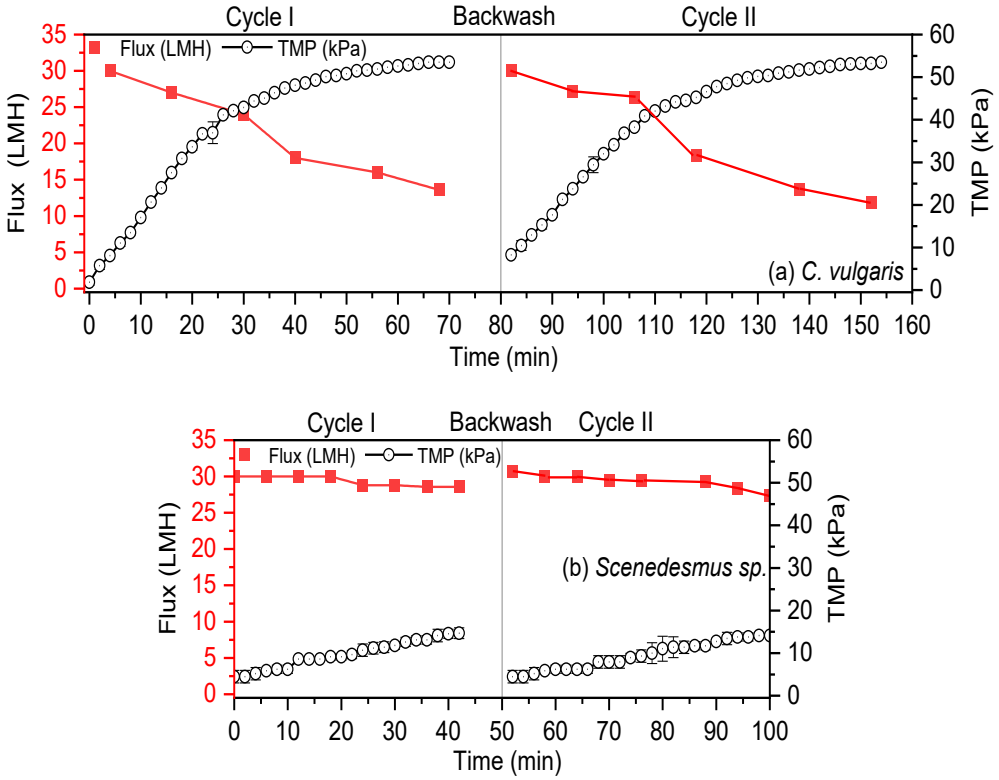

Figure 28. TMP profile and membrane flux (LMH) before and after backwashing for (a) *C. Vulgaris* and (b) *Scenedesmus sp*. Water-backwash was sufficient to restore the ceramic membrane to its original state. Experiments were conducted at 40% water recovery. The error bar represents the standard deviation from two measurements.

6.3.3. Multi filtration cycle performance

6.3.3.1. Initial permeate flux

The effect of initial permeate flux on membrane fouling was investigated in the range from 25 to 51 LMH under aerated conditions. T the effect of initial permeate flux on membrane fouling was microalgae species-specific. Notable fouling was observed in *C. Vulgaris* at the initial permeate flux of 50 LMH. TMP significantly increased and permeated flux significantly decreased during the first 20 min of the filtration experiment

with *C. Vulgaris*. Membrane fouling was lower when the initial permeate flux was 30 LMH. As filtration continued, a further decrease in flux was noticed in 30 and 50 LMH, although it is substantially smaller (referred to as steady-state flux). At initial permeate flux 25 LMH, permeate fluxes had not reached steady-state flux after 40% of water recovery. By contrast, *Scenedesmus sp.* Shows no discernible fouling of the aforementioned initial flux values. The initial flux of 51 LMH only resulted in mild fouling. The maximum TMP reached by 51 LMH was 25 kPa. 25 and 30 LMH initial permeate flux had a negligible effect on TMP and permeate flux. Since less membrane fouling was observed in 25 LMH, the initial permeate flux of 25 LMH was selected for subsequent multi-filtration cycle performance.

6.3.3.2. Multi filtration cycle performance

Long-term performance of the membrane was demonstrated with 10 repetitive filtration cycles. The results show a small, but discernible TMP increase when enriching *C. vulgaris* solution, especially after the first 5 cycles of filtration (Figure 29a). TMP increase was more discernible from the sixth cycle onward, resulting in about 10% higher TMP in the tenth cycle compared to the first cycle. Correspondingly, a notable drop in permeate flux was observable when comparing the tenth and first filtration cycles. In addition to forming a cake layer of microalgae cells on the membrane surface, cell membrane rupture during repetitive filtration/backwashing cycles may also contribute to membrane fouling. *C. vulgaris*. Evidence of cell rupture can be observed via the change in colour of *C. vulgaris* solution and the settlement of *C. vulgaris* biomass at the bottom of the membrane vessel.

By contrast to *C. vulgaris*, changes in TMP and permeate flux were insignificant when enriching *Scenedesmus sp.* Solution (Figure 29). Discernible increase in TMP was also observed over 10 repetitive filtration cycles. However, notwithstanding a tinge of green of *Scenedesmus sp* on the membrane surface, the TMP only reached 12 kPa at the tenth cycle. The decrease in actual water flux was insignificant (Figure 29b).

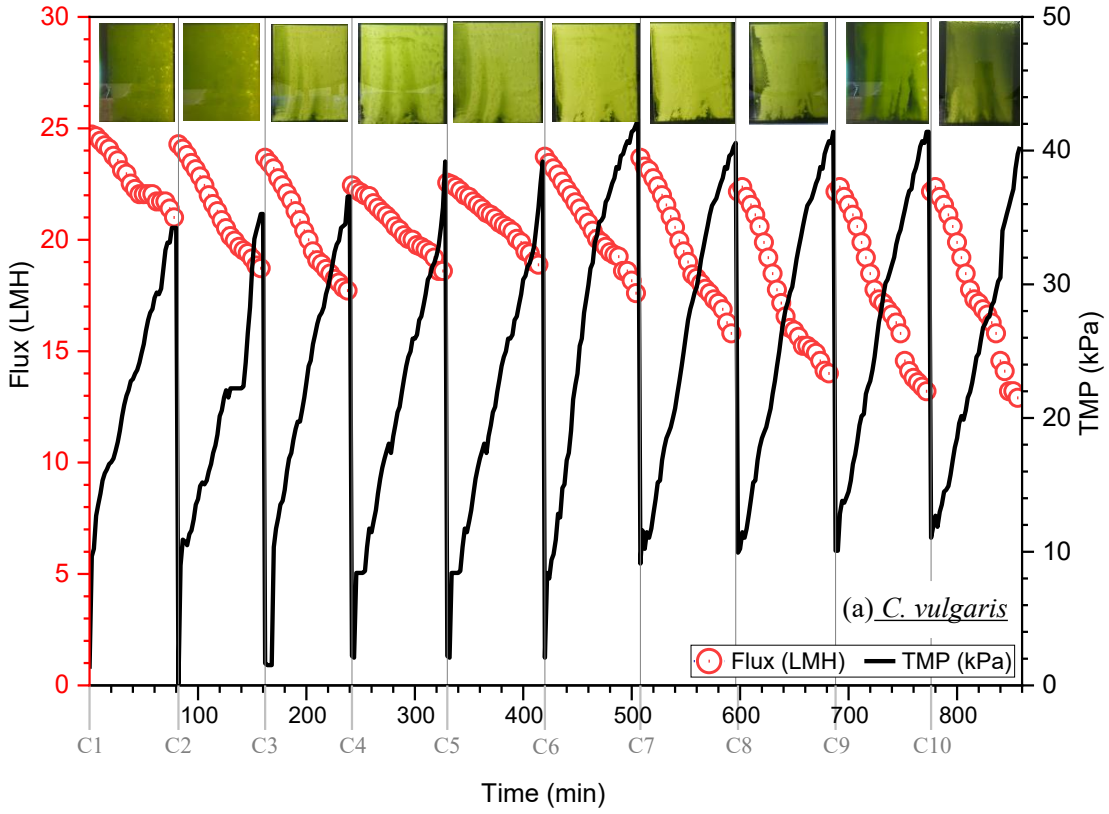

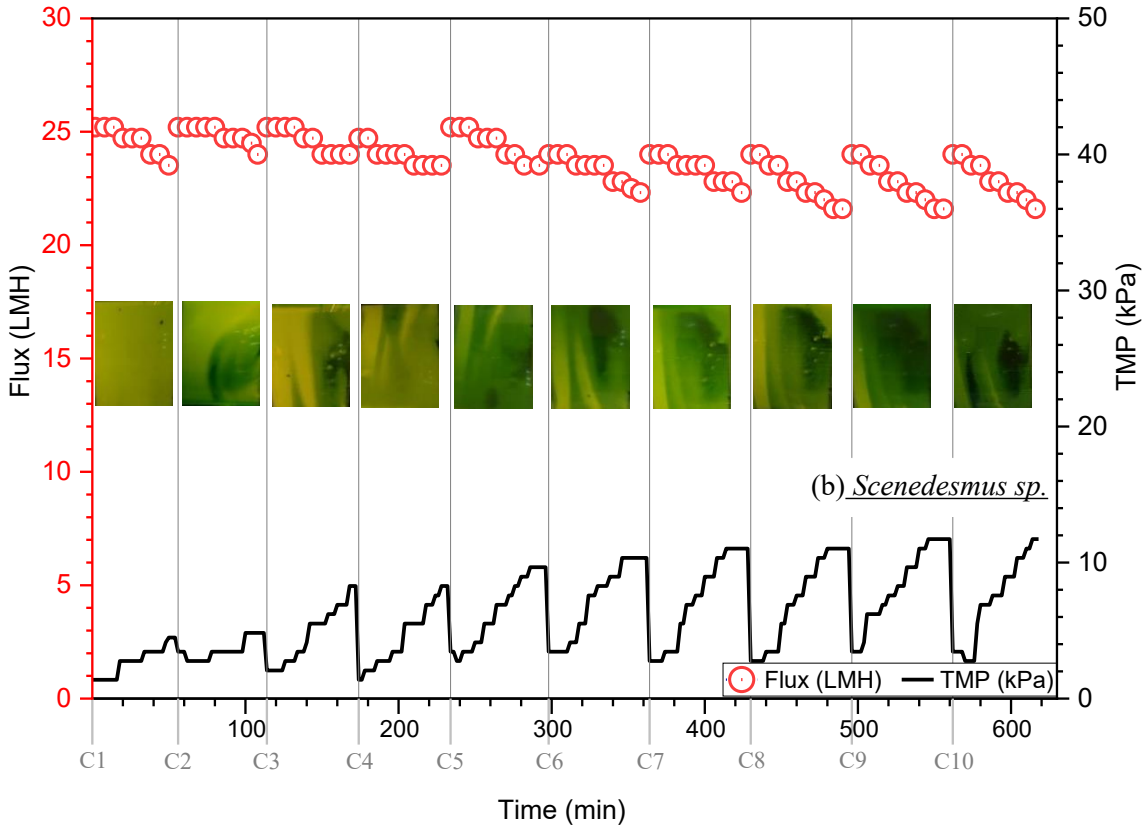

Figure 29. Comparison of TMP and permeate flux during the dewatering microalgae solution (a) *C. Vulgaris* and (b) *Scenedesmus sp.* In 10 repetitive filtration cycles. Water recovery of each cycle was 40%. The membrane image was captured at the end of a cycle.

Similar results were obtained when the water recovery from each cycle was increased to 80% (Figure 30). The magnitude of membrane fouling was more obvious with *C. vulgaris*. TMP increase beyond 50 kPa was observed at the third cycle (Figure 30a), where membrane cleaning was required to restore the flux to its original value. Leakage of cell content to the permeate (evidenced in a slight green tint) was observed, possibly due to excessive pressure. It is noteworthy that 2 min of backwashing could restore the TMP value to near original value (although excessive TMP increase would be observed again, unless the membrane was cleaned rather than backwashed).

In good agreement with the results reported above, no discernible fouling was observed with *Scenedesmus sp.* (Figure 30b). The TMP profile of *Scenedesmus sp.* was unaffected by continuous operation without backwashing. After one hour, the membrane was capable of self-cleaning and reverting to its initial value. It can be ascribed to *Scenedesmus sp*'s slimy outer layer and body size. It can be concluded that the size, shape, and morphology of microalgal cells explain the variation in filtering effectiveness between the two species. *Scenedesmus sp.* Solution can be enriched using ceramic membranes, and fouling can be effectively managed.

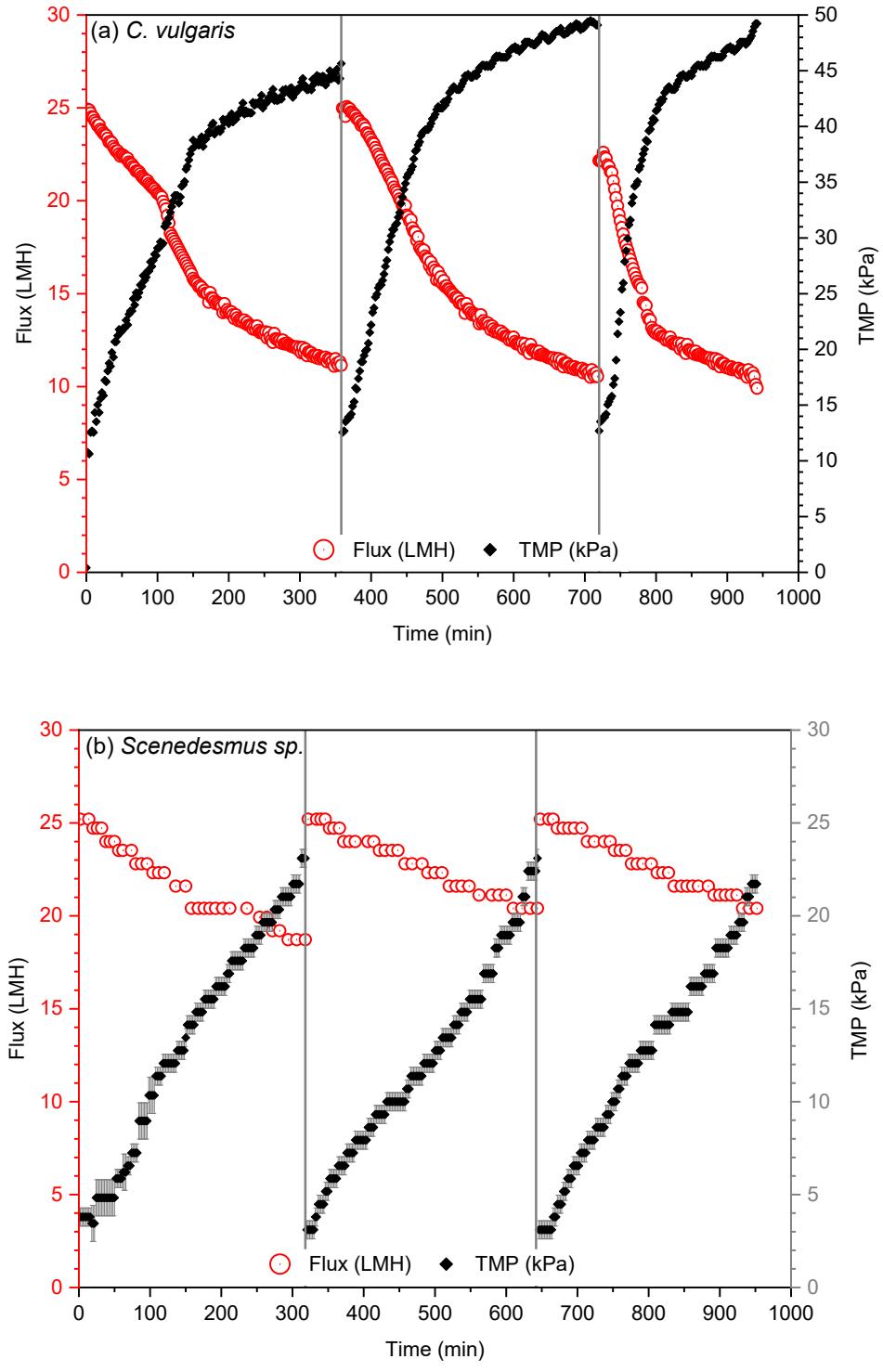

Figure 30. Comparison of TMP and permeate flux during the dewatering microalgae solution in 3 repetitive filtration cycles of 80% water recovery for (a) *C. Vulgaris* and

(b) *Scenedesmus sp* with and without backwashing, respectively. The error bar represents the standard deviation from two measurements.

6.3.4. Permeate reusability

Results in Figure 31 shows that permeate water extracted via membrane filtration can be reused to cultivate both *C. Vulgaris* and *Scenedesmus sp.* For both species, the biomass content in permeate water increased gradually as a function of cultivation time. The growth rate in permeate water was similar to or even slightly higher than that in the feed solution. This is because microalgae cells in the feed solution were already at the stationary growth phase, where there is a combination of cell production and mortality. Each of the two species responds differently to permeate reusability. In fact, from day 8^{th}, the *C. Vulgaris* feed solution had reached the decaying phase, and the microalgae population collapsed. By contrast, in the permeate solution, microalgae cells were diluted with 60% permeate water, thus, the growth was restored to the exponential phase. On the other hand, the growth rate of *Scenedesmus sp.* Was similar in both permeate and feed solutions. MF membrane could retain the microalgae cells while allowing the micro- and macro-nutrients to pass through to the permeate water to support microalgae growth and eliminate the need for additional nutrient input. The findings confirm that the permeate water can be reused as new growth media to develop a circular cultivation harvesting cycle.

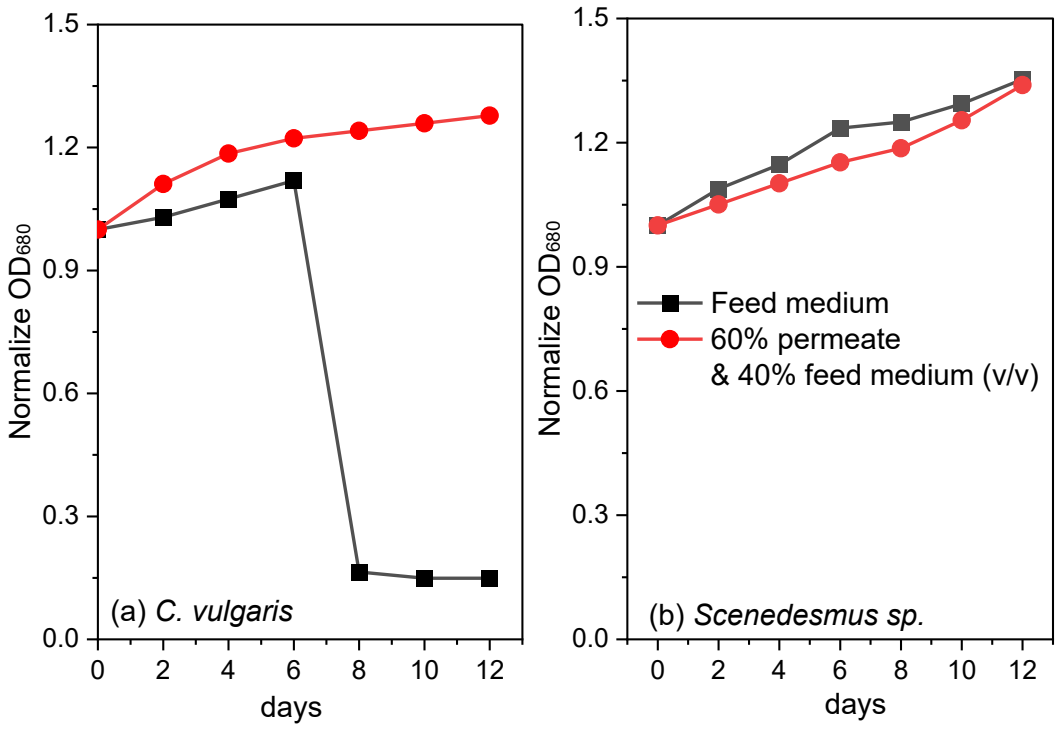

Figure 31. The growth rate in the feed medium and permeate medium (a) *C. Vulgaris* and (b) *Scenedesmus sp.* Growth rates were estimated through optical density measurements. The growth rate obtained from a mixture of 60% (v/v) permeates water, and 40% (v/v) microalgae feed solution (inoculum), which was used in membrane filtration experiments, as compared to the growth rate in the feed solution before the filtration experiment. The findings confirm that the permeate solutions can be reused as new growth media.

6.4. Summary

Harvesting and water reuse are two critical issues for large-scale microalgae cultivation. Using two representative microalgae species, namely *C. vulgaris* and *Scenedesmus sp.,* this study evaluates the performance of a ceramic microfiltration membrane to extract clean water for reuse and pre-concentrate the microalgae solution for subsequent harvesting. The results show that fouling was specific to each individual microalgae species due to the difference in cell properties (e.g. size, shape, and cell membrane). Importantly, membrane fouling could be efficiently mitigated by aeration

and regular backwashing without any chemical addition. Aeration reduced the transmembrane pressure when filtering *C. vulgaris* and *Scenedesmus sp.* by 56 and 38%, respectively. In long-term performance experiments, *C. vulgaris* showed considerable membrane fouling over time; by contrast, *Scenedesmus sp.* showed negligible fouling. The results reaffirmed that membrane filtration efficiency was microalgae species-specific. Permeate water reuse for growing another batch of microalgae was also demonstrated using both species. Results reported here suggest that ceramic microfiltration membrane can simultaneously enrich the microalgae solution and recycle permeated water for microalgae cultivation.

CHAPTER 7. Synthesising cationic polymers and tuning their properties for microalgae harvesting

Part of this chapter has been published as the following journal article:

L Aditya, HP Vu, MAH Johir, S Mao, A Ansari, Q Fu, LD Nghiem. Synthesising cationic polymers and tuning their properties for microalgae harvesting. 2024. Science of the Total Environment 917, 170423

7.1. Research objectives

This study aims to investigate a series of newly synthesised cationic polymers named PAPTAC for microalgae harvesting. The PAPTAC polymers were synthesised at various initial monomer concentrations, ranging from 60 to 360 mg/mL and at different UV power. Three microalgae species from freshwater and marine microalgae species, namely *Scenedesmus* sp. (UTS.LD), Chlorella *vulgaris* CS-41 (C. *vulgaris*), and *Porphyridium purpureum* CS-25 (*P. purpureum*) were examined at mentioned monomer concentrations. The flocculation harvesting efficiency of PAPTAC was evaluated to identify the optimal dose and compared with a commercially available flocculant (FO3801). The findings of this study could provide helpful guide for screening suitable polymer flocculants based on the specific characteristics of microalgae.

7.2. Material and method

7.2.1. Materials

The photo-initiator lithium phenyl-2,4,6-trimethylbenzoylphosphinate and monomer (3-acrylamidopropyl)-trimethylammonium chloride (APTAC, 75 wt% in H_2O)

were purchased from Merck (Australia) and used without further purification. A commercially available polymer denoted as FO3801 from SNF Pty Ltd (Australia) was used for comparison. FO3801 is a high molecular weight and highly positively charged polymer. According to a previous study [3], FO3801 has a molecular weight (MW) of over 15,000 kDa and zeta potential (ζ) of 75 mV [3]. Three reference poly(diallyldimethylammonium chloride) (PDADMAC) polymers from Merck (Australia) were used to determine the average viscosity molecular weight of the PAPTAC polymers synthesised in this study. The average molecular weight of these PDADMAC reference polymers were 100 KDa, 200 – 350 KDa, and 400 – 500 KDa [2].

Scenedesmus sp. (UTS-LD) was maintained in the MaxiGro medium. This microalgae species was previously isolated from environmental water in Australia by the University of Technology Sydney. *Chlorella vulgaris* (CS-41) was obtained from Australian National Algae Culture Collection at CSIRO Microalgae Research (Hobart, Tasmania, Australia). The stock culture was maintained in the MLA medium (Algaboost; Wallaroo, SA, Australia). The *Porphyridium purpureum* (CS-25) was obtained from the Australian National Algae Collection at CSIRO Microalgae Research (Hobart, Tasmania, Australia). *P. purpureum* is a marine microalgae species. *P. purpureum* was maintained in the f/2 medium at 33–35 ppm salinity. All three microalgae species were cultivated using a 10 L photobioreactor until the stationary growth phase (maturity) and used for the harvesting experiment. The cultivation procedure has been previously described in details [140, 246]. At the stationary growth phase, the dried biomass contents of *Scenedesmus sp., C.vulgaris*, and *P. purpureum* were 0.28, 0.75, and 0.70 g/L, respectively.

7.2.2. Synthesis of polymer flocculants

Poly(3-acrylamidopropyl)trimethylammonium chloride (PAPTAC) polymers were synthesised by UV-induced free-radical polymerisation in an aqueous solution with a range of monomer concentrations [2]. Each reaction mixture containing the monomer at a specific concentration ([M] = 60 - 360 mg/mL) and the photo-initiator lithium phenyl-2,4,6-trimethylbenzoylphosphinate (0.3 mg/mL) was sealed in a glass vial, subjected to degassing by introducing nitrogen gas at a flow rate of 0.5 L/min and positioned on top of a magnetic stirrer plate. The vials were irradiated by UV at λ_{max} = 365 nm with energy input of 36W to obtain the cationic polymers. Polymer flocculants were also produced at energy input of 60 W (λ_{max} = 390 nm). The photopolymerization reaction is completed within 30 minutes. The experimental conditions were consistent with our previous study [2].

7.2.3. Harvesting experiments

A stock solution with polymer concentration of 2.4 g/L was prepared by dissolving the above synthesised polymer in Milli-Q water with continuous mixing for 60 minutes using a magnetic stirrer. The stock solution was used for microalgae harvesting within one hour to avoid any hydrolysis. A specified volume of the polymer solution was added to 100 mL microalgae solution, thoroughly mixed, then allowed for settling. After 1 hour of settling, the aggregated microalgal biomass was separated from the water phase by decanting. All harvesting experiments were conducted in triplicate. The flocculation efficacy was determined by measuring optical density at 680 nm of the initial microalgal solution and the decanted water after harvesting as described in

Equation (2). Optical density was measured using an UV spectrophotometer (UV 6000 Shimadzu; Australia).

$$Flocculation\ efficiency\ (\%) = \frac{OD_{w/o} - OD_w}{OD_{w/o}} \times 100 \qquad (2)$$

where: OD_w and $OD_{w/o}$ is the optical density of the culture with flocculant addition and without flocculant addition (control), respectively.

The optimal dose of the polymer was determined by a dose–response relationship experiment. Polymer doses added to the microalgal solution were varied from 2.5 – 100 mg-polymer/g.dry-biomass. The polymer doses were normalised relative to the dried biomass concentration.

7.2.4. Analytical methods

The monomer conversion was measured using nuclear magnetic resonance spectroscopy (^{1}H NMR) (Varian Unity 400 MHz spectrometer). The polymers were dissolved in D_2O at 10-20 mg/mL for ^{1}H-NMR analysis. The photopolymerization reaction is completed within 30 minutes. The experimental conditions were consistent with our previous study [2]. The obtained ^{1}H-NMR spectra were used to determine monomer conversion. Specifically, the methine (*g*) and methylene (*f* and *j*) resonances of the resulting PAPTAC were obtained from the ^{1}H-NMR spectrum in Figure 32. In addition, proton resonance peaks of unreacted APTAC residues were also obtained from the ^{1}H-NMR spectrum (marked as '*'). The monomer conversion of the polymerization is calculated as shown in Equation (3).

$$Conv. = \frac{\frac{A_{f,g,j}}{5}}{\frac{Amonomer}{3} + \frac{A_{f,g,j}}{5}} \times 100\% \quad (3)$$

Where $A_{f,g,j}$ denotes the integral area of the protons on the 'f, g and j' groups, and the $A_{monomer}$ is the sum of the integral areas of all '*' labelled peaks.

The charges of polymers were measured using a Zetasizer nano instrument (Nano ZS Zen 3600, Malvern, UK). Polymer rheology was measured using a Brookfield DV2T equipped with a small sample adapter unit (Part SC4-45Y), a removable sample chamber with embedded RTD temperature probe (SC4-13RPY), and a coaxial cylinder spindle SC4-18. The sample chamber has a 19.05 mm diameter, a 64.77 mm depth, and an effective volume of 16.1 mL. The spindle speed was 100 rpm. Plastic viscosity, shear rate, shear stress, and torque were recorded for rheology analysis. The relationship between shear stress and shear rate is described using the Bingham Plastic model. Polymer sample acts as a Bingham plastic fluid, which indicates that the fluid will not flow until the applied shear stress exceeds the fluid's yield stress. The equation (3) shows The Bingham Plastic model:

$$\tau = \tau_y + \mu\gamma \quad (4)$$

where: τ is shear stress (Pa), τy is yield stress (Pa), μ is plastic viscosity (Pa) and γ is the shear rate (s^{-1}).

Both plastic viscosities were plotted against molecular weight on a logarithmic scale. The intercept on the shear stress axis corresponds to the yield stress, while the slope of the line corresponds to the plastic viscosity. This correlation was utilised to calculate the viscosity average molecular weight of the PAPTAC polymers by using PDADMAC standards.

7.3. Result and discussion

7.3.1. Polymer characterization

The nuclear magnetic resonance (^{1}H NMR) spectrum of a polymer synthesised in this study is presented in Figure 32 as evidence of successful polymerization. This NMR analysis with protium nuclei also provides the structural evidence of PAPTAC polymer formation. There were two main regions. The resonances for the methylene *(f, -C**H₂**-CH-)* and methine group *(g, -CH₂-C**H**-)* of the PAPTAC backbone and the methylene *(j, -CH₂C**H₂**CH₂-N(CH₃)₃)* of the pendant moiety occur at 1.10–2.45 ppm. The resonances for the methyl (l, -N(C**H₃**)$_3$)) and methylene groups *(i & k, -C**H₂**CH₂C**H₂**-)* of the pendant moiety occur in the region 3.0 and 3.5 ppm. The resonance for the unique *–N**H**–* group (h) was observed at 8.24 ppm. The strong signal at 4.7 ppm was attributed to the solvent H_2O. In addition, proton resonance peaks of unreacted *–C**H₂**=C**H**–* group of APTAC monomer (marked as '*') were also observed at 5.72, 6.18 and 6.85 ppm, respectively.

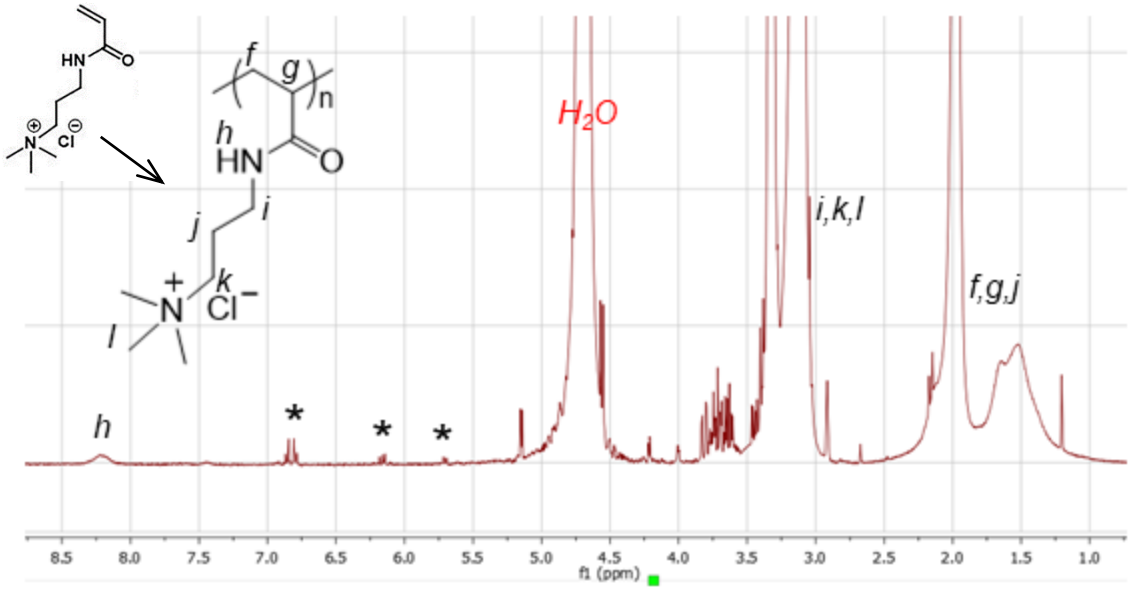

Figure 32. ^{1}H NMR spectrum of the prepared cationic polymer PAPTAC in D_2O. The '*' represents the signals of unreacted double bonds (-C***H*₂**=C***H***-) of monomer residue.

Table 4 summarises key properties of the six polymers individually synthesised with monomer concentrations from 60 to 360 mg/mL. These polymers were denoted as P-x, where x represents the initial monomer concentration (mg/mL). As expected, increasing monomer concentration results in an increase in the polymer's plastic viscosity, which can be used to calculate the polymer molecular weight. Results in Table 1 also show that monomer conversion decreased as the monomer concentration increased. This is due to the increase in monomer concentration leads to unreachable state of saturation, hence impeding the initiation of polymerisation of all available monomers. In other worlds, an increase in monomer concentration leads to an increase in viscosity and a reduction in diffusivity. Consequently, some monomers are unable to engage in the polymerisation process due to the excessive concentration. Likewise, an increased in UV power leads to faster photoinitiation, which resulted in lower monomer conversion. At

the monomer concentration of 240 mg/mL, two UV power level of 36W and 60W were used to produce polymer P-240-1 and P-240-2, respectively. As the UV power increased from 36 to 60 W, at the same monomer concentration of 240 mg/mL, the plastic viscosity increased from 60 to 100 mPa.s (or 67% increase in plastic viscosity) and the monomer conversion decreased from 98.2% to 85.1%. Results in Table 1 are consistent with previous studies, which reported a lower monomer concentration with lower UV power induced showed a higher rate of monomer conversion [265].

Table 4. Summary of the characterization of cationic polymers

Polymers	Monomer concentration (mg/mL)	UV-power (Watts)	Monomer conversion[a] (%)	Av. plastic viscosity (mPa.s)
P-60	60	36	99.2	10
P-90	90	36	99.3	20
P-120	120	36	99	30
P-240	240	36	98.2	60
P-360	360	36	90.3	90
P-240	240	60	85.1	100
FO3801		-	-	40

[a] The monomer conversion was determined by ^{1}H NMR analysis.

Using the reference polymers, plastic viscosity data in Table 1 were used to estimate the polymer molecular weight (section 2.4.1). Results in Figure 33 suggest that desirable polymer molecular weight can be achieved by tuning the monomer concentration. High molecular weight polymers can be obtained by increasing the monomer concentration. This is because the increase of monomer concentration results in a longer polymer chain being formed. The lengthening of the polymer chain is reflected by an increase in viscosity.

Similar to molecular weight, charge density (measured by Zeta potential) of the PAPTAC polymers is also related to monomer concentration. Surface charge density also increased almost linearly as the monomer concentration increased within the monomer concentration of between 60 and 120 mg/mL. As the monomer concentration increased to 240 mg/mL, the polymer's surface charge did not increase further. In fact, at monomer concentration 360 mg/mL, the polymer surface charge decreased slightly compared to monomer concentration of 120 mg/mL. This may be due to the relatively low monomer conversion (Table 4), compromising the overall zeta-potential. In addition, the long polymer chains may entangle to reduce their effective surface charge.

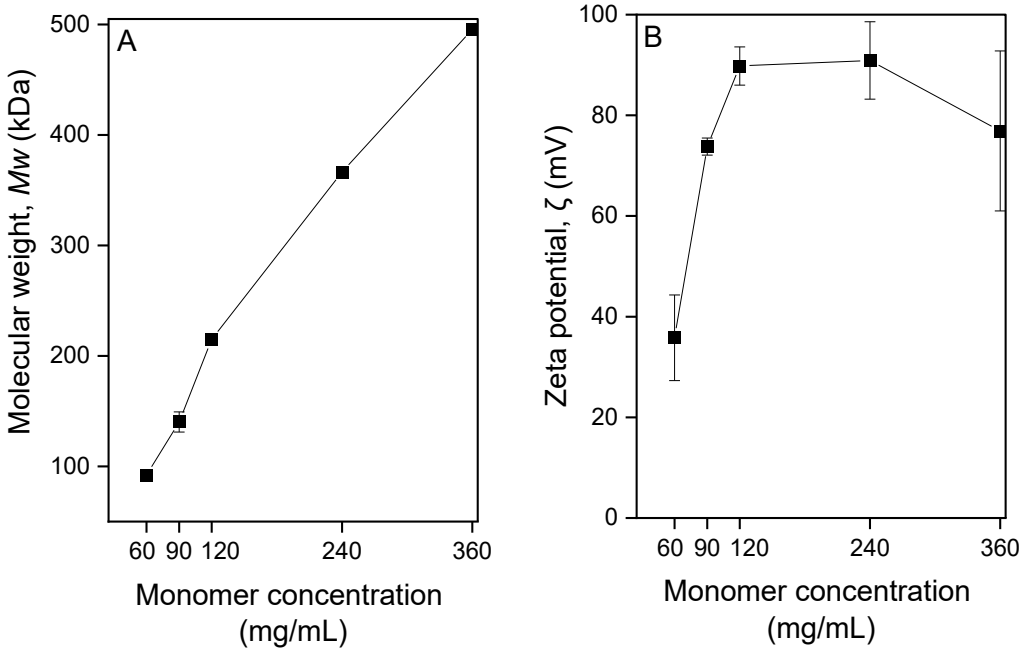

Figure 33. Correlation between monomer concentration (A) with molecular weight and (B) with zeta potential. The error bar represents the standard deviation from six replicate experiments.

UV irradiation energy can significantly influence on the molecular weight and zeta potential of the synthesised polymers. At the same monomer concentration of 240 mg/mL, by increasing the UV light energy from 36W to 60W, enhanced the molecular weight and charge density by about 50% as shown in Figure 34. In the polymerisation process, first, the monomers are converted to dimeric forms, then to J-aggregated forms or oligomeric forms at increased irradiated UV power [266]. Similar to aforementioned case of P-120 and P-240, which showed that polymer chains of high molecular weight entangle and shield the effective charge. This observation is also consistent with properties of the commercial polymer FO3801. As shown in Figure 34, the commercial polymer FO3801 has a very high molecular weight of 15,000 kDa but a relatively modest charge density of +55 mV (at pH 2.6).

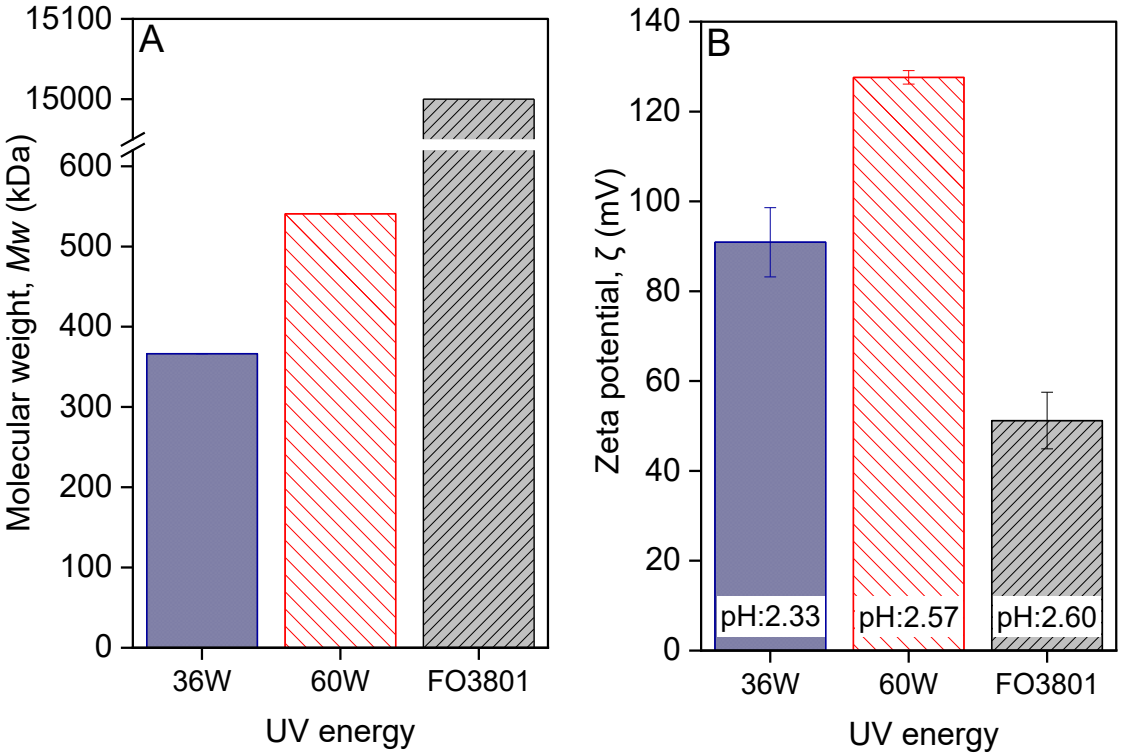

Figure 34. (A) Effect of UV power induced on polymer molecular weight and (B) zeta potential. The error bar represents the standard deviation from six replicate experiments.

7.3.2. Role of polymer properties

In this study, the type of monomer-repeat unit that forms a polymer also has a significant effect on polymer properties. The arrangement of monomer-repeat units along the backbone of a polymer chain, is affected by varying UV power induced to a monomer/polymer. It modifies polymer properties by modifying the molecular weight distribution, branching distribution, and number of terminal double bonds. Polymer properties play a vital role in the behavior, performance, and application of polymers in various industries. Polymers are macromolecules consisting of repeating structural units whose properties can be customized for specific applications. For instance, the chemical

structure of a polymer affects its overall properties. The arrangement of the monomer units and the presence of functional groups affect the polymer's reactivity, stability, and compatibility with other materials. In addition, molecular weight affects the physical properties of a polymer. High molecular weight polymers typically have higher mechanical strength, toughness, and resistance to abrasion. On the other hand, low molecular weight polymers may have better processability and flexibility. For instance, when P-240 was synthesised at UV power of 60W, the polymer charge density and molecular weight were greater than at UV power of 36W (at the same monomer concentration of 240 mg/mL).

Flocculation is governed by surface charge neutralisation of individual microalgae cells and polymer bridging. When cationic polymers are added to the microalgae solution, their highly cationic charge density can neutralise the negative charge of microalgae cells due to electrostatic attraction. This leads to a decrease in cell surface charge and biomass aggregation. At the optimal dosage, PAPTAC polymer can effectively neutralise microalgae cell surface charge for the highest level of aggregation and generate clear water as the supernatant as shown in the picture Table S1-S3. When the dose of polymer exceeds the optimum level, the excess polymer is adsorbed onto microalgae suspensions, the microalgae cells become coated with positive surface charges leading to a reversal of

surface charge. This reaction induces electrostatic repulsions among the cells, which reintroduces coulombic repulsion.

7.3.3. Microalgae flocculation efficiency

Surface morphology and properties of microalgae vary from one species to another as demonstrated by three different microalgae species in Table 5. The efficiency of microalgae flocculation is governed by the interplay among several factors including solution pH, cell membrane morphology, surface charge (or zeta potential). For example, cell surface charge (or zeta potential) is a function of the solution pH and microalgae density [3, 267]. In general, the zeta potential will become more negative as the density of microalgae increases and the pH rises. In this study, the pH of marine species (*Porphyridium purpureum)* was slightly lower, but it has a similar charge density to *Scenedesmus sp*. *Chlorella vulgaris* has the lowest charge density. This is because *Chlorella vulgaris* had a lowest dry weight than the other two species.

Table 5. Freshwater and marine microalgae properties

Microalgae species	Mature culture solution pH	Dry weight (g/L)	Zeta potential *(mV)*
Scenedesmus sp.	8.10	0.75	-23.2 ± 1.3
Porphyridium purpureum	6.89	0.70	-17.3 ± 1.1
Chlorella vulgaris	8.14	0.28	-9.9 ± 0.3

Microalgae species in Table 2 were evaluated for flocculation using the PAPTAC polymers with a range of molecular weight and charge density regulated by adjusting the monomer concentrations and UV power during polymerisation. As discussed above, flocculation by cationic polymers involves charge neutralisation and molecular bridging to induce aggregation. During charge neutralisation, the negative charge of the microalgae is neutralised by the positive charge of the polymer. Polymer with a high positive charge have stronger attraction and helps clumping microalgae efficiently like magnetic powder [2, 268].

On the other hand, the molecular weight of the polymer acts as a bridge to bind the cells. Polymers with a high molecular weight may show enhanced performance, due to their increased capacity to bridge between algae cells and enables them to generate larger and more stable flocs. This can enhance flocculation efficiency by promoting rapid aggregation of microalgae cells and simplifying the separation process. Efficient microalgae harvesting requires the identification of the optimal combination from surface charge and high molecular weight as illustrated in Figure 35. When they work together synergistically, it is like having the perfect set of tools for efficient microalgae harvesting. Thus, for effective microalgae harvesting, finding the optimal polymer dosage is necessary.

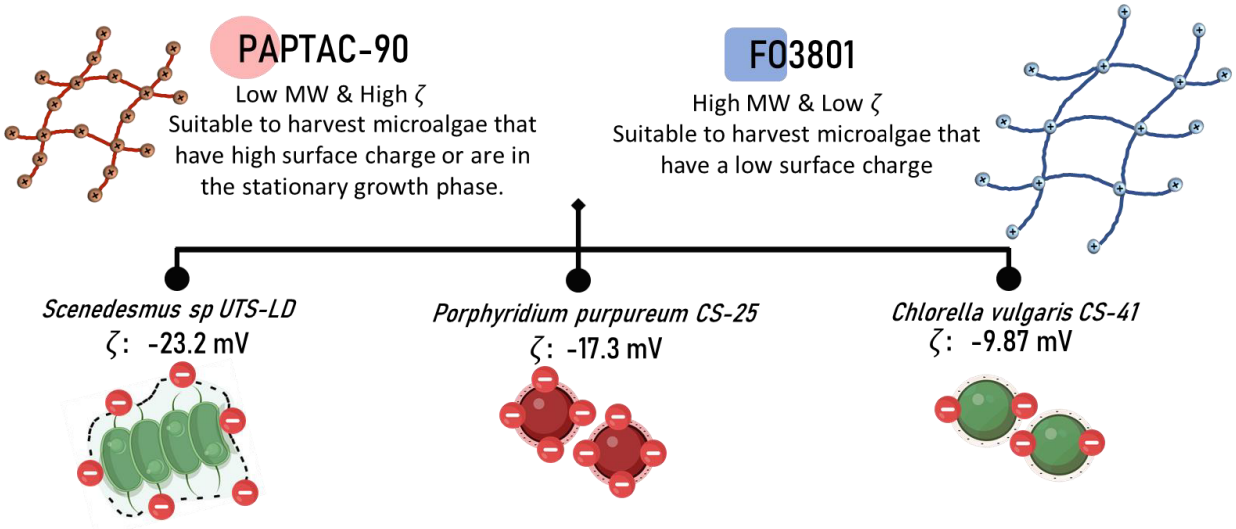

Figure 35. Illustrated polymer in different surface charge and molecular weight

The highest flocculation efficiency for *Scenedesmus sp* was observed at a dosage of 25 mg-polymer/gram of dry biomass, achieving a flocculation efficiency of 80% by using P-90. By contrast, the commercial polymer FO3801 requires a dosage four times higher to achieve the same flocculation efficiency as presented in Figure 36. The highest flocculation efficiency for FO3801 was 78% when using 100 mg-polymer/gram of dry biomass. This is because FO3801 has a molecular weight 10-times higher than P-90, but a lower charge density. Thus, additional flocculant should be used to enhance its charge density. Consequently, this will have a negative effect on the flocculation efficiency, since additional concentrations and costs will be required. The findings of this study also indicate that the flocculation efficiency of PAPTAC is threefold higher than FO3801 for *Scenedesmus sp*.

As discussed above, excessive polymer dose can be detrimental to flocculation efficiency. Flocculation efficiency in Figure 36 decreased after the optimal dose of 25

mg-polymer/gram of dry biomass was achieved. This observation aligns with prior research that elucidated the presence of an augmented coating layer with long polymer chains, leading to diminished flocculation efficiency [269, 270].

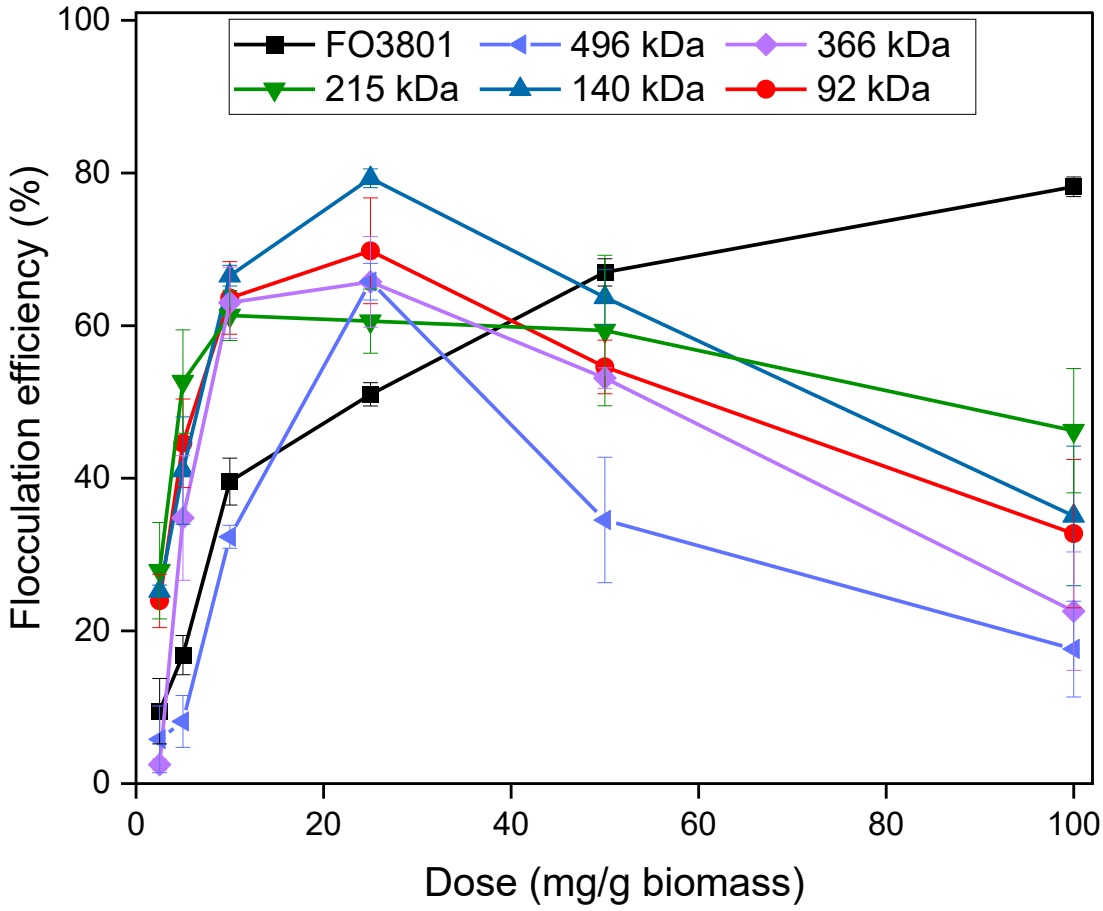

Figure 36. Flocculation efficiency of cationic polymers with freshwater microalgae *Scenedesmus sp.* The error bar represents the standard deviation from three replicate experiments.

UV power can also be used to tune the polymer properties. The zeta potential and molecular weight of the polymer (P-240) produced at UV power of 60W were significantly higher than that produced at 36W. Figure 37 demonstrates that higher

molecular weight resulted in more stable flocculation efficacy. However, the optimum flocculation efficiency of the polymer produced at 36W was slightly higher than that produced at 60W. It was probably due to charge density of microalgae EPS. *Scenedesmus sp* EPS has highly negative charge, thus it was easier to harvest at lower molecular weight and optimum charge density polymer compared to higher molecular weight and charge density polymer. The excessive amount of flocculant molecular weight resulted in a charge reversal on the surfaces of microalgae cells, leading to their destabilization in suspension. Consequently, resulted in a decrease in the efficiency of harvesting [271].

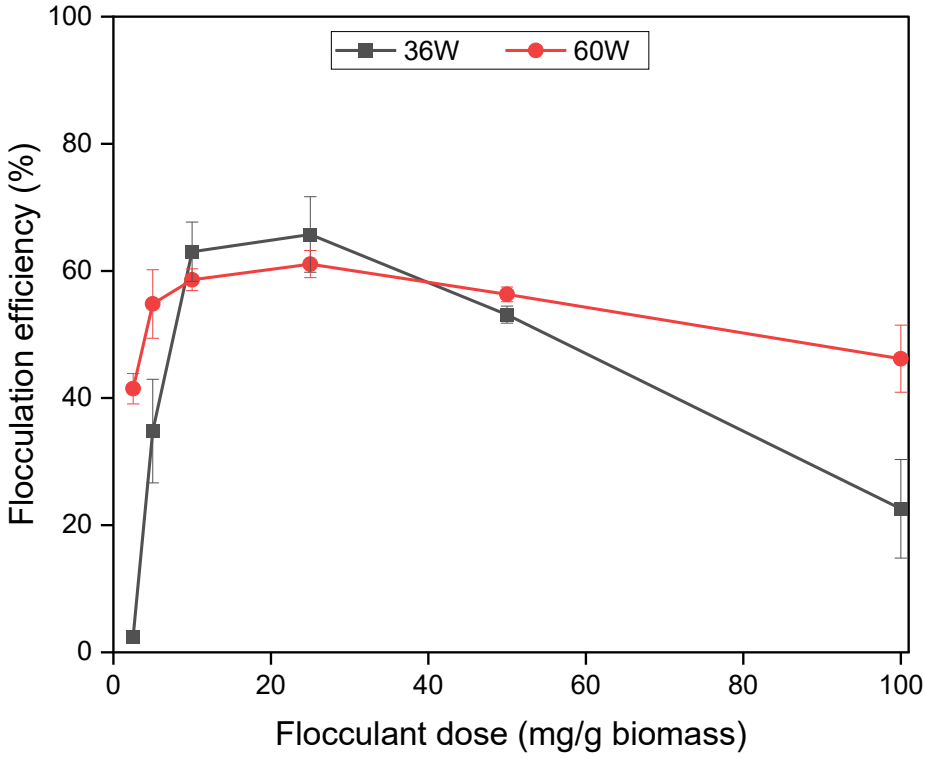

Figure 37. Flocculation efficiency of freshwater microalgae *Scenedesmus sp* with different UV power synthesised at P-240. The error bar represents the standard deviation from three replicate experiments.

High monomer concentration is liable for the transition toward large polymer molecular weight, thus, a more adhesive polymer. The effect is observable by the

adherence of microalgae to the bottom flask at increased dose of polymer. This result is in line with prior study which showed the polymer interaction alter from cohesive to adhesive, caused by increased in molecular weight [272].

The other possibility responsible for the disparity in flocculation efficiency is the distinct EPS types of each microalgal species. *Scenedesmus sp* excreted thick mucilage as its growth and the EPS composed of long chain polysaccharides (mannose and glucose) but lack in nucleic acid and protein [273]. The irregular shapes and charge distribution of EPS surface, often creates a patch between regions of uncoated. The positively charged patches can then interact with other negatively charged areas at the surface of other *Scenedesmus sp* cells and connect them together [274]. In this case the key parameters that will ensure successful flocculation are the length of the polymers, as only short chains (lower molecular weight) can form patches at the surface of the cells [273].

PAPTAC polymer showed excellent harvesting efficiency for *Scenedesmus sp.* This species is well-known for its ability to absorb CO_2 in high relatively concentration compared to other species [275-277]. The biomass has been acknowledged for its high lipid and protein content, which can be converted into essential vitamins for human or animal fed [278, 279]. For *Scenedesmus sp*. Other species that has similarity to *Scenedesmus sp* is *Chlorgonium*. This particular freshwater microalgae species has approximately 17 μm of width, this species has been well recognised as an ideal food source for shrimp [280]. Additional species that show comparable characteristics to *Scenedesmus sp* are *Coelastrum Nägeli* and *Cosmarium Corda*. These species have a thick mucilage in their EPS, with a size exceeding 10 μm, and are commonly found in

coenobium. The findings of this study could act as a helpful guide for selecting an appropriate polymer based on the specific characteristics of the microalgae.

Good harvesting efficiency was also observed with the marine microalgae *P.purpureum.* Due to the highly negative charge of *P.purpureum* cells, a small amount of flocculant is sufficient to effectively harvest *P.purpureum* biomass. Figure 38 shows by using P-90 PAPTAC achieved 93% flocculation efficiency at 25 mg-polymer/gram dry-biomass polymer dose, while FO3801 reached >80% efficiency at 10 mg-polymer/g. dry-biomass. However, considering its molecular weight, FO3801 required a considerably higher concentration than PAPTAC to achieve comparable flocculation efficiency. The production of high molecular weight polymers typically requires more demanding reaction conditions such as high temperatures, high pressures, high purity solvents, etc. In addition, the resulting high molecular weight polymers usually have a high viscosity, which requires more complex processes and consumes more energy to purify. Furthermore, as the molecular weight increases, the viscosity of the system increases dramatically, resulting in reduced monomer conversion and increased waste of raw materials. PAPTAC polymers, on the other hand, can be tailored to specific needs, using water as the solvent and light as the polymerization condition, resulting in 'green' synthesis and reduced environmental footprint.

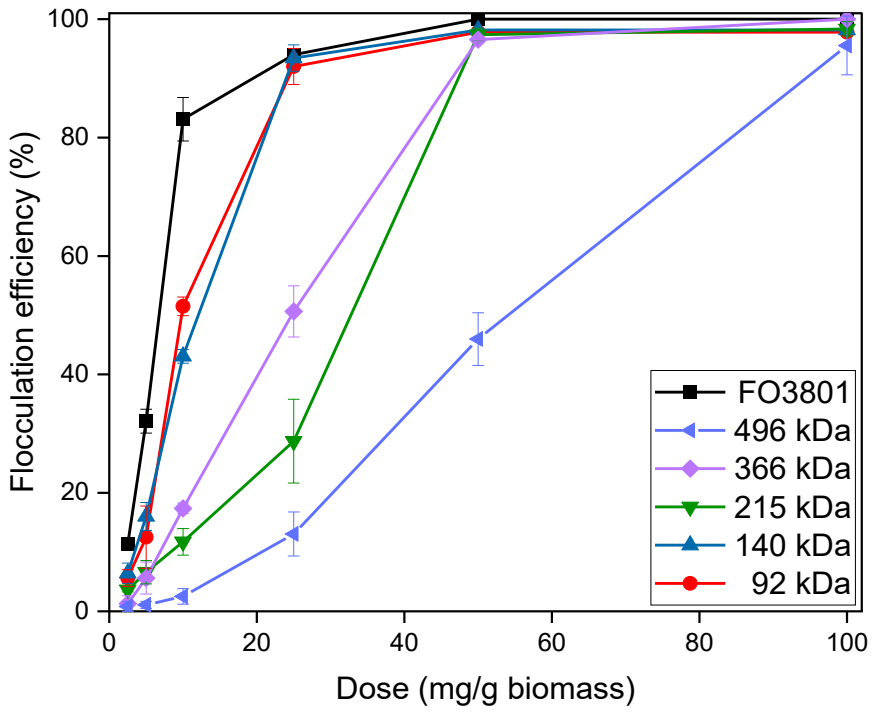

Figure 38. Flocculation efficiency of seven polymers with *P. purpureum*. The error bar represents the standard deviation from three replicate experiment deviation from three replicate experiments.

Despite the fact that marine water species have higher ionic strength and polymeric coiling could occur in high ionic strength solutions to degrade polymer properties and performance [281]. In this study marine microalgae had lower pH and the flocculation can be inhibited when the pH microalgae is excessively high/low [282]. Interestingly, PAPTAC resulted in the large clumps formation of *P. purpureum*, which indicated the stability of the polymer even in saltwater with high ionic strength. As the concentration increases, the size of the clumps formed also increases. This makes PAPTAC an appealing choice of flocculant because it easier to collect the biomass from water. The flocculated biomass can be collected by stainless steel sieving. This approach will effectively mitigate the substantial production expenses. Additionally, the

achievement of a high level of flocculation efficiency would additionally contribute to the viability of recycling leftover culture as a means to decrease the water footprint associated with the production of microalgal biomass.

C. vulgaris shows different results compared to the other two species. The PAPTAC polymer did not show any optimum doses. Instead, flocculation efficiency increased as the polymer dose increased to 100 mg-polymer/g.dry-biomass as illustrated in Figure 39. By contrast, an optimum dose of 25 mg-polymer/g.dry-biomass was observed with the commercial polymer FO3801. Table 5 delineates that *C. vulgaris* has a significantly lower surface charge density compared to the other two microalgae species. Thus, it is possible that flocculation is driven mostly by molecular bridging and sweeping rather than charge neutralisation. The former is governed by molecular weight and thus favours the commercial polymer FO3801. There could be other underlying reasons, and further research is necessary to explain for the different flocculation behaviour amongst the three microalgae species in this study.

In addition to surface charge density, cell morphology especially EPS content and type may also affect the disparity of flocculation efficiency. *C.vulgaris* has distinct type of EPS compared to *Scenedesmus sp*. For example, it can be indicated by the relationship between pH and zeta potential. *Scenedesmus sp* has a linear relationship between pH and zeta potential [283], whereas *C.vulgaris* has a curve relationship between pH and zeta potential with a peak at pH 7 [284].

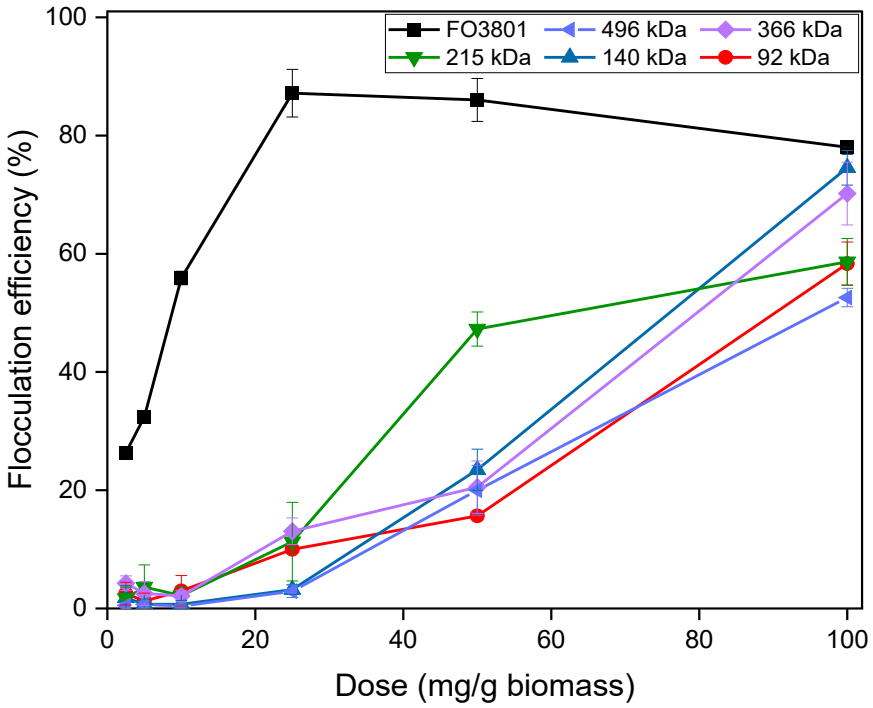

Figure 39. Flocculation efficiency of seven polymers with freshwater microalgae *C.vulgaris*. The error bar represents the standard deviation from three replicate experiments.

Overall, PAPTAC demonstrates a high level of flocculation efficiency at low dosages. Results in this study also demonstrate the ability to tune the PAPTAC polymer molecular weight and surface charge to improve microalgae harvesting. Several factors have been identified as potential contributors to flocculation performance but have not been investigated in this study. Examples include such as cell membrane morphology, the composition of the culture media [132, 271, 285]. Thus, further research is still needed to realise polymer tuning for microalgae harvesting.

7.4. Summary

This study demonstrates a facile technique to synthesize and tune the cationic Poly(3-acrylamidopropyl) trimethylammonium chloride (PAPTAC) polymer by UV-

induced free-radical polymerisation. By regulating the monomer concentration and UV energy for polymerisation, cationic PAPTAC polymer can be tuned in terms of molecular weight and surface change for harvesting three microalgae species. The obtained PAPTAC polymer shows excellent flocculation efficiency at low dosages. When evaluating for harvesting *Scenedesmus sp*. and *P.purpureum*, the optimised PAPTAC polymer has a lower optimum dosage of 25 mg-polymer/gram and higher harvesting performance than the commercial polymer. The observed performance can be attributed to effective neutralisation and molecular bridging by the optimised PAPTAC polymer. However, the obtained PAPTAC polymer and polymer tuning were less effective for harvesting C. *vulgaris*, possibly due to the cell morphology of this microalgae species. Further research is still needed to identify other underlying factors that account for the distinct flocculation behaviours observed in this study.

CHAPTER 8. Conclusion and recommendations

8.1. Conclusion

Results from this thesis provide new insights for improving the cultivation, harvesting, and utilisation of microalgae for simultaneously capturing CO_2 and producing valuable bioproducts. This work addresses key challenges in optimising microalgae systems, including the interplay between light intensity and CO_2 concentration, the effects of elevated sulphate levels and initial pH, and the impact of carbon-to-nutrient ratios. It also focuses on enhancing ceramic membrane microfiltration for preconcentrating solutions before harvesting, developing flocculants for efficient microalgae harvesting, reclaiming water, and enhancing biomass composition. These are the keys to improving the integrated microalgae system.

Results from this thesis show that microalgae growth rate can be optimised by balancing between CO_2 input and light intensity. The result shows light intensity and CO_2 input have opposing effects on the culture solution pH, which is essential to microalgae growth. Microalgae photosynthesis is mediated by the RuBisCo enzyme, which can only work in a specific pH range. CO_2 dissolution in the culture solution leads to acidification. On the other hand, the carboxylation process consumes protons and increases the solution pH. By balancing light intensity and CO_2 input, high-rate microalgae growth and CO_2 fixation can be achieved.

Results from this thesis reveal that *Scenedesmus sp* and *C.vulgar*is have different sulphate assimilation pathways. *Scenedesmus sp* relies on eukaryotic-type reductase enzymes, while *C. vulgaris* utilises prokaryotic-like plastid sulphate transporters on

chloroplast membranes. Elevated sulphate levels induced toxicity and disrupted osmotic balance. Acidic conditions disrupt sulphur metabolism and adenosine triphosphate production, impairing critical enzyme metabolism in microalgae. This demonstrates that an optimal concentration is necessary to balance metabolic processes while avoiding osmotic stress and toxicity.

This thesis demonstrates the importance of optimising carbon and nutrient inputs to enhance microalgae lipid and protein production. Results show that increasing carbon input can reduce nutrient demand for the same growth rate. Inputting excessive nutrients or carbon can negatively impact microalgae morphology and surface charge. Moreover, the nutrient composition of the growth media significantly influences lipid and protein production.

In this thesis, data were presented to evaluate the performance of a ceramic microfiltration membrane to extract clean water for reuse and pre-concentrate the microalgae solution for subsequent harvesting. The results show that fouling was specific to each individual microalgae species due to the difference in cell properties. Membrane fouling could be efficiently mitigated by aeration and regular backwashing, eliminating the need for chemical addition. Furthermore, permeate water was able to be reused for subsequent microalgae cultivation was demonstrated for both species.

Results from this thesis also demonstrate a facile technique to synthesise and tune the cationic Poly(3-acrylamidopropyl) trimethylammonium chloride (PAPTAC) polymer by UV-induced free-radical polymerisation. By regulating the monomer concentration and UV energy for polymerisation, cationic PAPTAC polymer can be tuned in terms of molecular weight and surface change for harvesting three microalgae species. The newly

synthesised polymer PAPTAC was also evaluated in this thesis for microalgae harvesting efficiency, which demonstrates a high level of flocculation efficiency at low dosages and outperforms the commercially available polymer FO3801.

Findings from this thesis underscore the potential of microalgae systems for greenhouse gas mitigation and biofuel production. By optimising cultivation conditions, advancing harvesting technologies, and promoting sustainable water reuse. This research contributes to the development of cost-effective and environmentally sustainable microalgae-based systems.

8.2. Recommendation

Greenhouse gas emission, particularly from CO_2, remains a serious problem. Microalgae have demonstrated the ability to absorb these pollutants, offering a potential sustainable solution. However, several technical challenges still need to be addressed. For example, the method for sparging the gas into the water and an efficient feeding rate. This study has not been able to reach an inorganic concentration higher than 200 mg/L. The challenges related to safety issues and mass transfer. The inorganic carbon concentration in some cases can be higher than in this study. For this reason, it is important to find a new technology that can provide higher concentrations of inorganic carbon. The study used ceramic membrane filtration to separate the growth medium with microalgae biomass (Chapter 6). This study uses the uncoated membrane, and a small aeration was placed at the bottom of the membrane. This study can be improved by coating the membrane with metal oxide or inorganic materials. This group of materials provides enhanced properties, such as fouling resistance, antimicrobial activity, and improved permeability. For example, graphene oxide has been widely used in water purification

membranes to enhance filtration efficiency to prevent microbial fouling. In Chapter 7, the study on cationic polymer for harvesting microalgae. Further research is still needed to identify other underlying factors that account for the distinct flocculation behaviours observed in this study. For a better understanding of the economic aspects of this integrated system, a cost analysis is recommended. This evaluation would be essential to assess the commercial feasibility of implementing microalgae systems for carbon capture and utilisation at industrial scale.

Reference

1. Nguyen, L.N., et al., *Microalgae-based carbon capture and utilization: A critical review on current system developments and biomass utilization.* Critical Reviews in Environmental Science and Technology, 2022: p. 1-23.

2. Nguyen, L.N., et al., *Synthesis and evaluation of cationic polyacrylamide and polyacrylate flocculants for harvesting freshwater and marine microalgae.* Chemical Engineering Journal, 2022. **433**: p. 133623.

3. Vu, H.P., et al., *Factors governing microalgae harvesting efficiency by flocculation using cationic polymers.* Bioresource technology, 2021. **340**: p. 125669.

4. Begum, H., et al., *Availability and Utilization of Pigments from Microalgae.* Crit Rev Food Sci Nutr, 2016. **56**(13): p. 2209-22.

5. Wang, Q., et al., *Effect of inoculation process on lycopene production by Blakeslea trispora in a stirred-tank reactor.* Applied biochemistry and biotechnology, 2015. **175**(2): p. 770-779.

6. Bjornland, T., *Distribution patterns of carotenoids in relation to chromophyte phylogeny and systematics.* The chromophyte algae: problems and perspectives. Systematics Association Special, 1989. **38**: p. 37-60.

7. Sukhinov, D.V., et al., *Increased C-phycocyanin extract purity by flocculation of Arthrospira platensis with chitosan.* Algal Research, 2021. **58**: p. 102393.

8. Macías-Sánchez, M., et al., *Comparison of supercritical fluid and ultrasound-assisted extraction of carotenoids and chlorophyll a from Dunaliella salina.* Talanta, 2009. **77**(3): p. 948-952.

9. Chauhan, U. and N. Pathak, *Effect of different conditions on the production of chlorophyll by Spirulina platensis.* J Algal Biomass Utln, 2010. **1**(4): p. 89-99.

10. Nwoba, E.G., C.N. Ogbonna, T. Ishika, and A. Vadiveloo, *Microalgal pigments: a source of natural food colors*, in *Microalgae biotechnology for food, health and high value products*. 2020, Springer. p. 81-123.

11. Wang, Z., et al., *Melanin produced by the fast-growing marine bacterium Vibrio natriegens through heterologous biosynthesis: characterization and application.* Applied and environmental microbiology, 2020. **86**(5): p. e02749-19.

12. Ward, C.S., et al., *Janthinobacter additions reduce rotifer grazing of microalga Microchloropsis salina in biotically complex communities.* Algal Research, 2021. **58**: p. 102400.

13. Becker, M.H., et al., *Genetically modifying skin microbe to produce violacein and augmenting microbiome did not defend Panamanian golden frogs from disease.* ISME Communications, 2021. **1**(1): p. 1-10.

14. Wei, J., et al., *Simultaneous Microcystis algicidal and microcystin synthesis inhibition by a red pigment prodigiosin.* Environ Pollut, 2020. **256**: p. 113444.

15. Zhang, S., W. Zheng, and H. Wang, *Physiological response and morphological changes of Heterosigma akashiwo to an algicidal compound prodigiosin.* J Hazard Mater, 2020. **385**: p. 121530.

16. Nelson, D.R., et al., *Large-scale genome sequencing reveals the driving forces of viruses in microalgal evolution.* Cell Host & Microbe, 2021. **29**(2): p. 250-266. e8.

17. Gaysina, L.A., A. Saraf, and P. Singh, *Cyanobacteria in diverse habitats*, in *Cyanobacteria*. 2019, Elsevier. p. 1-28.

18. Leliaert, F., *Green algae: Chlorophyta and Streptophyta*. 2019, Academic Press. p. 457-468.

19. Kottuparambil, S., R.L. Thankamony, and S. Agusti, *Euglena as a potential natural source of value-added metabolites. A review.* Algal Research, 2019. **37**: p. 154-159.

20. Borowitzka, M.A., *Microalgae in medicine and human health: A historical perspective*, in *Microalgae in health and disease prevention*. 2018, Elsevier. p. 195-210.

21. Bowler, C. and A. Falciatore, *Phaeodactylum tricornutum.* Trends in Genetics, 2019. **35**(9): p. 706-707.

22. Gaber, K., C. Rösch, and N. Biondi, *Life Cycle Assessment of Total Fatty Acid (TFA) Production from Microalgae Nannochloropsis oceanica at Different Sites and Under Different Sustainability Scenarios.* BioEnergy Research, 2021: p. 1-21.

23. Borowitzka, M.A., *Biology of microalgae*, in *Microalgae in health and disease prevention*. 2018, Elsevier. p. 23-72.

24. Villar, E., et al., *Chloroplasts of symbiotic microalgae remain active during bleaching induced by thermal stress in Collodaria (Radiolaria).* bioRxiv, 2018: p. 263053.

25. Putri, D.S., S.P. Astuti, and S. Alaa. *The growth of microalgae Chlorococcum sp. isolated from Ampenan estuary of Lombok Island in Walne's medium*. in *AIP Conference Proceedings*. 2019. AIP Publishing LLC.

26. Correia, N., et al., *Isolation, identification and biotechnological applications of a novel, robust, free-living Chlorococcum (Oophila) amblystomatis strain isolated from a local pond.* Applied Sciences, 2020. **10**(9): p. 3040.

27. Xiao, M., A. Willis, M.A. Burford, and M. Li, *a meta-analysis comparing cell-division and cell-adhesion in Microcystis colony formation.* Harmful algae, 2017. **67**: p. 85-91.

28. Xu, S., et al., *Polysaccharide biosynthesis-related genes explain phenotype-genotype correlation of Microcystis colonies in Meiliang Bay of Lake Taihu, China.* Scientific reports, 2016. **6**(1): p. 1-10.

29. Yang, Z., F. Kong, X. Shi, and H. Cao, *Morphological response of Microcystis aeruginosa to grazing by different sorts of zooplankton.* Hydrobiologia, 2006. **563**(1): p. 225-230.

30. Yang, Z., et al., *Changes in the morphology and polysaccharide content of Microcystis aeruginosa (Cyanobacteria) during flagellate grazing 1.* Journal of Phycology, 2008. **44**(3): p. 716-720.

31. Yang, Z., F. Kong, and X. Shi, *Effects of filtered lake water on colony formation and growth rate in Microcystis aeruginosa of different physiological phases.* Journal of Freshwater Ecology, 2005. **20**(3): p. 425-429.

32. Yang, Z. and J.-J. Li, *Effects of Daphnia-associated infochemicals on the morphology and growth of Scenedesmus obliquus and Microcystis aeruginosa.* Journal of Freshwater Ecology, 2007. **22**(2): p. 249-253.

33. Cao, H. and Z. Yang, *Variation in colony size of Microcystis aeruginosa in a eutrophic lake during recruitment and bloom formation.* Journal of Freshwater Ecology, 2010. **25**(3): p. 331-335.

34. Yang, Z., et al., *Effect of filtered cultures of flagellate Ochromonas sp. on colony formation in Microcystis aeruginosa.* International review of hydrobiology, 2009. **94**(2): p. 143-152.

35. Queiroz, M.I., J.G. Vieira, and M.M. Maroneze, *Morphophysiological, structural, and metabolic aspects of microalgae*, in *Handbook of Microalgae-Based Processes and Products*. 2020, Elsevier. p. 25-48.

36. Buzalewicz, I., M. Karwanska, A. Wieliczko, and H. Podbielska, *On the application of multi-parametric optical phenotyping of bacterial colonies for multipurpose microbiological diagnostics.* Biosens Bioelectron, 2021. **172**: p. 112761.

37. Ansari, A.J., et al., *Forward osmosis as a platform for resource recovery from municipal wastewater-A critical assessment of the literature.* Journal of membrane science, 2017. **529**: p. 195-206.

38. Vu, M.T., et al., *Wastewater to R3–resource recovery, recycling, and reuse efficiency in urban wastewater treatment plants*, in *Clean Energy and Resource Recovery*. 2022, Elsevier. p. 3-16.

39. Feng, S., et al., *Roles and applications of enzymes for resistant pollutants removal in wastewater treatment.* Bioresource technology, 2021. **335**: p. 125278.

40. Chong, C.C., et al., *Anaerobic digestate as a low-cost nutrient source for sustainable microalgae cultivation: A way forward through waste valorization approach.* Science of The Total Environment, 2022. **803**: p. 150070.

41. Nguyen, T.-T., et al., *Nutrient recovery and microalgae biomass production from urine by membrane photobioreactor at low biomass retention times.* Science of the Total Environment, 2021. **785**: p. 147423.

42. Chan, S.S., et al., *Recent advances biodegradation and biosorption of organic compounds from wastewater: Microalgae-bacteria consortium - A review.* Bioresour Technol, 2022. **344**(Pt A): p. 126159.

43. Xiao, R. and Y. Zheng, *Overview of microalgal extracellular polymeric substances (EPS) and their applications.* Biotechnology Advances, 2016. **34**(7): p. 1225-1244.

44. Blifernez-Klassen, O., et al., *Phytoplankton consortia as a blueprint for mutually beneficial eukaryote-bacteria ecosystems based on the biocoenosis of Botryococcus consortia.* Scientific reports, 2021. **11**(1): p. 1-13.

45. Lopez, B.R., et al., *Riboflavin and lumichrome exuded by the bacterium Azospirillum brasilense promote growth and changes in metabolites in Chlorella sorokiniana under autotrophic conditions.* Algal Research, 2019. **44**: p. 101696.

46. Huang, X., et al., *Nitrate assimilation, dissimilatory nitrate reduction to ammonium, and denitrification coexist in Pseudomonas putida Y-9 under aerobic conditions.* Bioresource Technology, 2020. **312**: p. 123597.

47. Nhut, H.T., et al., *Removal of nutrients and organic pollutants from domestic wastewater treatment by sponge-based moving bed biofilm reactor.* Environmental Engineering Research, 2020. **25**(5): p. 652-658.

48. Qu, W., C. Zhang, X. Chen, and S.-H. Ho, *New concept in swine wastewater treatment: development of a self-sustaining synergetic microalgae-bacteria symbiosis (ABS) system to achieve environmental sustainability.* Journal of Hazardous Materials, 2021: p. 126264.

49. Chen, X., et al., *The interactions of algae-activated sludge symbiotic system and its effects on wastewater treatment and lipid accumulation.* Bioresour Technol, 2019. **292**: p. 122017.

50. Bankston, E., Q. Wang, and B.T. Higgins, *Algae support populations of heterotrophic, nitrifying, and phosphate-accumulating bacteria in the treatment of poultry litter anaerobic digestate.* Chemical Engineering Journal, 2020. **398**: p. 125550.

51. Maza-Márquez, P., et al., *Microalgae-bacteria consortia for the removal of phenolic compounds from industrial wastewaters*, in *Approaches in Bioremediation*. 2018, Springer. p. 135-184.

52. Higgins, B.T., et al., *Algal–bacterial synergy in treatment of winery wastewater.* npj Clean Water, 2018. **1**(1): p. 1-10.

53. Xu, Y., et al., *Using microbial aggregates to entrap aqueous phosphorus.* Trends in biotechnology, 2020. **38**(11): p. 1292-1303.

54. Chai, W.S., et al., *Multifaceted roles of microalgae in the application of wastewater biotreatment: A review.* Environ Pollut, 2021. **269**: p. 116236.

55. Sells, M.D., N. Brown, and A.N. Shilton, *Determining variables that influence the phosphorus content of waste stabilization pond algae.* Water research, 2018. **132**: p. 301-308.

56. Qi, F., et al., *Convergent community structure of algal-bacterial consortia and its effects on advanced wastewater treatment and biomass production.* Sci Rep, 2021. **11**(1): p. 21118.

57. Khan, M.I., J.H. Shin, and J.D. Kim, *The promising future of microalgae: current status, challenges, and optimization of a sustainable and renewable industry for biofuels, feed, and other products.* Microb Cell Fact, 2018. **17**(1): p. 36.

58. Meyer, K.J. and J.R. Nodwell, *Biology and applications of co-produced, synergistic antimicrobials from environmental bacteria.* Nat Microbiol, 2021. **6**(9): p. 1118-1128.

59. Jia, W., X. Huang, and C. Li, *A preliminary study of the algicidal mechanism of bioactive metabolites of Brevibacillus laterosporus on Oscillatoria in prawn ponds.* ScientificWorldJournal, 2014. **2014**: p. 869149.

60. González-González, L.M. and L.E. de-Bashan, *Toward the enhancement of microalgal metabolite production through microalgae–bacteria consortia.* Biology, 2021. **10**(4): p. 282.

61. Gou, Y., et al., *Feasibility of using a novel algal-bacterial biofilm reactor for efficient domestic wastewater treatment.* Environmental Technology, 2020. **41**(4): p. 400-410.

62. Foladori, P., S. Petrini, M. Nessenzia, and G. Andreottola, *Enhanced nitrogen removal and energy saving in a microalgal-bacterial consortium treating real municipal wastewater.* Water Sci Technol, 2018. **78**(1-2): p. 174-182.

63. Barreiro-Vescovo, S., C. González-Fernández, and I. de Godos, *Characterization of communities in a microalgae-bacteria system treating domestic wastewater reveals dominance of phototrophic and pigmented bacteria.* Algal Research, 2021. **59**: p. 102447.

64. Purba, L.D., et al., *Rapid Development of Microalgae-Bacteria Granular Sludge Using Low-Strength Domestic Wastewater.* Journal of Water and Environment Technology, 2021. **19**(2): p. 96-107.

65. Fan, J., et al., *Performance of Chlorella sorokiniana-activated sludge consortium treating wastewater under light-limited heterotrophic condition.* Chemical Engineering Journal, 2020. **382**: p. 122799.

66. Goswami, G., B.B. Makut, and D. Das, *Sustainable production of bio-crude oil via hydrothermal liquefaction of symbiotically grown biomass of microalgae-bacteria coupled with effective wastewater treatment.* Sci Rep, 2019. **9**(1): p. 15016.

67. Raza, N., M. Rizwan, and G. Mujtaba. *TREATMENT OF REAL TEXTILE WASTEWATER IN SINGLE STAGE AND MICROALGAE–BACTERIA CONSORTIUM*. in *BOOK OF ABSTRACTS*. 2021.

68. Huo, S., et al., *Co-culture of Chlorella and wastewater-borne bacteria in vinegar production wastewater: Enhancement of nutrients removal and influence of algal biomass generation.* Algal Research, 2020. **45**: p. 101744.

69. Shetty, P., et al., *Exploitation of algal-bacterial consortia in combined biohydrogen generation and wastewater treatment.* Frontiers in Energy Research, 2019. **7**: p. 52.

70. Udaiyappan, A.F.M., et al., *Microalgae-bacteria interaction in palm oil mill effluent treatment.* Journal of Water Process Engineering, 2020. **35**: p. 101203.

71. Rasouli, Z., et al., *Nutrient recovery from industrial wastewater as single cell protein by a co-culture of green microalgae and methanotrophs.* Biochemical Engineering Journal, 2018. **134**: p. 129-135.

72. Biswas, T., S. Bhushan, S.K. Prajapati, and S. Ray Chaudhuri, *An eco-friendly strategy for dairy wastewater remediation with high lipid microalgae-bacterial biomass production.* J Environ Manage, 2021. **286**: p. 112196.

73. Makut, B.B., D. Das, and G. Goswami, *Production of microbial biomass feedstock via co-cultivation of microalgae-bacteria consortium coupled with effective wastewater treatment: A sustainable approach.* Algal Research, 2019. **37**: p. 228-239.

74. You, K., et al., *Nutrients recovery from piggery wastewater and starch wastewater via microalgae-bacteria consortia.* Algal Research, 2021. **60**: p. 102551.

75. Sánchez-Zurano, A., et al., *Abaco: a new model of microalgae-bacteria consortia for biological treatment of wastewaters.* Applied Sciences, 2021. **11**(3): p. 998.

76. Okurowska, K., et al., *Adapting the algal microbiome for growth on domestic landfill leachate.* Bioresour Technol, 2021. **319**: p. 124246.

77. Tighiri, H.O. and E.A. Erkurt, *Biotreatment of landfill leachate by microalgae-bacteria consortium in sequencing batch mode and product utilization.* Bioresour Technol, 2019. **286**: p. 121396.

78. Sniffen, K.D., C.M. Sales, and M.S. Olson, *The fate of nitrogen through algal treatment of landfill leachate.* Algal research, 2018. **30**: p. 50-58.

79. Nair, A.T. and S.S. Nagendra, *Chlorella Pyrenoidosa mediated phycoremediation of landfill leachate.* Impact of global atmospheric changes on natural resources, 2018: p. 65-68.

80. Wulan, D.R., et al., *Domestic wastewater in Indonesia: generation, characteristics and treatment.* Environmental Science and Pollution Research, 2022: p. 1-18.

81. Thomas, D.G., N. Minj, N. Mohan, and P.H. Rao, *Cultivation of microalgae in domestic wastewater for biofuel applications–an upstream approach.* J Algal Biomass Utln, 2016. **7**(1): p. 62-70.

82. Fallahi, A., et al., *Interactions of microalgae-bacteria consortia for nutrient removal from wastewater: A review.* Chemosphere, 2021. **272**: p. 129878.

83. Foladori, P., S. Petrini, and G. Andreottola, *Evolution of real municipal wastewater treatment in photobioreactors and microalgae-bacteria consortia using real-time parameters.* Chemical Engineering Journal, 2018. **345**: p. 507-516.

84. You, X., L. Yang, X. Zhou, and Y. Zhang, *Sustainability and carbon neutrality trends for microalgae-based wastewater treatment: A review.* Environ Res, 2022. **209**: p. 112860.

85. Serrano-Bermúdez, L.M., L.C. Montenegro-Ruíz, and R.D. Godoy-Silva, *Effect of CO2, aeration, irradiance, and photoperiod on biomass and lipid accumulation in a microalga autotrophically cultured and selected from four Colombian-native strains.* Bioresource Technology Reports, 2020. **12**: p. 100578.

86. Hena, S., L. Gutierrez, and J.-P. Croué, *Removal of pharmaceutical and personal care products (PPCPs) from wastewater using microalgae: A review.* Journal of hazardous materials, 2021. **403**: p. 124041.

87. Osman, N.A., et al., *The effect of palm oil mill effluent final discharge on the characteristics of Pennisetum purpureum.* Scientific reports, 2020. **10**(1): p. 1-10.

88. Noguchi, M., et al., *Application of real treated wastewater to starch production by microalgae: Potential effect of nutrients and microbial contamination.* Biochemical Engineering Journal, 2021. **169**: p. 107973.

89. Passos, F., et al., *Anaerobic co-digestion of coffee husks and microalgal biomass after thermal hydrolysis.* Bioresource technology, 2018. **253**: p. 49-54.

90. Arif, M., et al., *A complete characterization of microalgal biomass through FTIR/TGA/CHNS analysis: An approach for biofuel generation and nutrients removal.* Renewable Energy, 2021. **163**: p. 1973-1982.

91. Posadas, E., et al., *Microalgae-based agro-industrial wastewater treatment: a preliminary screening of biodegradability.* Journal of applied phycology, 2014. **26**(6): p. 2335-2345.

92. Hemalatha, M., J.S. Sravan, B. Min, and S. Venkata Mohan, *Microalgae-biorefinery with cascading resource recovery design associated to dairy wastewater treatment.* Bioresour Technol, 2019. **284**: p. 424-429.

93. Gramegna, G., et al., *Exploring the potential of microalgae in the recycling of dairy wastes.* Bioresource Technology Reports, 2020. **12**: p. 100604.

94. Talapatra, N., R. Gautam, V. Mittal, and U. Ghosh, *A comparative study of the growth of microalgae-bacteria symbiotic consortium with the axenic culture of microalgae in dairy wastewater through extraction and quantification of chlorophyll.* Materials Today: Proceedings, 2021.

95. Svierzoski, N.D.S., et al., *Treatment of a slaughterhouse wastewater by anoxic-aerobic biological reactors followed by UV-C disinfection and microalgae bioremediation.* Water Environ Res, 2021. **93**(3): p. 409-420.

96. Fuentes-Grünewald, C., et al., *Towards a circular economy: A novel microalgal two-step growth approach to treat excess nutrients from digestate and to produce biomass for animal feed.* Bioresource Technology, 2021. **320**: p. 124349.

97. Nawaz, T., et al., *A review of landfill leachate treatment by microalgae: Current status and future directions.* Processes, 2020. **8**(4): p. 384.

98. Porto, B., et al., *Assessing the potential of microalgae for nutrients removal from a landfill leachate using an innovative tubular photobioreactor.* Chemical Engineering Journal, 2021. **413**: p. 127546.

99. Li, X., et al., *Effect of ammonium nitrogen on microalgal growth, biochemical composition and photosynthetic performance in mixotrophic cultivation.* Bioresour Technol, 2019. **273**: p. 368-376.

100. Sánchez-Zurano, A., et al., *Wastewater treatment using Scenedesmus almeriensis: effect of operational conditions on the composition of the microalgae-bacteria consortia.* Journal of Applied Phycology, 2021: p. 1-13.

101. Hernandez-Garcia, A., et al., *Wastewater-leachate treatment by microalgae: Biomass, carbohydrate and lipid production.* Ecotoxicol Environ Saf, 2019. **174**: p. 435-444.

102. Chia, S.R., et al., *Algae as potential feedstock for various bioenergy production.* Chemosphere, 2022. **287**: p. 131944.

103. Dang, B.-T., et al., *Current application of algae derivatives for bioplastic production: A review.* Bioresource Technology, 2022: p. 126698.

104. Yaakob, M.A., et al., *Influence of nitrogen and phosphorus on microalgal growth, biomass, lipid, and fatty acid production: an overview.* Cells, 2021. **10**(2): p. 393.

105. Zarrinmehr, M.J., et al., *Effect of nitrogen concentration on the growth rate and biochemical composition of the microalga, Isochrysis galbana.* The Egyptian Journal of Aquatic Research, 2020. **46**(2): p. 153-158.

106. Michelon, W., et al., *Amino acids, fatty acids, and peptides in microalgae biomass harvested from phycoremediation of swine wastewaters.* Biomass Conversion and Biorefinery, 2021: p. 1-12.

107. de Souza, M.P., et al., *Concepts and Trends for Extraction and Application of Microalgae Carbohydrates.* Microalgae-From Physiology to Application, 2019.

108. Rocha, C.J.L., et al., *Development of bioplastics from a microalgae consortium from wastewater.* Journal of Environmental Management, 2020. **263**: p. 110353.

109. Ramos-Romero, S., et al., *Edible microalgae and their bioactive compounds in the prevention and treatment of metabolic alterations.* Nutrients, 2021. **13**(2): p. 563.

110. Soletto, D., et al., *Batch and fed-batch cultivations of Spirulina platensis using ammonium sulphate and urea as nitrogen sources.* Aquaculture, 2005. **243**(1-4): p. 217-224.

111. Dosta, J., et al., *Integration of a Coagulation/Flocculation step in a biological sequencing batch reactor for COD and nitrogen removal of supernatant of anaerobically digested piggery wastewater.* Bioresource technology, 2008. **99**(13): p. 5722-5730.

112. Rodolfi, L., et al., *Microalgae for oil: Strain selection, induction of lipid synthesis and outdoor mass cultivation in a low-cost photobioreactor.* Biotechnology and bioengineering, 2009. **102**(1): p. 100-112.

113. Levasseur, W., P. Perré, and V. Pozzobon, *A review of high value-added molecules production by microalgae in light of the classification.* Biotechnology advances, 2020. **41**: p. 107545.

114. Sajjadi, B., W.-Y. Chen, A.A.A. Raman, and S. Ibrahim, *Microalgae lipid and biomass for biofuel production: A comprehensive review on lipid enhancement strategies and their effects on fatty acid composition.* Renewable and Sustainable Energy Reviews, 2018. **97**: p. 200-232.

115. Peng, H., L.E. de-Bashan, Y. Bashan, and B.T. Higgins, *Indole-3-acetic acid from Azosprillum brasilense promotes growth in green algae at the expense of energy storage products.* Algal Research, 2020. **47**: p. 101845.

116. Vuong, T.T., et al., *Interaction between marine bacterium Stappia sp. K01 and diatom Phaeodactylum tricornutum through extracellular fatty acids.* Journal of Applied Phycology, 2020. **32**(1): p. 71-82.

117. Kiran, B.R. and S. Venkata Mohan, *Microalgal Cell Biofactory—Therapeutic, Nutraceutical and Functional Food Applications.* Plants, 2021. **10**(5): p. 836.

118. Vethathirri, R.S., E. Santillan, and S. Wuertz, *Microbial community-based protein production from wastewater for animal feed applications.* Bioresour Technol, 2021. **341**: p. 125723.

119. Saadaoui, I., et al., *Microalgal-based feed: promising alternative feedstocks for livestock and poultry production.* J Anim Sci Biotechnol, 2021. **12**(1): p. 76.

120. Ekmay, R., et al., *Nutritional and metabolic impacts of a defatted green marine microalgal (Desmodesmus sp.) biomass in diets for weanling pigs and broiler chickens.* Journal of agricultural and food chemistry, 2014. **62**(40): p. 9783-9791.

121. Wu, Y., et al., *Dual functions of eicosapentaenoic acid-rich microalgae: enrichment of yolk with n-3 polyunsaturated fatty acids and partial replacement for soybean meal in diet of laying hens.* Poultry science, 2019. **98**(1): p. 350-357.

122. Torregrosa-Crespo, J., et al., *Exploring the valuable carotenoids for the large-scale production by marine microorganisms.* Marine drugs, 2018. **16**(6): p. 203.

123. Sakarika, M., et al., *The type of microorganism and substrate determines the odor fingerprint of dried bacteria targeting microbial protein production.* FEMS Microbiol Lett, 2020. **367**(18): p. fnaa138.

124. Das, P., et al., *Microalgal nutrients recycling from the primary effluent of municipal wastewater and use of the produced biomass as bio-fertilizer.* International journal of environmental science and technology, 2019. **16**(7): p. 3355-3364.

125. Solovchenko, A., P. Zaitsev, and V. Zotov, *Phosphorus biofertilizer from microalgae*, in *Biofertilizers*. 2021, Elsevier. p. 57-68.

126. Rachidi, F., et al., *Evaluation of microalgae polysaccharides as biostimulants of tomato plant defense using metabolomics and biochemical approaches.* Scientific reports, 2021. **11**(1): p. 1-16.

127. Yan, C., et al., *Microalgal bioremediation of heavy metal pollution in water: Recent advances, challenges, and prospects.* Chemosphere, 2022. **286**(Pt 3): p. 131870.

128. Garcia-Gonzalez, J. and M. Sommerfeld, *Biofertilizer and biostimulant properties of the microalga Acutodesmus dimorphus.* Journal of applied phycology, 2016. **28**(2): p. 1051-1061.

129. Umamaheswari, J. and S. Shanthakumar, *Paddy-soaked rice mill wastewater treatment by phycoremediation and feasibility study on use of algal biomass as biofertilizer.* Journal of Chemical Technology & Biotechnology, 2021. **96**(2): p. 394-403.

130. Renuka, N., et al., *Exploring the efficacy of wastewater-grown microalgal biomass as a biofertilizer for wheat.* Environmental Science and Pollution Research, 2016. **23**(7): p. 6608-6620.

131. Ferreira, A., et al., *Scenedesmus obliquus microalga-based biorefinery–from brewery effluent to bioactive compounds, biofuels and biofertilizers–aiming at a circular bioeconomy.* Biofuels, Bioproducts and Biorefining, 2019. **13**(5): p. 1169-1186.

132. Okoro, V., et al., *Microalgae cultivation and harvesting: Growth performance and use of flocculants-A review.* Renewable and Sustainable Energy Reviews, 2019. **115**: p. 109364.

133. Zullaikah, S., et al., *Ecofuel conversion technology of inedible lipid feedstocks to renewable fuel*, in *Advances in Eco-Fuels for a Sustainable Environment*. 2019, Elsevier. p. 237-276.

134. Kim, T.-H., et al., *A novel process for the coproduction of biojet fuel and high-value polyunsaturated fatty acid esters from heterotrophic microalgae Schizochytrium sp. ABC101.* Renewable Energy, 2021. **165**: p. 481-490.

135. Yao, L., et al., *Microalgae lipid characterization.* Journal of agricultural and food chemistry, 2015. **63**(6): p. 1773-1787.

136. Siddiki, S.Y.A., et al., *Microalgae biomass as a sustainable source for biofuel, biochemical and biobased value-added products: An integrated biorefinery concept.* Fuel, 2022. **307**: p. 121782.

137. Mofijur, M., et al., *Selection of microalgae strains for sustainable production of aviation biofuel.* Bioresource Technology, 2021: p. 126408.

138. O'Malley, J., N. Pavlenko, and S. Searle, *Estimating sustainable aviation fuel feedstock availability to meet growing European Union demand*. 2021, Retrieved from the International Council on Clean Transportation, https ….

139. Peter, A.P., et al., *Microalgae for biofuels, wastewater treatment and environmental monitoring.* Environmental Chemistry Letters, 2021. **19**(4): p. 2891-2904.

140. Aditya, L., et al., *Microalgae enrichment for biomass harvesting and water reuse by ceramic microfiltration membranes.* Journal of Membrane Science, 2023. **669**: p. 121287.

141. Zerveas, S., M.S. Mente, D. Tsakiri, and K. Kotzabasis, *Microalgal photosynthesis induces alkalization of aquatic environment as a result of H+ uptake independently from CO2 concentration–New perspectives for environmental applications.* Journal of Environmental Management, 2021. **289**: p. 112546.

142. Iñiguez, C., P. Aguiló-Nicolau, and J. Galmés, *Improving photosynthesis through the enhancement of Rubisco carboxylation capacity.* Biochemical Society Transactions, 2021. **49**(5): p. 2007-2019.

143. Mott, K.A. and J.A. Berry, *Effects of pH on activity and activation of ribulose 1, 5-bisphosphate carboxylase at air level CO2.* Plant physiology, 1986. **82**(1): p. 77-82.

144. Chen, Y., C. Xu, and S. Vaidyanathan, *Influence of gas management on biochemical conversion of CO2 by microalgae for biofuel production.* Applied Energy, 2020. **261**: p. 114420.

145. Wang, Z., et al., *Mutation adaptation and genotoxicity of microalgae induced by Long-Term high CO2 stress.* Chemical Engineering Journal, 2022. **445**: p. 136745.

146. Manzi, H.P., M. Zhang, and E.-S. Salama, *Extensive investigation and beyond the removal of micro-polyvinyl chloride by microalgae to promote environmental health.* Chemosphere, 2022. **300**: p. 134530.

147. Qu, D. and X. Miao, *Carbon flow conversion induces alkali resistance and lipid accumulation under alkaline conditions based on transcriptome analysis in Chlorella sp. BLD.* Chemosphere, 2021. **265**: p. 129046.

148. Rao, M., et al., *Light Conditions Determine Optimal CO2 Concentrations for Nannochloropsis oceanica Growth with Carbon Fixation.* ACS Sustainable Chemistry & Engineering, 2022. **10**(27): p. 8799-8814.

149. Wang, Z., et al., *Comprehensive understanding of regulatory mechanisms, physiological models and key enzymes in microalgal cells based on various concentrations of CO2.* Chemical Engineering Journal, 2023. **454**: p. 140233.

150. Nikkanen, L. and E. Rintamäki, *Chloroplast thioredoxin systems dynamically regulate photosynthesis in plants.* Biochemical Journal, 2019. **476**(7): p. 1159-1172.

151. Gao, P., et al., *Enhancing microalgae growth and product accumulation with carbon source regulation: New perspective for the coordination between photosynthesis and aerobic respiration.* Chemosphere, 2021. **278**: p. 130435.

152. Zhang, Z., D. Sun, K.-W. Cheng, and F. Chen, *Investigation of carbon and energy metabolic mechanism of mixotrophy in Chromochloris zofingiensis.* Biotechnology for Biofuels, 2021. **14**: p. 1-16.

153. Zhang, X., et al., *Effects of different concentrations of CO2 on Scenedesmus obliquus to overcome sludge extract toxicity and accumulate biomass.* Chemosphere, 2022. **305**: p. 135514.

154. Li, S., X. Li, and S.-H. Ho, *How to enhance carbon capture by evolution of microalgal photosynthesis?* Separation and Purification Technology, 2022. **291**: p. 120951.

155. Choi, H.I., et al., *Augmented CO2 tolerance by expressing a single H+-pump enables microalgal valorization of industrial flue gas.* Nature communications, 2021. **12**(1): p. 6049.

156. Kang, N.K., et al., *Photoautotrophic organic acid production: glycolic acid production by microalgal cultivation.* Chemical Engineering Journal, 2022. **433**: p. 133636.

157. Casey, J.R., S. Ferrón, and D.M. Karl, *Light-enhanced microbial organic carbon yield.* Frontiers in Microbiology, 2017. **8**: p. 2157.

158. Cordoba-Perez, M. and H. de Lasa, *CO2-derived carbon capture and photon absorption efficiency by microalgae in novel PhotoBioCREC.* Industrial & Engineering Chemistry Research, 2020. **59**(33): p. 14710-14716.

159. Shibagaki, N. and A. Grossman, *The state of sulfur metabolism in algae: from ecology to genomics*, in *Sulfur metabolism in phototrophic organisms*. 2008, Springer. p. 231-267.

160. Kumari, K., S. Samantaray, D. Sahoo, and B.C. Tripathy, *Modulation of photosynthesis, biomass and lipid production by sulfur and CO2 supplementation in Chlorella vulgaris.* Journal of Applied Phycology, 2024: p. 1-16.

161. Zhang, Y., et al., *Growth, biochemical composition and photosynthetic performance of Scenedesmus acuminatus under different initial sulfur supplies.* Algal Research, 2020. **45**: p. 101728.

162. Mera, R., E. Torres, and J. Abalde, *Effects of sodium sulfate on the freshwater microalga Chlamydomonas moewusii: implications for the optimization of algal culture media.* Journal of Phycology, 2016. **52**(1): p. 75-88.

163. Giordano, M., V. Pezzoni, and R. Hell, *Strategies for the allocation of resources under sulfur limitation in the green alga Dunaliella salina.* Plant Physiology, 2000. **124**(2): p. 857-864.

164. Giordano, M. and J.A. Raven, *Nitrogen and sulfur assimilation in plants and algae.* Aquatic botany, 2014. **118**: p. 45-61.

165. Zhang, Y., et al., *Photosynthetic physiological performance and proteomic profiling of the oleaginous algae Scenedesmus acuminatus reveal the mechanism of lipid accumulation under low and high nitrogen supplies.* Photosynthesis research, 2018. **138**: p. 73-102.

166. Li, T., et al., *Morphology, growth, biochemical composition and photosynthetic performance of Chlorella vulgaris (Trebouxiophyceae) under low and high nitrogen supplies.* Algal Research, 2016. **16**: p. 481-491.

167. Ota, S., et al., *Highly efficient lipid production in the green alga Parachlorella kessleri: draft genome and transcriptome endorsed by whole-cell 3D ultrastructure.* Biotechnology for biofuels, 2016. **9**: p. 1-10.

168. Takeshita, T., et al., *Starch and lipid accumulation in eight strains of six Chlorella species under comparatively high light intensity and aeration culture conditions.* Bioresource Technology, 2014. **158**: p. 127-134.

169. Ballin, G., J. Doucha, V. Zachleder, and I. Šetlík, *Macromolecular syntheses and the course of cell cycle events in the chlorococcal alga Scenedesmus quadricauda under nutrient starvation: effect of nitrogen starvation.* Biologia plantarum, 1988. **30**: p. 81-91.

170. Yildiz, F.H., J.P. Davies, and A.R. Grossman, *Characterization of sulfate transport in Chlamydomonas reinhardtii during sulfur-limited and sulfur-sufficient growth.* Plant physiology, 1994. **104**(3): p. 981-987.

171. Takahashi, H., et al., *Sulfur assimilation in photosynthetic organisms: molecular functions and regulations of transporters and assimilatory enzymes.* Annual review of plant biology, 2011. **62**(1): p. 157-184.

172. Mizuno, Y., et al., *Sequential accumulation of starch and lipid induced by sulfur deficiency in Chlorella and Parachlorella species.* Bioresource Technology, 2013. **129**: p. 150-155.

173. Carfagna, S., et al., *Cross-effects of nitrogen and sulphur starvation in Chlorella sorokiniana 211/8K.* Natural Resources, 2015. **6**(4): p. 221-229.

174. D'Hooghe, P., S. Escamez, J. Trouverie, and J.-C. Avice, *Sulphur limitation provokes physiological and leaf proteome changes in oilseed rape that lead to perturbation of sulphur, carbon and oxidative metabolisms.* BMC Plant Biology, 2013. **13**: p. 1-15.

175. Zhang, L., T. Happe, and A. Melis, *Biochemical and morphological characterization of sulfur-deprived and H 2-producing Chlamydomonas reinhardtii (green alga).* Planta, 2002. **214**: p. 552-561.

176. Sugimoto, K., M. Tsuzuki, and N. Sato, *Regulation of synthesis and degradation of a sulfolipid under sulfur-starved conditions and its physiological significance in Chlamydomonas reinhardtii.* New Phytologist, 2010. **185**(3): p. 676-686.

177. Fu, J., et al., *How the sulfur dioxide in the flue gas influence microalgal carbon dioxide fixation: From gas dissolution to cells growth.* Renewable Energy, 2022. **198**: p. 114-122.

178. Van Den Hende, S., H. Vervaeren, and N. Boon, *Flue gas compounds and microalgae:(Bio-) chemical interactions leading to biotechnological opportunities.* Biotechnology advances, 2012. **30**(6): p. 1405-1424.

179. Novosel, N., et al., *Salinity-induced chemical, mechanical, and behavioral changes in marine microalgae.* Journal of applied phycology, 2022. **34**(3): p. 1293-1309.

180. Jothibasu, K., et al., *Impact of microalgal cell wall biology on downstream processing and nutrient removal for fuels and value-added products.* Biochemical Engineering Journal, 2022. **187**: p. 108642.

181. Singh, D.V., A. Upadhyay, R. Singh, and D. Singh, *Implication of municipal wastewater on growth kinetics, biochemical profile, and defense system of Chlorella vulgaris and Scenedesmus vacuolatus.* Environmental Technology & Innovation, 2022. **26**: p. 102334.

182. Zafar, A.M., et al., *Recent updates on ions and nutrients uptake by halotolerant freshwater and marine microalgae in conditions of high salinity.* Journal of Water Process Engineering, 2021. **44**: p. 102382.

183. Ramos-Ibarra, J.R., R. Snell-Castro, J.A. Neria-Casillas, and F.J. Choix, *Biotechnological potential of Chlorella sp. and Scenedesmus sp. microalgae to endure high CO 2 and methane concentrations from biogas.* Bioprocess and biosystems engineering, 2019. **42**: p. 1603-1610.

184. Rachlin, J.W. and A. Grosso, *The effects of pH on the growth of Chlorella vulgaris and its interactions with cadmium toxicity.* Archives of environmental contamination and toxicology, 1991. **20**: p. 505-508.

185. Gong, Q., et al., *Effects of light and pH on cell density of Chlorella vulgaris.* Energy Procedia, 2014. **61**: p. 2012-2015.

186. Baker, M., C. Mayfield, W. Inniss, and P. Wong, *Toxicity of pH, heavy metals and bisulfite to a freshwater green alga.* Chemosphere, 1983. **12**(1): p. 35-44.

187. Sakarika, M. and M. Kornaros, *Effect of pH on growth and lipid accumulation kinetics of the microalga Chlorella vulgaris grown heterotrophically under sulfur limitation.* Bioresource technology, 2016. **219**: p. 694-701.

188. Peng, H., et al., *Deciphering mechanism of sulfide stress on microalgae and overcoming its inhibition by regulation growth acclimatization period.* Chemical Engineering Journal, 2024. **495**: p. 153045.

189. Chauhan, D.S., L. Sahoo, and K. Mohanty, *Maximize microalgal carbon dioxide utilization and lipid productivity by using toxic flue gas compounds as nutrient source.* Bioresource Technology, 2022. **348**: p. 126784.

190. Vega, J.M., *Nitrogen and sulfur metabolism in microalgae and plants: 50 years of research.* Progress in Botany Vol. 81, 2020: p. 1-40.

191. Peng, L., et al., *Alleviation of oxygen stress on Neochloris oleoabundans: effects of bicarbonate and pH.* Journal of Applied Phycology, 2017. **29**: p. 143-152.

192. Radmann, E.M., F.V. Camerini, T.D. Santos, and J.A.V. Costa, *Isolation and application of SOX and NOX resistant microalgae in biofixation of CO2 from thermoelectricity plants.* Energy Conversion and Management, 2011. **52**(10): p. 3132-3136.

193. Liu, X., et al., *Sulfur heterogeneity: A non-negligible factor in manipulating growth and lipid accumulation of Scenedesmus obliquus at a relatively high ratio of carbon to nitrogen.* Bioresource Technology, 2022. **360**: p. 127599.

194. Li, Q.-D., et al., *Effects of elevated temperature and acidification on sulfate assimilation and reduction of microalgae.* Journal of Applied Phycology, 2023. **35**(4): p. 1603-1619.

195. Wang, C., H. Li, Q. Wang, and P. Wei, *Effect of pH on growth and lipid content of Chlorella vulgaris cultured in biogas slurry.* Sheng wu gong cheng xue bao= Chinese journal of biotechnology, 2010. **26**(8): p. 1074-1079.

196. Cho, H.U., et al., *Effects of pH control and concentration on microbial oil production from Chlorella vulgaris cultivated in the effluent of a low-cost organic waste fermentation system producing volatile fatty acids.* Bioresource technology, 2015. **184**: p. 245-250.

197. Cheng, C.-L., et al., *Effect of pH on biomass production and carbohydrate accumulation of Chlorella vulgaris JSC-6 under autotrophic, mixotrophic, and photoheterotrophic cultivation.* Bioresource technology, 2022. **351**: p. 127021.

198. Xin, L., H. Hong-Ying, and Z. Yu-Ping, *Growth and lipid accumulation properties of a freshwater microalga Scenedesmus sp. under different cultivation temperature.* Bioresource technology, 2011. **102**(3): p. 3098-3102.

199. Wu, Y.-H., Y. Yu, H.-Y. Hu, and L.-L. Zhuang, *Effects of cultivation conditions on the production of soluble algal products (SAPs) of Scenedesmus sp. LX1.* Algal Research, 2016. **16**: p. 376-382.

200. Liu, X., et al., *Effects of sulfate ions on growth and lipid synthesis of Scenedesmus obliquus in synthetic wastewater with various carbon-to-nitrogen ratios altered by different ammonium and nitrate additions.* Bioresource Technology, 2021. **341**: p. 125766.

201. Ajala, S.O. and M.L. Alexander, *Assessment of Chlorella vulgaris, Scenedesmus obliquus, and Oocystis minuta for removal of sulfate, nitrate, and phosphate in*

wastewater. International Journal of Energy and Environmental Engineering, 2020. **11**(3): p. 311-326.

202. Tao, R., et al., *Use of factorial experimental design to study the effects of iron and sulfur on growth of Scenedesmus acuminatus with different nitrogen sources.* Journal of Applied Phycology, 2020. **32**: p. 221-231.

203. Cai, Y., et al., *The relationship between amino acid and lipid metabolism in oleaginous eukaryotic microorganism.* Applied Microbiology and Biotechnology, 2022. **106**(9): p. 3405-3417.

204. Ho, S.-H., W.-M. Chen, and J.-S. Chang, *Scenedesmus obliquus CNW-N as a potential candidate for CO2 mitigation and biodiesel production.* Bioresource technology, 2010. **101**(22): p. 8725-8730.

205. Griffiths, M.J. and S.T. Harrison, *Lipid productivity as a key characteristic for choosing algal species for biodiesel production.* Journal of applied phycology, 2009. **21**: p. 493-507.

206. Wang, H., et al., *Oxidative stress response mechanism of Scenedesmus obliquus to ionic liquids with different number of methyl-substituents.* Journal of Hazardous Materials, 2020. **399**: p. 122847.

207. Zheng, H., et al., *Cultivation of Chlorella vulgaris in manure-free piggery wastewater with high-strength ammonium for nutrients removal and biomass production: Effect of ammonium concentration, carbon/nitrogen ratio and pH.* Bioresource Technology, 2019. **273**: p. 203-211.

208. Huang, Y., C. Lou, L. Luo, and X.C. Wang, *Insight into nitrogen and phosphorus coupling effects on mixotrophic Chlorella vulgaris growth under stably controlled nutrient conditions.* Science of the total environment, 2021. **752**: p. 141747.

209. Solovchenko, A., et al., *Phosphorus starvation and luxury uptake in green microalgae revisited.* Algal Research, 2019. **43**: p. 101651.

210. Su, Y., *Revisiting carbon, nitrogen, and phosphorus metabolisms in microalgae for wastewater treatment.* Science of the total environment, 2021. **762**: p. 144590.

211. Yaakob, M.A., et al., *Influence of nitrogen and phosphorus on microalgal growth, biomass, lipid, and fatty acid production: an overview.* Cells, 2021. **10**(2): p. 393.

212. Ibrahim, T.N.B.T., et al., *Biological active metabolites from microalgae for healthcare and pharmaceutical industries: a comprehensive review.* Bioresource Technology, 2023. **372**: p. 128661.

213. Singh, D., et al., *Combination of calcium and magnesium ions prevents substrate inhibition and promotes biomass and lipid production in thraustochytrids under higher glycerol concentration.* Algal research, 2016. **15**: p. 202-209.

214. Dukic, E., et al., *Chloroplast magnesium transporters play essential but differential roles in maintaining magnesium homeostasis.* Frontiers in Plant Science, 2023. **14**: p. 1221436.

215. Chen, Z., et al., *Simultaneous improvements on nutrient and Mg recoveries of microalgal bioremediation for municipal wastewater and nickel laterite ore wastewater.* Bioresource Technology, 2020. **297**: p. 122517.

216. Ermis, H., U. Guven-Gulhan, T. Cakir, and M. Altinbas, *Effect of iron and magnesium addition on population dynamics and high value product of microalgae grown in anaerobic liquid digestate.* Scientific reports, 2020. **10**(1): p. 3510.

217. Koyande, A.K., et al., *Integration of osmotic shock assisted liquid biphasic system for protein extraction from microalgae Chlorella vulgaris.* Biochemical engineering journal, 2020. **157**: p. 107532.

218. Tan, C.H., et al., *Examination of indigenous microalgal species for maximal protein synthesis.* Biochemical engineering journal, 2020. **154**: p. 107425.

219. Singh, A., et al., *A sustainable approach for the production of formate from CO2 using microalgae as a clean biomass and improvement using potassium-doped g-C3N4.* Chemical Engineering Journal, 2023. **454**: p. 140303.

220. Xu, F. and J. Pan, *Potassium channel KCN11 is required for maintaining cellular osmolarity during nitrogen starvation to control proper cell physiology and TAG accumulation in Chlamydomonas reinhardtii.* Biotechnology for biofuels, 2020. **13**: p. 1-11.

221. Zhang, B., C. Cai, and Y. Zhou, *Iron and nitrogen regulate carbon transformation in a methanotroph-microalgae system.* Science of The Total Environment, 2023. **904**: p. 166287.

222. Behnke, J. and J. LaRoche, *Iron uptake proteins in algae and the role of Iron Starvation-Induced Proteins (ISIPs).* European Journal of Phycology, 2020. **55**(3): p. 339-360.

223. Wang, Z., et al., *Mitigating nutrient accumulation with microalgal growth towards enhanced nutrient removal and biomass production in an osmotic photobioreactor.* Water Research, 2020. **182**: p. 116038.

224. Li, J., C. Li, C.Q. Lan, and D. Liao, *Effects of sodium bicarbonate on cell growth, lipid accumulation, and morphology of Chlorella vulgaris.* Microbial Cell Factories, 2018. **17**: p. 1-10.

225. Polat, E., E. Yüksel, and M. Altınbaş, *Mutual effect of sodium and magnesium on the cultivation of microalgae Auxenochlorella protothecoides.* Biomass and bioenergy, 2020. **132**: p. 105441.

226. Zhu, C., et al., *Efficient CO2 capture from the air for high microalgal biomass production by a bicarbonate Pool.* Journal of CO2 Utilization, 2020. **37**: p. 320-327.

227. Wang, F., et al., *Effects of sodium selenite on the growth, biochemical composition and selenium biotransformation of the filamentous microalga Tribonema minus.* Bioresource Technology, 2023. **384**: p. 129313.

228. Salama, E.-S., et al., *Biomass, lipid content, and fatty acid composition of freshwater Chlamydomonas mexicana and Scenedesmus obliquus grown under salt stress.* Bioprocess and biosystems engineering, 2013. **36**: p. 827-833.

229. von Alvensleben, N., M. Magnusson, and K. Heimann, *Salinity tolerance of four freshwater microalgal species and the effects of salinity and nutrient limitation on biochemical profiles.* Journal of applied phycology, 2016. **28**: p. 861-876.

230. Salbitani, G., et al., *Rapid and positive effect of bicarbonate addition on growth and photosynthetic efficiency of the green microalgae Chlorella sorokiniana (Chlorophyta, Trebouxiophyceae).* Applied Sciences, 2020. **10**(13): p. 4515.

231. Srinivasan, R., et al., *Bicarbonate supplementation enhances growth and biochemical composition of Dunaliella salina V-101 by reducing oxidative stress induced during macronutrient deficit conditions.* Scientific reports, 2018. **8**(1): p. 6972.

232. Michael A. Borowitzka, J.B., John A. Raven *The Physiology of Microalgae*. 2016: Springer.

233. Sun, X.-M., et al., *Microalgae for the production of lipid and carotenoids: a review with focus on stress regulation and adaptation.* Biotechnology for biofuels, 2018. **11**: p. 1-16.

234. Rengel, R., et al., *Simultaneous production of carotenoids and chemical building blocks precursors from chlorophyta microalgae.* Bioresource Technology, 2022. **351**: p. 127035.

235. Singh, R.P. and A. Kumar, *Physiological and biochemical responses of bicarbonate supplementation on biomass and lipid content of green algae Scenedesmus sp. BHU1 isolated from wastewater for renewable biofuel feedstock.* Frontiers in Microbiology, 2022. **13**: p. 839800.

236. Araujo, G.S., J.W. Silva, C.A. Viana, and F.A. Fernandes, *Effect of sodium nitrate concentration on biomass and oil production of four microalgae species.* International Journal of Sustainable Energy, 2020. **39**(1): p. 41-50.

237. Mahendra, A., et al. *Effects of sodium bicarbonate supplementation on lipid accumulation of Chlorella sp. cultivated in artificial medium*. in *AIP Conference Proceedings*. 2024. AIP Publishing.

238. Singh, R., A. Upadhyay, P. Chandra, and D. Singh, *Sodium chloride incites reactive oxygen species in green algae Chlorococcum humicola and Chlorella vulgaris: implication on lipid synthesis, mineral nutrients and antioxidant system.* Bioresource technology, 2018. **270**: p. 489-497.

239. Li, N., et al., *Electrostatic charges on microalgae surface: mechanism and applications.* Journal of Environmental Chemical Engineering, 2022. **10**(3): p. 107516.

240. Matho, C., et al., *Bio-compatible flotation of Chlorella vulgaris: Study of zeta potential and flotation efficiency.* Algal Research, 2019. **44**: p. 101705.

241. Cui, Y., W. Yuan, and J. Cheng, *Understanding pH and ionic strength effects on aluminum sulfate-induced microalgae flocculation.* Applied biochemistry and biotechnology, 2014. **173**: p. 1692-1702.

242. Saavedra, R., R. Muñoz, M.E. Taboada, and S. Bolado, *Influence of organic matter and CO2 supply on bioremediation of heavy metals by Chlorella vulgaris and Scenedesmus almeriensis in a multimetallic matrix.* Ecotoxicology and Environmental Safety, 2019. **182**: p. 109393.

243. Huang, Y., et al., *Biodegradable branched cationic starch with high C/N ratio for Chlorella vulgaris cells concentration: Regulating microalgae flocculation performance by pH.* Bioresource technology, 2019. **276**: p. 133-139.

244. Flora, J.R., M.T. Suidan, P. Biswas, and G.D. Sayles, *Modeling algal biofilms: role of carbon, light, cell surface charge, and ionic species.* Water Environment Research, 1995. **67**(1): p. 87-94.

245. Zheng, Y., et al., *A rapid inoculation method for microalgae biofilm cultivation based on microalgae-microalgae co-flocculation and zeta-potential adjustment.* Bioresource technology, 2019. **278**: p. 272-278.

246. Vu, H.P., et al., *Harvesting Porphyridium purpureum using polyacrylamide polymers and alkaline bases and their impact on biomass quality.* Science of the Total Environment, 2021. **755**: p. 142412.

247. Yao, L., J. Shi, and X. Miao, *Mixed wastewater coupled with CO2 for microalgae culturing and nutrient removal.* PloS one, 2015. **10**(9): p. e0139117.

248. Xia, L., R. Huang, Y. Li, and S. Song, *The effect of growth phase on the surface properties of three oleaginous microalgae (Botryococcus sp. FACGB-762, Chlorella sp. XJ-445 and Desmodesmus bijugatus XJ-231).* Plos one, 2017. **12**(10): p. e0186434.

249. Wei, C., et al., *Analysis of the energy barrier between Chlorella vulgaris cells and their interfacial interactions with cationic starch under different pH and ionic strength.* Bioresource technology, 2020. **304**: p. 123012.

250. Ma, X., Y. Mi, C. Zhao, and Q. Wei, *A comprehensive review on carbon source effect of microalgae lipid accumulation for biofuel production.* Science of The Total Environment, 2022. **806**: p. 151387.

251. García-Martínez, J.B., et al., *The circular economy approach to improving CNP ratio in inland fishery wastewater for increasing algal biomass production.* Water, 2022. **14**(5): p. 749.

252. Lai, Y.-C., et al., *Towards protein production and application by using Chlorella species as circular economy.* Bioresource technology, 2019. **289**: p. 121625.

253. Zada, S., et al., *Biosorption of iron ions through microalgae from wastewater and soil: optimization and comparative study.* Chemosphere, 2021. **265**: p. 129172.

254. Esakkimuthu, S., V. Krishnamurthy, R. Govindarajan, and K. Swaminathan, *Augmentation and starvation of calcium, magnesium, phosphate on lipid production of Scenedesmus obliquus.* Biomass and Bioenergy, 2016. **88**: p. 126-134.

255. Chu, F.-F., et al., *Effect of phosphorus on biodiesel production from Scenedesmus obliquus under nitrogen-deficiency stress.* Bioresource technology, 2014. **152**: p. 241-246.

256. Liu, X., et al., *Carbon dioxide fixation coupled with ammonium uptake by immobilized Scenedesmus obliquus and its potential for protein production.* Bioresource technology, 2019. **289**: p. 121685.

257. El Ouaer, M., et al., *Recovery of landfill leachate as culture medium for two microalgae: Chlorella sp. and Scenedesmus sp.* Environment, Development and Sustainability, 2020. **22**: p. 2651-2671.

258. Muthurathinam, S.G. and A.V. Perumal, *Synthesis, characterization and tribological investigation of vegetable oil methyl esters based bio-lubricants.* Industrial Crops and Products, 2023. **203**: p. 117098.

259. Medicine, N.L.o., *Methyl tetradecanoate*. National Library of Medicine: PubChem.

260. Chemical, C., *Methyl Myristate 98%.*

261. Wu, Y., et al., *Experimental study on lubrication performance of main components of biodiesel.* Energy Sources, Part A: Recovery, Utilization, and Environmental Effects, 2022: p. 1-15.

262. Nayak, M., W.I. Suh, B. Lee, and Y.K. Chang, *Enhanced carbon utilization efficiency and FAME production of Chlorella sp. HS2 through combined supplementation of bicarbonate and carbon dioxide.* Energy conversion and management, 2018. **156**: p. 45-52.

263. Vu, M.T., et al., *Biogas sparging to control fouling and enhance resource recovery from anaerobically digested sludge centrate by forward osmosis.* Journal of Membrane Science, 2021. **625**: p. 119176.

264. Ricceri, F., et al., *Microalgae biomass concentration and reuse of water as new cultivation medium using ceramic membrane filtration.* Chemosphere, 2022: p. 135724.

265. Lin, J.-T., D.-C. Cheng, K.-T. Chen, and H.-W. Liu, *Dual-wavelength (UV and blue) controlled photopolymerization confinement for 3D-printing: Modeling and analysis of measurements.* Polymers, 2019. **11**(11): p. 1819.

266. Li, Q., et al., *Visualizing molecular weights differences in supramolecular polymers.* Proceedings of the National Academy of Sciences, 2022. **119**(9): p. e2121746119.

267. Pandey, A., et al., *Experimental studies on zeta potential of flocculants for harvesting of algae.* Journal of environmental management, 2019. **231**: p. 562-569.

268. Zhu, L., et al., *Effects of operating parameters on algae Chlorella vulgaris biomass harvesting and lipid extraction using metal sulfates as flocculants.* Biomass and bioenergy, 2020. **132**: p. 105433.

269. Scheepers, D., B. Chatillon, Z. Borneman, and K. Nijmeijer, *Influence of charge density and ionic strength on diallyldimethylammonium chloride (DADMAC)-based polyelectrolyte multilayer membrane formation.* Journal of Membrane Science, 2021. **617**: p. 118619.

270. Babiak, W. and I. Krzemińska, *Extracellular polymeric substances (EPS) as microalgal bioproducts: A review of factors affecting EPS synthesis and application in flocculation processes.* Energies, 2021. **14**(13): p. 4007.

271. Shaikh, S.M., et al., *A comprehensive review on harvesting of microalgae using Polyacrylamide-Based Flocculants: Potentials and challenges.* Separation and Purification Technology, 2021. **277**: p. 119508.

272. Siebert, H.M. and J.J. Wilker, *Improving the molecular weight and synthesis of a renewable biomimetic adhesive polymer.* European Polymer Journal, 2019. **113**: p. 321-327.

273. Demir, I., A. Besson, P. Guiraud, and C. Formosa-Dague, *Towards a better understanding of microalgae natural flocculation mechanisms to enhance flotation harvesting efficiency.* Water Science and Technology, 2020. **82**(6): p. 1009-1024.

274. Zhao, F., et al., *An effective method for harvesting of microalga: Coculture-induced self-flocculation.* Journal of the Taiwan Institute of Chemical Engineers, 2019. **100**: p. 117-126.

275. Esmaeili, A., H.A. Moghadam, and A. Golzary, *Application of marine microalgae in biodesalination and CO2 biofixation: A review.* Desalination, 2023: p. 116958.

276. López-Pacheco, I.Y., et al., *Phycocapture of CO2 as an option to reduce greenhouse gases in cities: Carbon sinks in urban spaces.* Journal of CO2 Utilization, 2021. **53**: p. 101704.

277. Xu, P., et al., *Recent advances in CO2 fixation by microalgae and its potential contribution to carbon neutrality.* Chemosphere, 2023: p. 137987.

278. Poli, M.A., et al., *Pacific white shrimp and Nile tilapia integrated in a biofloc system under different fish-stocking densities.* Aquaculture, 2019. **498**: p. 83-89.

279. Chen, B.-L., et al., *Genome sequencing, assembly, and annotation of the self-flocculating microalga Scenedesmus obliquus AS-6-11.* BMC genomics, 2020. **21**: p. 1-14.

280. Nishida, Y., R. Hoshina, S. Higuchi, and T. Suzaki, *The unicellular green alga Chlorogonium capillatum as a live food promotes the growth and survival of Artemia larvae.* Aquaculture, 2023. **566**: p. 739227.

281. Verfaillie, A., et al., *Harvesting of marine microalgae using cationic cellulose nanocrystals.* Carbohydrate polymers, 2020. **240**: p. 116165.

282. Nayak, M., et al., *Performance evaluation of different cationic flocculants through pH modulation for efficient harvesting of Chlorella sp. HS2 and their impact on water reusability.* Renewable Energy, 2019. **136**: p. 819-827.

283. Aljuboori, A.H.R., Y. Uemura, and N.T. Thanh, *Flocculation and mechanism of self-flocculating lipid producer microalga Scenedesmus quadricauda for biomass harvesting.* Biomass and Bioenergy, 2016. **93**: p. 38-42.

284. Hao, W., et al., *Surface characteristics of microalgae and their effects on harvesting performance by air flotation.* International journal of agricultural and biological engineering, 2017. **10**(1): p. 125-133.

285. Deepa, P., K. Sowndhararajan, and S. Kim, *A Review of the Harvesting Techniques of Microalgae.* Water, 2023. **15**(17): p. 3074.